UNIVERSITÀ
DEGLI STUDI
FIRENZE

DOTTORATO DI RICERCA IN FARMACOLOGIA,
TOSSICOLOGIA E TRATTAMENTI INNOVATIVI

CICLO XXVI

COORDINATORE Prof.ssa Teodori Elisabetta

Acute actions of parkinsonizing toxin MPP^+ reveal new functions for the hyperpolarization-activated current in the physiology and pathology of midbrain dopaminergic neurons

Settore scientifico discliplinare BIO/14

Dottorando:
Dr. Narducci Roberto

Tutore:
Prof. Mannaioni Guido

Coordinatore:
Prof.ssa Teodori Elisabetta

Anni 2011-2013

Contents

I. Introduction **1**

1. Parkinson's disease . . . **2**
1.1. Clinical characteristics of PD . . . 2
1.2. Neurochemical and neuropathological features of PD . . . 3
1.3. Anatomy and physiology of the basal ganglia . . . 4
1.4. Neural substrate of Parkinsonian motor symptoms . . . 6

2. Physiological properties of midbrain DA neurons . . . **8**
2.1. Hyperpolarization-activated current and HCN channels . . . 9
2.1.1. Hyperpolarization- activated current (I_{h}) . . . 9
2.1.2. Regulation . . . 10
2.1.3. Pharmacology . . . 11
2.2. HCN channels . . . 11
2.2.1. Structure . . . 11
2.2.2. Tissue and subcellular expression . . . 12
2.3. Physiological roles of I_{h} in neural function . . . 14
2.3.1. I_{h} and spontaneous activity . . . 14
2.3.2. I_{h} role in synaptic transmission . . . 15
2.3.3. I_{h} in dendritic integration . . . 15

3. Causes and pathogenesis of PD . . . **17**
3.1. Etiology of PD . . . 17
3.2. Pathogenesis of PD . . . 18
3.2.1. Misfolding and aggregation of proteins . . . 18
3.2.2. Free radicals and deficits in energy metabolism . . . 19

4. Animal models of Parkinson's Disease . . . **23**
4.1. The MitoPark mouse . . . 24
4.2. Toxin-treated models . . . 24
4.2.1. 6-hydroxydopamine . . . 24
4.2.2. Rotenone . . . 25
4.2.3. Paraquat . . . 25

4.2.4. The MPTP/MPP$^+$ model 26
4.2.5. Mechanisms of action of MPTP/MPP$^+$ 27
4.3. Unanswered issues in the mitochondrial hypothesis 28

II. Aim of the thesis **30**

5. Aim of the thesis **31**

III. Methods **32**

6. Methods **33**
6.1. Animals 33
6.2. Midbrain slices preparation 33
6.3. The patch-clamp technique 33
6.4. Electrophysiology 34
6.5. Drugs and chemicals 35
6.6. Data analysis and statistic 36

IV. Results **37**

7. Results **38**
7.1. MPP$^+$ causes rapid, ATP-independent, hyperpolarization and reduction of spontaneous activity in SNc DA neurons 38
7.2. MPP$^+$ inhibits I_h by slowing its gating properties and reducing current amplitude 40
7.3. MPP$^+$-mediated I_h inhibition is voltage-depentent and changes I_h kinetic properties 41
7.4. Effect of MPP$^+$ on I_h does not depend on complex I poisoning, D_2R signalling or cAMP metabolism 43
7.5. MPP$^+$ increases temporal summation of EPSPs at STN-SNc glutamatergic synapse 44
7.6. I_h inhibition increases temporal summation of EPSPs in VTA DA neurons 46
7.7. Presynaptic I_h does not influence integration of incoming synaptic signals in SNc DA neurons 48
7.7.1. Presynaptic I_h inhibition doesn't affect evoked release 48
7.7.2. Spontaneous activity of SNc DA neurons is not affected by presynaptic I_h inhibition 49

V. Discussion **51**

8. Discussion **52**
8.1. MPP$^+$ affects membrane potential and spontaneous activity through inhibition of I_h 52

8.2. MPP$^+$ likely inhibits I_h in a direct way 53
8.3. MPP$^+$ increases temporal summation of eEPSPs in SNc DA neurons via inhibition of I_h 54
8.4. I_h contribution to DA synaptic activity is mainly due to postsynaptic HCN channels 54
8.5. Relevance of I_h inhibition in PD pathogenesis 55

9. List of abbreviations 57

Part I.

Introduction

Chapter 1

Parkinson's disease

Parkinson's disease (PD) is a chronic, progressive neurologic disease. The prevalence of PD is 1% in persons above 55 years and, due to ageing of population, the number of patients worldwide is expected to rise considerably in the future.
It equally affects people from different ethnicities and socio-economic status, but it is more common in men than in women (Samii et al., 2004).
It was first formally identified by physician James Parkinson in 1817 as "The Shaking Palsy", where he described the daily lives and symptoms of six patients affected by problems such as constant shaking, rigidity and slowness of movement. Later in the 19^{th} century, the disease was formally named after Dr. Parkinson by the french neurologist Charcot.
PD presents with four cardinal motor manifestations: tremor at rest, rigidity, bradykinesia (slowing of movement), and postural instability. At later stages patients also develop cognitive impairment.
These clinical manifestations of the disease result from the massive degeneration of nigral dopaminergic neurons and the consequent drastic fall of dopamine (DA) levels in projection areas, such as the striatum.
Replenishment of striatal DA through the oral administration of the DA precursor levodopa (L-3, 4-dihydroxyphenylalanine) alleviates most of the symptoms. Nonetheless, after several years of treatment with levodopa most patients develop involuntary movements, termed, dyskinesias, which are difficult to control and impair the quality of life.
Still today all current treatments are symptomatic and none halt or retard DA neuron degeneration.

1.1. Clinical characteristics of PD

In about 95% of PD cases, there is no apparent genetic linkage (referred to as "sporadic" PD), but in the remaining cases, the disease is inherited. Over time, symptoms worsen, and prior to the introduction of levodopa, the mortality rate among PD patients was three times that of the normal age-matched subjects.
Clinically, any disease that includes striatal DA deficiency or direct striatal damage may lead to "parkinsonism", a syndrome characterized by tremor at rest, rigidity,

slowness or absence of voluntary movement, postural instability, and freezing. PD is the most common cause of parkinsonism, accounting for $\sim 80\%$ of cases.
In PD we can observe a variety of tremors: most frequently, a rest tremor or postural or kinetic tremor with equal frequency ranging from 4–7 Hz is found (classical parkinsonian tremor) although in the early stages and in severe akinetic-rigid symptoms higher frequencies may occur (Deuschl et al., 2000). Whereas it is not required for diagnosis, the prolonged absence of tremor in the course of a patient's illness should lead to the careful consideration of other neurologic conditions that can present with signs of parkinsonism (Lang and Lozano, 1998a).
Rigidity is a motor sign detected as an increased resistance (stiffness) to passive movement of a patient's limbs.
Bradykinesia refers to a slowness and paucity of movement; it manifests as a variety of symptoms, including paucity of normal facial expression (hypomimia), decreased voice volume (hypophonia) and drooling (failure to swallow without thinking about it).
Bradykinesia is not due to limb rigidity since it can be observed in the absence of rigidity during treatment and it may significantly impair the quality of life because it takes much longer to perform everyday tasks such as dressing or eating.
PD patients also typically develop a stooped posture and may lose normal posture reflexes. Of the cardinal motor signs, postural instability is the most potentially dangerous, because it can lead to falls with resulting fractures. It is also one of the manifestation that responds less well to levodopa treatment (Lang and Lozano, 1998b).
An additional motor feature of PD is the phenomenon called freezing or "motor block". It consists in the inability to begin a voluntary movement such as walking. It is transient, lasting for seconds or minutes, and suddenly abates. Combined with postural instability, it can be devastating and levodopa administration not always improves it, but can make it worse.
Depression is common, and dementia is significantly more frequent in PD, especially in older patients.

1.2. Neurochemical and neuropathological features of PD

The two pathological hallmarks of PD, essentials for it pathologic diagnosis, are the loss of the nigrostriatal DA neurons and the presence of intraneuronal proteinacious cytoplasmic inclusions, termed "Lewy Bodies" (LBs).
LBs are spherical eosinophilic cytoplasmic protein aggregates composed of numerous proteins involved in protein degradation, including α-synuclein, parkin, ubiquitin, and neurofilaments. LBs are commonly observed in the brain regions showing the most neuron loss in PD, including substantia nigra, locus coeruleus, the dorsal motor nucleus of the vagus and the nucleus basalis of Meynert, but they are also observed in neocortex, diencephalon, spinal cord, and even peripheral autonomic ganglia (Gibb et al., 1991). LBs are generally 5 µm to 25 µm in diameter and have an organized structure containing a dense hyaline core surrounded by a clear halo. Electron microscopy reveals a dense granulovesicular core surrounded by a ring of radiating 8 nm to 10 nm

fibrils (Pappolla, 1986). They usually are observed within the cell soma, but also can be seen in neuritis or free in the extracellular space. The role of LBs in neuronal cell death is controversial and, moreover, they are not specific for PD: they are also found in Alzheimer disease, in a condition called "dementia with LBs disease".
The cell bodies of nigrostriatal neurons are in the substantia nigra pars compacta (SNc), and they project primarily to the putamen. The loss of these neurons, which normally contain conspicuous amounts of neuromelanin (Marsden, 1983), produces the classic gross neuropathological finding of SNc depigmentation. The pattern of SNc cell loss appears to parallel the level of expression of the DA transporter (DAT) mRNA (Blanchard et al., 1994) and is consistent with the finding that depletion of DA is most pronounced in the dorsolateral putamen (Bernheimer et al., 1973), the main site of projection for these neurons.
At the onset of symptoms, putamenal DA is depleted $\sim 80\%$, and $\sim 60\%$ of SNc DA neurons have already been lost.
The degree of terminal loss in the striatum appears to be more pronounced than the magnitude of SNc DA neuron loss (Bernheimer et al., 1973), suggesting that striatal dopaminergic nerve terminals are the primary target of the degenerative process and that neuronal death in PD may result from a "dying back" process.
Mesolimbic DA neurons residing in the ventral tegmental area (VTA) are much less affected in PD (Uhl et al., 1985), consequently, there is significantly less depletion of DA in the caudate (Price et al., 1978), the main site of projection for these neurons.
Although some DA neurons are spared in PD, neurodegeneration is also found in noradrenergic (locus coeruleus), serotonergic (raphe), and cholinergic (nucleus basalis of Meynert, dorsal motor nucleus of vagus) systems, as well as in the cerebral cortex (especially cingulate and entorhinal cortices), olfactory bulb, and autonomic nervous system (Hornykiewicz and Kish, 1987).
While involvement of these neurochemical systems is generally thought to occur in more severe or late-stage disease, the temporal relationship of damage to specific neurochemical systems is not well established. For example, some patients develop depression months or years prior to the onset of PD motor symptoms, which could be due to early involvement of nondopaminergic pathways (Dauer and Przedborski, 2003).

1.3. Anatomy and physiology of the basal ganglia

The basal ganglia are a collection of nuclei located at the base of the forebrain and strongly connected with the cerebral cortex, thalamus, and other brain areas. They are formed by the striatum (putamen and caudate nucleus), the globus pallidus, the subthalamic nucleus (STN) and the substantia nigra. Over the last few years it has been demonstrated that these nuclei play a key role in mediating motor and non-motor behaviour, cognition and emotion.
Several models of the functional anatomy of the basal ganglia have been proposed. The most familiar model was introduced in the 1980's (Alexander and Crutcher, 1990; DeLong, 1990). This model is based on the existence of separate parallel loops, mediating motor, cognitive and emotional functions, and running through the basal ganglia in a more or less uniform fashion (Figure 1.1).

Two important characteristics of basal ganglia are convergence and segregation. Convergence refers to the fact that along the circuits the number of neurons decreases by each step, thus converging information following each relay. Segregation not only implies separation of the individual circuits along their path through the basal ganglia, but also the separation of information flow for motor functions (Santens et al., 2003).
The striatum is the major recipient of inputs to the basal ganglia. These excitatory afferents arise from the cerebral cortex, from the intralaminar nuclei of the thalamus and from the brainstem. The medium spiny neurons (MSNs) are inhibitory neurons of the striatum that project to the globus pallidus and the substantia nigra, giving rise to the main output projections of the basal ganglia. The internal segment of globus pallidus (GPi) is functionally related to the pars reticulata of the substantia nigra (SNr) and both segments use γ-aminobutyric acid (GABA) as neurotransmitter. In addition to its reticular portion, the substantia nigra has also a compact zone or pars compacta (SNc). Its cells are dopaminergic and also contain neuromelanin, a dark pigment derived from oxidized and polymerized DA. Dopaminergic cells are also present in the ventral-tegmental area (VTA), a medial extension of SNc.
Dopamine neurons in the VTA primarily project to the ventral striatum (nucleus accumbens and olfactory tubercle) as part of the so-called mesolimbic pathway, and to the prefrontal cortex (the mesocortical pathway)
MSNs also project directly to SNc, which in turn sends widespread dopaminergic projections back to the spiny neurons.
STN is closely connected anatomically with both segments of the globus pallidus (GP) and the SN and its glutaminergic cells are the only excitatory projections of the basal ganglia.
Based on the type of neurotransmitters and the predominant type of DA receptor they contain, MSNs can be divided into two populations. One population contains GABA, dynorphin, and substance P, and primarily expresses D_1 DA receptors (D_1R) coupled to a stimulatory G protein (G_s). These neurons project to the basal ganglia output nuclei, GPi and SNr (Albin et al., 1989) and form the"direct" striatal output pathway (Alexander and Crutcher, 1990). The second population contains GABA and enkephalin and primarily expresses D_2 DA receptors (D_2R) coupled to an inhibitory G protein (G_i). These neurons project to the external segment of the globus pallidus (GPe)(Albin et al., 1989) and are the origin of the"indirect" striatal output pathway.
When DA binds to the D_1 receptor , facilitates the release of GABA on output nuclei, thus resulting in less tonic inhibition of thalamus which leads to the transient activation of cortical nuclei via glutamate.
On the other hand when DA binds to the D_2R, decreases the release of inhibitory GABA from the MSNs, thereby increasing GPe's output of GABA which results in decreased STN output of excitatory glutamate and in a subsequent reduction in GABA release from the output nuclei. This finally manifests as a reduction in the inhibition of glutamatergic, thalmo-cortical neurons.

Summarizing, DA released from striatal terminals of SNc neurons has opposite effects on both pathways, resulting in a net release of thalamic output to cortical motor areas. In this way a release of motor programs and inhibition of unwanted movements can be balanced to result in finely tuned motor behaviour.

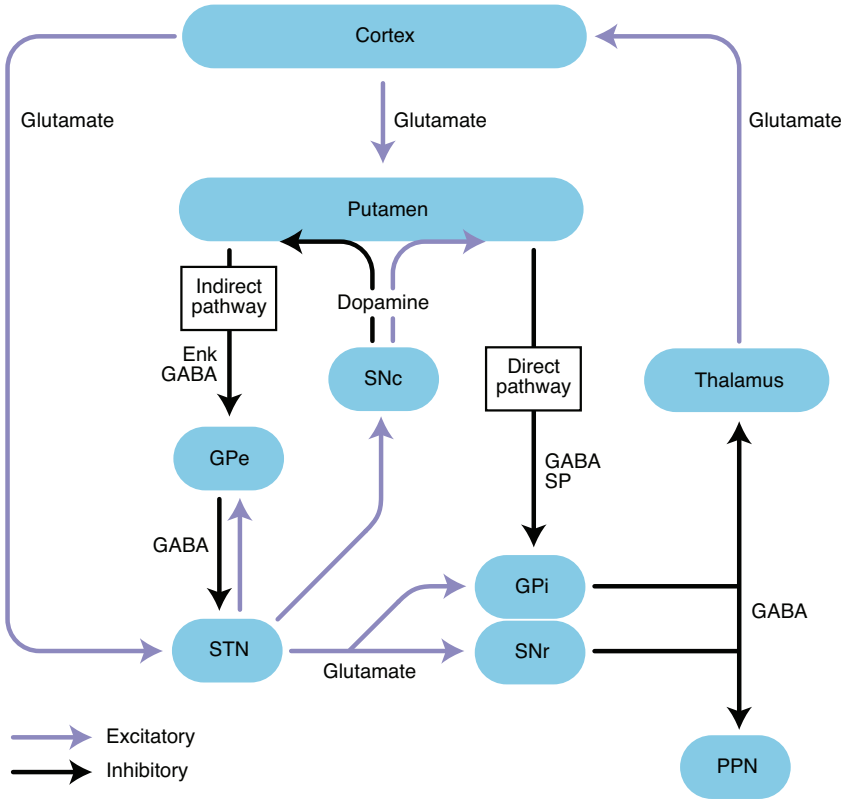

Figure 1.1.: Basal ganglia circuitry in normal conditions. Excitatory projections are shown in blue; inhibitory connections are shown in black. (Expert Reviews in Molecular Medicine, Volume 5, 2003).

1.4. Neural substrate of Parkinsonian motor symptoms

According to the classic patophysiologic model of the basal ganglia, DA deficiency leads to the loss of D_1R-mediated stimulation of the direct pathway that becomes underactive, while the indirect pathway becomes overactive due to the loss of D_2R-mediated inhibition with a consequent overinhibition of GPe, disinhibition of STN, and excessive glutamatergic drive of the GPi and SNr (Albin et al., 1989; DeLong, 1990). Similarly, the decreased activation of neurons in the direct pathway reduces its inhibition of GPi/SNr and contributes to the excessive basal ganglia output activity, whose influence is an inhibition of the thalamus (Figure1.2).
As dopaminergic neurons continue to die, the striatal DA deficit increases, leading to an excess inhibition of the GPe. In turn, hypoactivity of GPe reduces its inhibitory output onto the GPi and STN, which now became more overtly hyperactive with consequent aggravation of parkinsonian motor states (Blandini et al., 2000; Obeso et al., 2004; Wichmann and DeLong, 2006). These changes are thought to represent the neural substrate for parkinsonian motor symptoms. Therefore strategies for restore the balance of this pathways might be beneficial to treating PD.

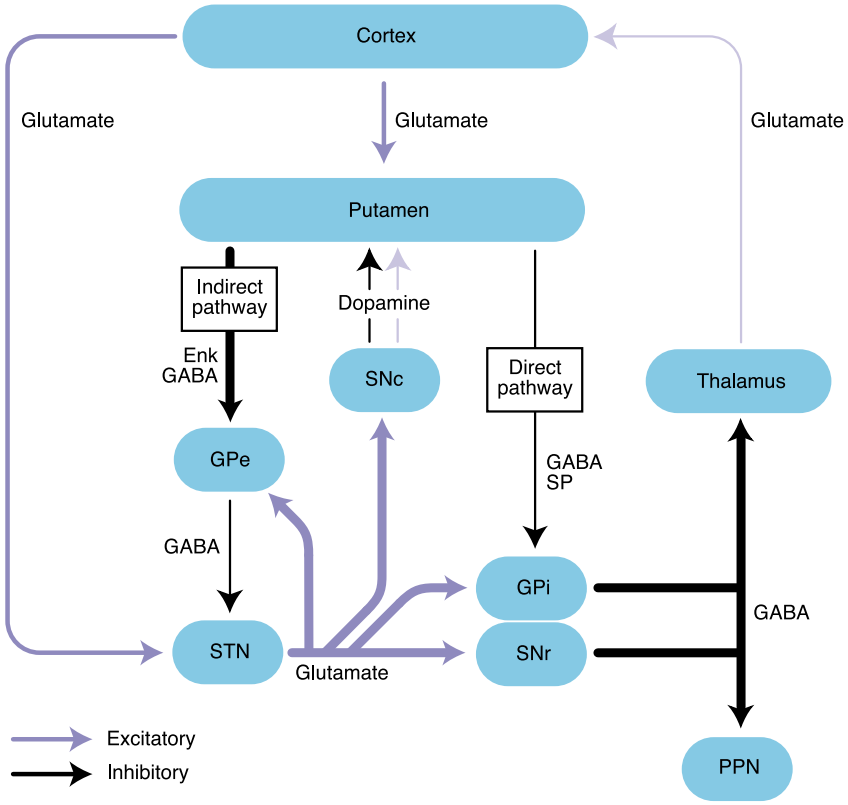

Figure 1.2.: Basal ganglia circuitry in Parkinson's disease. Excitatory projections are shown in blue; inhibitory connections are shown in black. (Expert Reviews in Molecular Medicine, Volume 5, 2003).

Chapter 2

Physiological properties of midbrain DA neurons

Midbrain DA cells are medium to large size (11-22 µm, German and Manaye (1993)) and present a multipolar, fusiform or polygonal shape. They emit 3-5 large, rapidly tapering smooth dendrites and, within the SNc, they don't show local axon collateral arborization (Juraska et al., 1977).
Molecular markers as DAT and tyrosine hydroxyalse (TH), the latter being the enzyme responsible for catalyzing the conversion of the aminoacid levodopa, allow the identification of this type of neuron. Neuromelanin is not equally expressed in all DA cell groups, but the largest clusters are found in SNc and VTA (82 % and 42 % of all TH-immunoreactive neurons respectively (Herrero et al., 1993a)).
Midbrain DA neurons are spontaneously active both *in vitro* and *in vivo*, with an average of 1-5 spikes per second (Grace and Bunney, 1983, 1984b). They exhibit three distinct modes or patterns of firing *in vivo* (Grace and Bunney, 1984a; Tepper and Lee, 2007)):

- Random or occasional mode of firing
- Pacemaker-like firing with regular interspike intervals, low coefficient of variations and lack of bursting
- Bursty firing, characterized by stereotyped bursts around 15 Hz in which the first intraburst interspike interval is around 60 ms, followed by progressively increasing interspike intervals and progressively decreasing spike amplitudes

In *in vitro* recordings the bursting firing activity is not observed because of the lost of afferent inputs, while the pacemaking activity is retained thanks to an endogenous calcium-dependent oscillatory mechanism sufficient to drive action potential generation (Puopolo et al., 2007).
VTA and SN DA neurons express D_2 autoceptors that play in important role in the regulation of DA neuronal firing activity by means of auto-inhibition (Olijslagers et al., 2006).
A distinctive electrophysiological property of SNc DA neurons is a pronounced hyperpolarization-activated current (I_h), which is used to distinguish them from non-DA

cells. Despite the anatomical proximity of VTA and SNc, this criterion is not valid for VTA, where the presence of I_h doesn't definitely represent a DA neuron, while its absence always indicates a VTA neuron not being dopaminergic (Margolis et al., 2006).

2.1. Hyperpolarization-activated current and HCN channels

The hyperpolarization-activated current (I_h) was first described in sino-atrial node cells and later identified in different types of neurons (Noma and Irisawa, 1976). Because of its unique properties, especially the activation upon hyperpolarization of the membrane potential, it was termed I_f (f for funny).
The ion channels underlying I_h have been discovered about a decade ago and, because of their complex dual gating mode, these proteins were termed hyperpolarization-activated cyclic nucleotide-gated (HCN) channels.
In mammals, four different genes encoding HCN isoforms ($HCN_{1–4}$) have been discovered, each isoform forming channels with significantly different physiological properties (Santoro et al., 1998).
Currents obtained after heterologous expression of $HCN_{1–4}$ channels cDNA reveal the principal features of native I_h, confirming that HCN channels indeed represent the molecular correlate of I_h.
I_h contributes to a wide range of physiological functions, including the determination of resting membrane potential (RMP), generation of neuronal oscillation, and regulation of dendritic integration and synaptic transmission, and is implicated in multiple physiological processes, such as sleep and arousal, learning and memory, sensation and perception.
Different HCN isoforms have been found in the same cells and their co-assembly has been suggested using electrophysiological analyses (Chen et al., 2001).

2.1.1. Hyperpolarization- activated current (I_h)

I_h is a mixed cationic current carried by Na^+ and K^+ with permeability ratios of about 1 : 4; however recent findings support the evidence of a small but significant Ca^{2+} permeability (Michels et al., 2008). Given its reversal potential around $-20\,mV$ and $-30\,mV$ at physiological ionic conditions (Biel et al., 2009), I_h is inwardly directed at rest and depolarizes the membrane potential.
Unlike most voltage-gated currents, is activated by hyperpolarizing voltage steps to potentials negative to $-55\,mV$, near the RMP, and does not display voltage-dependent inactivation. Although Na^+ constitutes the major inward cation current in HCN channels at physiological membrane potentials, the I_h current amplitude depends on the extracellular K^+ concentration (Wollmuth and Hille, 1992).
Upon activation of I_h, two kinetic components can be distinguished: a minor instantaneous current (IINS) fully activated within a few milliseconds (Macri and Accili, 2004; Macri et al., 2002; Proenza et al., 2002), and the major slowly developing component (ISS), which reaches the steady-state level under fully activating conditions in a range of tens of milliseconds to several seconds.

To date the ionic nature of IINS is not clear and is generally considered as a leak conductance or an experimental artifact (Macri and Accili, 2004; Macri et al., 2002). In general HCN channels activate quite slowly with time constants and the ISS can be empirically described by either a single (Womble and Moises, 1993) (see formula 2.2) or double exponential function (see equation 2.1), where I_{ht} is the amplitude of the current at time t, C is a constant, A_1 and A_2 reflect the amplitude coefficients of the fast (τ_1) and slow (τ_2) time constants, respectively. (van Ginneken and Giles, 1991).

$$I_{ht} = A_1 \times e^{-t/\tau_1} + A_2 \times e^{-t/\tau_2} + C \tag{2.1}$$

The diversity of time constants probably results from an interplay of several factors: in addition to the intrinsic activation properties of HCN channel isoforms, cellular microenvironment (e.g. auxiliary subunits, concentration of cellular factors, etc.) can affect I_h properties as well as experimental conditions (e.g. pH, temperature, ionic composition of solutions, etc.).
The voltage-dependence of I_h activation can be assessed by tail current activation curves, in which the amplitude of the tail current upon return to a fixed holding potential is plotted against the hyperpolarizing potential step used to activate the current. These activation curves show a typical sigmoidal profile and can be well fitted by Boltzmann function (see equation 2.2), providing estimation of the half-maximal activation potential ($V_{1/2}$) and steepness factor (k).

$$I_h = \frac{I_{h_{max}}}{1 + \exp\left(\frac{V - V_{1/2}}{k}\right)} \tag{2.2}$$

2.1.2. Regulation

External temperature can modulate I_h current by shifting the midpoint of voltage-dependent activation curve towards more depolarized potentials and reducing I_h time constants (Watts et al., 1996); thus performing experiments with a constant temperature is fundamental when investigating I_h .
Another positive I_h modulator is phosphatidylinositol 4,5-bisphosphate (PIP_2), which positively shifts the activation curve of cloned HCN_2 channels by 20-30 mV (Zolles et al., 2006). Conversely, in SN DA neurons, PIP_2 depletion, obtained by wortmannin-mediated inhibition of the PI 4-kinase, negatively shifted steady-state activation of the HCN channels by 10 mV. PIP_2 effect is largely cAMP-independent and prevents the hyperpolarized shift normally observed in excised patches (Chen et al., 2001; DiFrancesco, 1986), meaning that endogenous PIP_2 levels counterbalance the opposing action of corresponding kinases and phospahtases on native I_h current voltage dependence (Pian et al., 2006; Zolles et al., 2006).
In addition it has been shown that in hippocampal neurons, the inhibition p38 mitogen associated protein kinase (MAPK) negatively shifts the activation curve by 25 mV, whereas its activation induced a positive shift by 11 mV (Poolos et al., 2006).

2.1.3. Pharmacology

The common characteristic of all I_h blockers is their lack of full selectivity for HCN channels; in addition there are no isoform-specific compounds allowing identification of subunit-specific roles in various tissues.
Like K^+ channels, HCN channels are almost completely blocked by low millimolar concentrations of Cs, however, in contrast to inward rectifier K^+ currents, I_h is insensitive to millimolar concentrations of external Ba^{2+} and tetraethylammonium (TEA). I_h is also insensitive to 4-Aminopyridine (4-AP), a blocker of voltage-gated K^+ channels (Ludwig et al., 1998).
A number of organic blockers have been described to inhibits HCN channels; among them, the most widely used is a bradycardic one termed ZD7288 (originally named ICI 7288)(Briggs et al., 1994). ZD7288 blocks I_h at concentrations between 10 µM to 100 µM (Gasparini and DiFrancesco, 1997; Satoh and Yamada, 2000) and exibits slow kinetics, ranging in the order of minutes; in addition is poorly reversible and its I_h inhibition is not use dependent in moderate voltage ranges. These properties suggest that the localization of ZD7288 binding site is near the intracellular portion of the HCN channel pore as confirmed by a specific analysis carried on HCN_1 expressing HEK293 cells, where it was demonstrated that, to exert its action, ZD7288 needs the channel to be open and is trapped by its closing (Shin et al 2001). In addition, the block of I_h by ZD7288 is significantly relieved by hyperpolarization, therefore the reduced affinity of the binding site for the blocker can be a result of a conformational change that occurs during membrane hyperpolarizaton (Harris and Constanti, 1995).
Ivrabradine is the only organic I_h blocker used in therapy, in particular for symptomatic treatment of chronic stable angina pectoris. It reduces heart rate via inhibition of HCN_4 channels, which role in regulating pacemaker activity in the sinoatrial node cells is crucial. Ivrabradine blocks HCN channels in a use-dependent manner by occupying a cavity below the channel pore and shows an IC_{50} between 2 and 3 µM (Bucchi et al., 2013).
Finally, QX-314, the quaternary derivative of lidocaine normally employed to abolish voltage-activated Na channels, completely blocks I_h in CA1 pyramidal cells (Perkins and Wong, 1995).

2.2. HCN channels

2.2.1. Structure

Each HCN subunit features six alpha-helical segments (referred to as S1-S6) forming a transmembrane channel core. The region forming the ion-conducting pore loop is between S5 and S6, while the ion selectivity filter is constituted by the pore region carrying the GYG motif between S5 and S6.
The S4 segment carries nine arginine or lysine regularly spaced at every third position (Chen et al., 2000); its resulting positive charge confers to it the role of voltage-sensitive domain.
All the voltage-dependent members of the pore-loop cation channel superfamily present positively charged S4 segments (Yu and Catterall, 2004), but while inward movement

of S4 charges leads to the closure of depolarization-activated channels, in HCN channel it triggers their opening.
Following S6 is a region called "cAMP-sensing domain" (CSD), formed by a cyclic nucleotide binding domain (CNBD) and a carboxyl terminus segment termed C-linker.
The CSD is needed in order to elicit a cAMP-induced positive shift of the voltage-dependent activation of HCN channels.

HCN channels commonly exist in both homomeric and heteromeric tetramer configurations *in vivo* (Chen et al., 2001; Much et al., 2003). The four subtypes of HCN channels exhibit distinct cAMP-sensitivity and activation kinetics: HCN_1 channels show the more positive threshold for activation, the fastest activation kinetics, and the lowest sensitivity to cAMP, while HCN_4 channels are slowly gating and strongly sensitive to cAMP. HCN_2 and HCN_3 have intermediate properties (Baruscotti et al., 2005; Santoro et al., 1998).

2.2.2. Tissue and subcellular expression

Studies at mRNA and protein levels have demonstrated distinct expression patterns in the central nervous system (CNS) of the four HCN subunits (Notomi and Shigemoto, 2004).
HCN_1 is mainly expressed in neocortex, hippocampus, cerebellar cortex and brain stem (Santoro et al., 2000). HCN_2 subunit is widespread throughout the brain with the highest expression in the thalamus, GPe and brainstem nuclei (Chan et al., 2011; Moosmang et al., 1999; Santoro et al., 2000). HCN_3 distributes sparsely with the lowest expression level in CNS, but is present in olfactory bulb, hypothalamus and SNc. The distributed pattern of HCN_4 is complimentary to HCN_1, and HCN_4 is selectively expressed in various thalamic nuclei and distinct neuronal populations of the basal ganglia and habenular complex (Moosmang et al., 1999; Poller et al., 2011; Santoro et al., 2000).
HCN channels have also been identified in peripheral neurons, such as the dorsal root and trigeminal ganglion neurons. All four HCN subunits and I_h have been identified in the dorsal root ganglion, with HCN_1 exhibiting the highest expression (Chaplan et al., 2003; Moosmang et al., 2001), and the majority of trigeminal ganglion neurons were immune-positive for HCN_1, HCN_2 and HCN_3 (Wells et al., 2007). In SNc DA neurons, only the mRNA of HCN_2, HCN_3 and HCN_4 were detected by using qualitative single-cell RT-mPCR or *in situ* hybridization (Franz et al., 2000). In accordance with the lack of HCN_1 subunit, native I_h recorded in SNc DA neurons show larger activation time constants and bigger cAMP sensitivity than their counterparts in hippocampal pyramidal neurons (Franz et al., 2000), suggesting that in this area I_h is mainly mediated by HCN_2-HCN_4 subunits.
The subcellular localization of HCN channels can be neuron-type-specific and can influence the effects that they exert on neuronal properties and activity.
For example, in neocortical and CA1 hippocampal pyramidal neurons, HCN_1 channels are concentrated in the apical dendrites, and channel density is much higher in the distal compared with the proximal dendritic span (Lörincz et al., 2002). This gradient has been shown to contribute to normalizing dendritic inputs arriving at different locations along the dendrite (Magee, 1998).

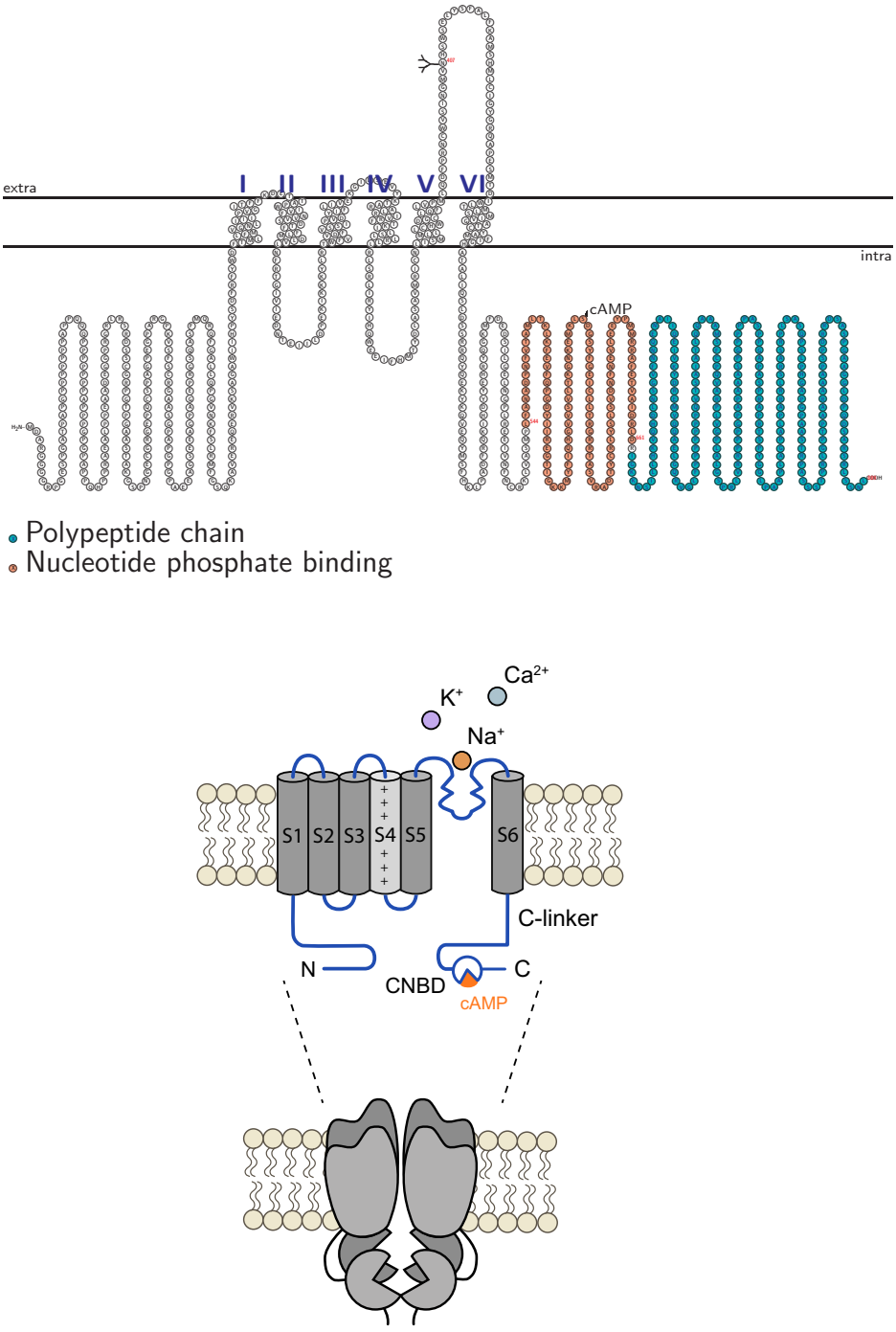

Figure 2.1.: Primary structure of human HCN_2 channel (top), generic structure of HCN channels (bottom)

In the interneurons of medial septum, hippocampus and cerebellum, all the HCN isoforms except for the HCN_3 are expressed at somatic and axonal regions, where they regulate membrane properties and influence neurotransmitters release (Bender and Baram, 2008). In the entorhinal cortex, localization of HCN_1 channels is prevalent in the axon terminal during development and their presynaptic expression and functions disappear with maturation. (Bender et al., 2007).
Interestingly, patterns of distribution of HCN_1 channels have been recently shown to depend on neuronal network activity: e.g. after the elimination of synchronized neuronal input to the distal dendrites of CA1 pyramidal neurons the gradient of HCN_1 channel distribution was abolished (Shin and Chetkovich, 2007).

2.3. Physiological roles of I_h in neural function

2.3.1. I_h and spontaneous activity

Given it activation near RMP and its non-activating properties, I_h exerts a depolarizing action on neural resting properties in many different cell types (Pape, 1996).
Activation of I_h around rests stabilizes membrane potential against hyperpolarization (Nolan et al., 2003; Stieber et al., 2003), while its deactivation antagonizes membrane depolarization (Magee, 1999).
In isolated thalamic cortical relay neurons the interaction between I_h and T-type calcium channels promotes a self-sustained intrinsic conductance driven oscillation (Yue and Huguenard, 2001). Up-regulation of I_h can alter the structure of oscillation by increasing the frequency and therefore producing an overall depression of activity; on the other hand I_h down-regulation has an opposite effect, leading to an enhancement of the network response deriving from a slowing of the oscillation (Yue and Huguenard, 2001).
Interactions between HCN channels and inwardly rectifying potassium channels (KIR) in pyramidal cell dendrites maintain I_h sufficiently high for its control of temporal summation (Day et al., 2005).
In rat interneurons of the stratum oriens/alveus of hippocampus, I_h inhibition causes a reduction in action potential frequency and a membrane hyperpolarization concomitant with an increased input resistance in current-clamp recordings (Maccaferri and McBain, 1996). Therefore, I_h can affect the excitability of these neurons in two ways: reducing the probability of cell firing induced by an excitatory stimulus and increasing the voltage change after a given amount of injected current because of the increased membrane input resistance.
In contrast, in rat cerebellar Purkinje neurons, I_h does not control the frequency of action potentials (Raman and Bean, 1999) but rather maintains the membrane potential within a range where the inward sodium current operates. As a consequence, tonic firing could persist even when challenged by several spontaneous inhibitory postsynaptic inputs (Häusser and Clark, 1997).

2.3.2. I_h role in synaptic transmission

It has been demonstrated that in invertebrate neurons, I_h increases excitatory synaptic release in a "non-ionic" way via a pathway involving actin depolymerization. These findings suggest that HCN channels might modulate synaptic release by triggering processes altering the cytoskeleton or modifying the terminal resistance or RMP, as demonstrated in cortical neurons postsynaptic dendrites (Beaumont et al., 2002).
In addition to their dendritic localization, HCN channels are also present on certain axons and synaptic terminals suggesting that I_h influences synaptic transmission. It has been shown that presynaptic I_h affects inhibitory synaptic transmission in rodents cerebellum, hippocampus and GP, but the underlying mechanism is still unknown (Huang et al., 2011).
Recently it has been demonstrated that in entorhinal cortical layer III pyramidal neurons, HCN_1 subunits colocalize with Cav3.2 T-type Ca^{2+} channel on synaptic terminals and depolarize RMP, restricting Ca^{2+} entry via T-type Ca^{2+} channel activity and preventing glutamate release.
I_h driven alteration of T-type Ca^{2+} channel activity has been also observed in hippocampal dendrites (Huang et al., 2011); therefore this might be a common mechanism by which these channels affect neuronal excitability.

2.3.3. I_h in dendritic integration

Great part of synaptic inputs are located within dendritic arbors, where inhibitory and excitatory signals are blended together to form a coherent output response.
While synaptic inputs are widely distributed across complicated dendritic arbors, the action potential output is confined in a relatively localized region of the soma or in the proximal axon (Colbert and Johnston, 1996).
Amplitude and temporal characteristics of signals can differ at the final integration site depending on variation in their synaptic distance, meaning that the effect of any given synapse on output depends upon its location (Mainen and Sejnowski, 1996).
Under passive conditions, the amplitude and kinetics of a given excitatory postsynaptic potential (EPSP) vary inversely with the distance of the synapse from the soma; thus, EPSPs from distal synapse will be smaller and slower than their proximal counterparts (Magee, 2000).
Location-dependent synaptic variability could interfere with a neuron's ability to accurately determinate the total amount of incoming synaptic activity or increase the variability of action potential discharge; therefore mechanisms for contrasting the dependence of synaptic summation on input location might be very advantageous.
I_h seems to be well suited to influencing the integration of subthreshold synaptic input: during synaptic activity, I_h deactivation by synaptic depolarization produces a hyperpolarizing current that tends to counterbalance the location-dependent kinetic (but not amplitude) filtering effects for a wide range of spatiotemporal input patterns (Magee, 1999; Williams and Stuart, 2000).
In neocortical and CA1 pyramidal neurons, HCN channels density is distributed as a gradient, reaching in dendrites a density nearly sevenfold bigger than the one observed in the soma (Pettit and Augustine, 2000; Sayer et al., 1990), and therefore producing a sustained hyperpolarization current which amplitude increases with the distance from

the soma.
This hyperpolarization gradient permits primarily proximal input to produce the same temporal output pattern as distal input, allowing the generation of a neuron's response largely reflecting the temporal pattern of the synaptic input.
With I_h blocked, neurons fires indiscriminately during both coincident and temporally dispersed input; therefore a spatially normalized temporal summation allows a neuron to lower the variability of action potential firing, improving the synchrony of neuronal population activity (Jaffe and Carnevale, 1999; Rinzel and Rall, 1974).

Chapter 3

Causes and pathogenesis of PD

3.1. Etiology of PD

Despite many years of focused research, the causes of this disease remain to be elucidated.

Age is an important risk factor for PD, however it remains unclear what precise role aging plays in pathogenesis. Even though the gradual loss of striatal dopaminergic markers (Kish et al., 1992; Scherman et al., 1989) and SNc neurons (Fearnley and Lees, 1991) with age has recently been confirmed, the pattern and timing of these losses differ from what occurs in PD, indicating that aging itself is not likely to play a direct role in the degenerative process. For example, although the number of dopaminergic terminals appears to decrease with age, this takes place with a different temporal and spatial pattern than occurs in PD (Scherman et al., 1989). The loss of DA neurons in aging is linear and predominantly in the dorsal tier of the SNc, whereas in PD it is exponential and predominantly in the lateral ventral tier (Fearnley and Lees, 1991; Scherman et al., 1989). In addition, the SNc in PD contains numerous reactive microglia, which are much less frequent in age-matched control brains, indicating an active destructive process that is not present in the normal aged brain (McGeer et al., 1988).

The relative contributions of genetic versus environmental factors regarding the cause of PD have been hotly debated.

The environmental toxin hypothesis, stating that PD-related neurodegeneration results from exposure to a dopaminergic neurotoxin, was dominant for much of the 20^{th} century. However, the discovery of PD genes has renewed interest in hereditary susceptibility factors. Both probably play a role.

The discovery that the protoxin n-methyl-4-phenyl-1,2,3,6-tetrahydropyridine (MPTP) causes a syndrome nearly identical to PD (Langston et al., 1983) in both humans and nonhumans is a prototypic example of how an exogenous toxin can mimic the clinical and pathological features of PD.

Other environmental toxins have been shown to induce a parkinsonian state as well, supporting this view (McCormack et al., 2002). However, the recent discovery of inherited forms of PD shifted the emphasis back to genetic factors.

Among the different genetic forms of PD, mutations in the gene encoding for α-

synuclein have received the most attention. Mutations in this gene cause rare forms of PD. Furthermore, α-synuclein is also present in the LBs, one of the PD markers.
Another possibility, which does not fit neatly into a genetic or environmental category, is that an endogenous toxin may be responsible for PD neurodegeneration. Distortions of normal metabolism might create toxic substances because of environmental exposures or inherited differences in metabolic pathways.

3.2. Pathogenesis of PD

Toxic PD models and the functions of genes implicated in inherited forms of PD suggest two major hypotheses regarding the pathogenesis of the disease. One hypothesis posits that misfolding and aggregation of proteins are instrumental in the death of SNc DA neurons, while the other proposes that the culprit is mitochondrial dysfunction and the consequent oxidative stress, including toxic oxidized DA species.
These hypotheses are not mutually exclusive, and one of the key aims of current PD research is to elucidate the sequence in which they act and whether points of interaction between these pathways are key to the demise of SNc DA neurons.

3.2.1. Misfolding and aggregation of proteins

Aggregated or unsoluble misfolded proteins could be neurotoxic through a variety of mechanisms. Protein aggregates could directly cause damage, perhaps by deforming the cell or interfering with intracellular trafficking in neurons. Protein inclusions might also sequester proteins that are important for cell survival. If so, there should be a direct correlation between inclusion formation and neurodegeneration.
A growing body of evidence, particularly from studies of Huntington disease and other polyglutamine diseases (Cummings et al., 1999; Saudou et al., 1998), suggests that there is no correlation between inclusion formation and cell death.
Cytoplasmic protein inclusions may not result simply from precipitated misfolded proteins but rather from an active process meant to sequester soluble misfolded proteins from the cellular milieu (Kopito, 2000).
Accordingly, inclusion formation, while possibly indicative of a cell under attack, may be a defensive measure aimed at removing toxic soluble misfolded proteins (Auluck et al., 2002; Cummings et al., 2001).
On the other hand, the ability of chaperones such as Hsp-70 to protect against neurodegeneration provoked by disease-related proteins (including α-synuclein-mediated dopaminergic neuron loss) is consistent with the view that soluble misfolded proteins are neurotoxic (Auluck et al., 2002; Muchowski, 2002). The possibility that protein aggregation may play a role in PD had long been suggested by the presence of LBs in disease brains. However, this concept was given powerful support upon discovery of the mutations in α-synuclein, the primary structural component of LBs fibrills.
Human α-synuclein was originally identified as a proteolytic fragment derived from Alzheimer senile plaques (Uéda et al., 1993). The isolated fragment, termed the non-αβ component (NAC), corresponded to a 35 aminoacid hydrophobic portion of α-synuclein, a domain responsible for aggregation (El-Agnaf et al., 1998b). NAC aggregates have been demonstrated to have cellular toxicity: they induce apoptotic death

in cultured human neuroblastoma cells (El-Agnaf et al., 1998a) moreover low concentrations of aggregated NAC are toxic to DA neurons in primary culture (Forloni et al., 2000) and *in vivo* application of α-synuclein oligomers induced death of SN DA neurons (Winner et al., 2011). Based on these demonstrations of the ability of α-synuclein and NAC to aggregate and the possible toxicity of aggregates, an abnormality of protein aggregation has become one of the principal hypotheses for the pathogenesis of PD.
In patients with inherited PD, pathogenic mutations are thought to cause disease directly by inducing abnormal and possibly toxic protein conformations (Bussell and Eliezer, 2001) or indirectly by interfering with the processes that normally recognize or process misfolded proteins.
In sporadic PD, there is a similar focus both on direct protein-damaging modifications and on dysfunction of chaperones or the proteasome that may indirectly contribute to the accumulation of misfolded proteins.
One trigger of protein aggregation may be oxidative stress.
The tissue content of abnormally oxidized proteins (which may misfold) increases with age (Beckman and Ames, 1998), and neurons may be particularly susceptible because they are postmitotic. In PD, LBs contain oxidatively modified α-synuclein, which *in vitro* exhibits a greater propensity to aggregate than unmodified α-synuclein (Giasson et al., 1999).
Cells respond to misfolded proteins by inducing chaperones, but if not properly refolded they are targeted for proteasomal degradation by polyubiquitination.
With aging, the ability of cells to induce a variety of chaperones is impaired as is the activity of the proteasome. Proteasomal dysfunction and the consequent accumulation of misfolded proteins may provoke a vicious cycle, with excess misfolded proteins further inhibiting an already compromised proteasome.

3.2.2. Free radicals and deficits in energy metabolism

The leading hypothesis for the neuronal degeneration observed in PD continues to be the free radical-mediated injury, also referred to as the "oxidant stress hypothesis" or the "endogenous toxin hypothesis".
Oxidative stress occurs when an imbalance is formed between production of reactive oxygen species (ROS) and cellular antioxidant activity.
DA neurons are particularly prone to oxidative stress because of four aspects of their neurochemistry and their local environment. First, DA degradation consists in its oxidative deamination by monoamine oxidase A (MAO-A) and B (MAO-B), two enzymes found in the outer membrane of mitochondria. As a consequence of this process, the enzymatic production of H_2O_2 can lead to the formation of highly reactive hydroxyl-radicals through non-enzymatic reactions with ferrous or cupric ions via Fenton-type reactions.
Second, DA can form quinines and semiquinones reacting nonenzimatically with oxygen, producing superoxide, hydrogen peroxide, and hydroxyl radicals. Third, the formation of hydroxyl radicals from H_2O_2 may be augmented in the SNr because of the high presence of iron of this region.
Fourth, neuromelanin generates from DA auto-oxidation and it may contribute to neurodegeneration by catalyzing ROS formation, through an interaction with iron, se-

lectively in pigmented neurons (Zecca et al., 2001).
Because of this intrinsic sensitivity to reactive species, a moderate oxidative stress can trigger a cascade of events that lead to cell demise. The major sources of such oxidative stress generated for the nigral DA neurons are thought to be the ROS produced during DA metabolism, mitochondrial dysfunction, and neuroinflammation.

DA metabolism

Although DA is normally stored in vesicles, excess cytosolic DA is easily oxidized both spontaneously and enzymatically to produce DA quinone.
The DA quinone species are capable of covalently modifying cellular nucleophiles, including low molecular weight sulfhydryls such as glutathione (GSH) and protein cysteinyl residues, whose normal functions are important for cell survival. Notably, DA quinone has been shown to modify a number of proteins whose dysfunctions have been linked to PD pathophysiology, such as α-synuclein, parkin, DJ-1, and UCH-L1. DA quinone covalently modifies α-synuclein monomer and promotes the conversion of α-synuclein to the cytotoxic protofibril form (Conway et al., 2001). The DA quinone-modified α-synuclein is not only poorly degraded but also inhibits the normal degradation of other proteins by chaperone-mediated autophagy (Martinez-Vicente et al., 2008).
Conversely, α-synuclein can bind to and permeabilize the vesicle membrane, causing leakage of DA into the cytosol (Lotharius and Brundin, 2002) and this would in turn induce DA quinone generation.
DA quinone has also been shown to cause inactivation of the DAT and TH (Kuhn et al., 1999). In addition, it leads to mitochondrial dysfunction (Lee et al., 2002) and swelling of brain mitochondria (Berman and Hastings, 1999). Accordingly, the subunits of Complex I and Complex III of the electron transport chain, whose dysfunction will deter mitochondrial respiration and cause ROS production, were also shown to be targets of DA quinone modification (Van Laar et al., 2009).
Furthermore, DA quinone can cyclize to become the highly reactive aminochrome, which ultimately polymerizes to form neuromelanin which, in turn, can exacerbate the neurodegenerative process by triggering neuroinflammation (Zecca et al., 2008).
Evidence of the existence of *in vivo* DA oxidation and its toxicity is also available. Higher levels of cysteinyl-catechol derivatives are found in postmortem nigral tissues of PD patients compared to age-matched controls, suggesting cytotoxic nature of DA oxidation (Spencer et al., 1998).

Mitochondrial dysfunction

The most direct evidence for disrupted mitochondrial metabolism has come from studies of autopsy tissue and other tissue samples and *in vitro* cell cultures derived from patients with PD. One finding at autopsy is that the activity of complex I, a major component of the electron transport chain, is decreased in the SN (Schapira et al., 1990) and frontal cortex (Parker et al., 2008) in patients with PD, and sophisticated immunocapture techniques have demonstrated increased oxidative damage and reduced electron transfer rates through complex I subunits in these individuals (Keeney et al., 2006).

Inhibition of complex I can impair ATP synthesis, making cells vulnerable to "weak excitotoxicity", which is proposed to result from changes in the energy-dependent cell membrane potential. It also induces an "energy crisis" *in vitro* and *in vivo* (Mizuno et al., 1988) and increases the production of the ROS superoxide, which may form toxic hydroxyl radicals or react with nitric oxide to form peroxynitrite. These molecules may cause cellular damage by reacting with nucleic acids, proteins, and lipids. One target of these reactive species may be the electron transport chain itself (Cohen, 2000), leading to mitochondrial damage and further production of ROS.
Several complex I inhibitors such as 1-methyl-4-phenylpyridinium (MPP^+) and rotenone, replicate some of the key motor features of PD and are used in PD neurotoxic models. For example, chronic infusion of the rotenone reproduces a parkinsonian syndrome in rats that is associated with selective loss of DA neurons and LBs-like fibrillar cytoplasmic inclusions containing ubiquitin and α-synuclein (Betarbet et al., 2000).
Mitochondrial dysfunction leads to increased oxidative stress. These findings provide a plausible link between oxidative damage and formation of LBs, as oxidative damage induces α-synuclein aggregation and impairs proteasomal ubiquitination and degradation of proteins (Jenner, 2003).
Mitochondria-related energy failure may also disrupt vesicular storage of DA. Cytosolic monoamines are accumulated in storage vesicles by the vesicular monoamine transporter (VMAT), an integral membrane protein embedded in synaptic vesicles membrane. This active transport is driven by a transmembrane pH and electrochemical gradient generated by the vesicular H^+-ATPase in the granule membrane; the inward transport of the monoamine is coupled with the efflux of two protons per monoamine (Parsons, 2000).
Two closely related vesicular monoamine transporters, VMAT1 and VMAT2 have been cloned, expressed and characterized. VMAT2 is primarily expressed in multiple monoaminergic cells in the brain, sympathetic nervous system, mast cells, and histamine containing cells in the gut (Erickson et al., 1996; Weihe and Eiden, 2000).
The lack of energy deriving from complex I inhibition may compromise the VMAT2-mediated antiport, causing the release of DA in the cytosol and allowing harmful DA-mediated reactions to damage cellular macromolecules.
Mitochondria also have an important role in the apoptotic cell death pathway. When the outer mitochondrial membrane is rendered permeable by the action of "death agonists", such as Bax, cytochrome c is released into the cytosol, leading to caspase activation and apoptosis (Chipuk and Green, 2004). Similar pathways are also activated by opening of the mitochondrial permeability transition pore, an event that can occur under conditions of oxidative stress or electron transport chain inhibition, leading to collapse of the mitochondrial membrane potential.

Neuroinflammation

Neuronal loss in PD is associated with chronic neuroinflammation, which is controlled primarily by microglia, the resident innate immune cells and the main immune responsive cells in the central nervous system. Microglial reaction has been found in the SN of sporadic PD patients (McGeer et al., 1988) as well as familial PD patients (Yamada et al., 1993) and in the SN and/or striatum of PD animal models elicited by MPTP (O'Callaghan and Miller, 1993).

Microglia are activated in response to injury or toxic insult as a self-defensive mechanism to remove cell debris and pathogens. When activated, they release free radicals such as nitric oxide and superoxide, which can in turn contribute to oxidative stress in the microenvironment.
Damaged neurons could release inflammatory signals and thus overactivate microglia, leading to induction of reactive microgliosis. The oxidized or ROS-induced molecules that are released from damaged nigral DA neurons and trigger microglial activation include neuromelanin and α-synuclein.
Insoluble extraneuronal neuromelanin granules have been observed in patients of juvenile PD (Ishikawa and Takahashi, 1998) and idiopathic PD, as well as those with MPTP-induced parkinsonism (Langston et al., 1999).
Intracerebral injection of neuromelanin caused strong microglia activation and a loss of DA neurons in the SN (Zecca et al., 2008). Neuromelanin appears to remain for a very long time in the extracellular space (Langston et al., 1999) and thus thought to be one of the molecules responsible for inducing chronic neuroinflammation in PD.

Chapter 4

Animal models of Parkinson's Disease

Animal models of PD can be divided into those using environmental or synthetic toxic molecules or those utilizing the *in vivo* expression of PD-related mutations (genetic models).
Toxic models represent the classic experimental PD models. They aim to reproduce the pathological and behavioural changes of the human disease in rodents or primates by using pharmacological agents that induce the selective degeneration of nigrostriatal neurons.
A common feature of all toxin-induced models is their ability to produce an oxidative stress and to cause cell death in DA neuronal populations that reflect what is seen in PD (see Table 4.1).

Among several neurotoxins used to induce nigrostriatal damage, only MPTP is clearly linked to a form of human parkinsonism, and it is thus the most widely studied model. Although toxic models of PD have provided an invaluable bulk of information on disease pathology, the lack of an age-dependent, slowly progressive lesion and the fact that LBs are typically not observed in these models represent major drawbacks. The discovery of monogenic "Mendelian" forms of PD has provided considerable insights into the disease pathogenesis and the recent burst of genomewide association studies has provided evidence that familial and sporadic forms of PD may share common genetic backgrounds. Recently, the identification of different genetic mutations such as α-synuclein, parkin, LRKK2, PINK1 and DJ-1 has prompted the development of genetic models of PD (see Table 4.2).
One strength of the genetic models is that they are primarily based on identified

Model	Behavioral symptoms	Nigrostrital damage	α-syn aggregation/LB	Disadvantages
6-OHDA	Rotational behavior after unilateral injection	Loss of DA innervation at injection site (striatum)	No inclusions	Requires intracerebral injection, very little synuclein involvement.
MPTP/MPP$^+$	Motor impairments in primates	Specific nigrostriatal degeneration and reduced DA levels in striatum nonhuman primates	Few cases of synuclein aggregation in	Nonprogressive model of cell death. Inclusiones are rare.
Rotenone	Reports of decreased motor activity in rodents	Loss of DA neurons and reduced DA innervation in striatum	Synuclein aggregation in DA neurons	Substantial morbidity and mortality.
Paraquat	No clear motor deficits	Decreased striatal TH immunoreactivity	No inclusions present	Effects in other neurotransmitter systems.

Table 4.1.: Principal characteristic of toxic models of PD

Model	Behavioral symptoms	Nigrostrital damage	α-syn aggregation/LB	Disadvantages
α-synuclein	Severe motor deficits in the A53T model, less in A30P model	Generally no neuron degeneration observed	α-synuclein aggregates in DA neurons (A53T model)	No DA neuron death observed
LRRK2	Few motor deficits observed in Drosophila model	Minimal levels of degeneration in mutation models	Generally not observed	Lack of neurodegeneration and α-synuclein aggregates
DJ-1	No changes in basic motor activity. Slight hypoactivity	Generally no neuron degeneration observed	Generally not observed	Lack of neurodegeneration and α-synuclein aggregates
PINK1	Gait alterations and olfactory dysfunctions	Generally no neuron degeneration observed	Generally not observed	Lack of neurodegeneration and α-synuclein aggregates
MitoPark	Decreased locomotion, tremors, limb rigidity	Selective nigrostriatal neurodegeneration	Inclusions lacking α-synuclein	Not based on human genetic mutation

Table 4.2.: Principal characteristic of genetic models of PD

targets associated with potential mechanisms known to cause PD in humans (Bezard and Przedborski, 2011; Meredith et al., 2008a). However, currently available models do not display appreciable neurodegeneration and phenotypes (Dawson et al., 2010).

4.1. The MitoPark mouse

The MitoPark mouse model was designed to directly test the hypothesis that mitochondrial dysfunction in DA neurons can cause a progressive parkinsonian phenotype. The model is based on the specific inactivation of a gene coding for a protein required for both transcription and maintenance of mitochondrial DNA. This mutation leads to a decreased mitochondrial transcription with consequent respiratory chain failure; the expression of the cre-recombinase under the DAT promoter restricts this effect to DA neurons only.
Among all PD animal models, MitoPark is the only one that reproduce typical aspects of the disease like the delayed onset and progressive course of symptoms, allowing the assessment of the extent and type of DA neuron dysfunction occurring before the onset of behavioral deficits.
Although after 6 weeks mitochondrial DNA expression is dramatically reduced and inclusions lacking α-synuclein start appearing; the onset of nigrostriatal death, decreased locomotion and reduced exploratory behavior starts only after 12-14 weeks. As in PD, L-DOPA is able to improve motor performance and its effect weakens as the animals age.
Regarding the neurodegeneration, SNc DA neurons of MitoPark mice degenerate before those in the VTA, a condition found also in PD.
Motor symptoms progress and at 20 weeks the mice display more evident phenotypic manifestation like tremors and limb rigidity (Ekstrand and Galter, 2009). Albeit MitoPark mice has to be sacrificed after 45 weeks, this animal model provides a 30 week time window where the progression of the disease can be studied.

4.2. Toxin-treated models

4.2.1. 6-hydroxydopamine

6-OHDA is a hydroxylated analogue of DA that, because of the structural similarity with DA and high affinity for DAT, accumulates specifically in catecholaminergic neu-

rons, where it causes DA and norepinephrine depletion and inflicts structural damage to these neurons. Once in the cytosol, it generates ROS and quinones that inactivate some biological macromolecules by binding to their nucleophilic groups (Saner and Thoenen, 1971). Available evicences suggest that the dominant neurotoxic action is driven by ROS production after 6-OHDA auto-oxidation (Graham et al., 1978; Jonsson, 1980). In *in vivo* experiments, local administration is required because the toxin doesn't cross the blood-brain barrier (BBB) and the injection sites are preferably the medial forebrain bundle, SNc and striatum (Javoy et al., 1976). An injection in the latter brain region leads to a prompt damage of striatal terminals, followed by delayed, progressive cell loss of DA neurons due to a dying back mechanism. This lesion is highly reproducible and, after 4-5 weeks, the maximum level of DA neuron loss reaches 50 % to 70 % (Blandini et al., 2007). Within the ventral midbrain DA neuronal group, the highest loss is found in SNc, followed by retrobulbar field and VTA (Rodríguez et al., 2001).
When 6-OHDA is injected unilaterally, with the contralateral side serving as internal control, it induces typical stereotypies like asymmetric circling behavior in response to the stimulation of striatal DA receptors (Ungerstedt, 1971); over the years the circling behavior has been quantified and used to verify antiparkinsonian properties of new drugs.

4.2.2. Rotenone

Rotenone is a highly lipophilic flavonoid that easily crosses the BBB and freely diffuses into cells. Once inside them, it binds and inhibits mitochondrial complex I, causing formation of ROS and inhibiting proteasome activity. In rats it produces selective nigrostriatal degeneration and is the only PD toxic model where LBs-like cytoplasmic inclusions containing both ubiquitin and α-synuclein are reported (Betarbet et al., 2000). Since the toxin freely enters into all cells, the nigrostriatal cell death suggested that DA neurons are more susceptible to complex I poisoning. Rat injected intraperitoneally with rotenone develop classical PD motor symptoms as bradykinesia, postural instability and/or rigidity, which can be reversed by apomorphine (Cannon et al., 2009).
Rotenone is considered as a milestone among PD experimental models because of the crucial insights it provided into the mitochondria-related DA neurodegeneration and the link between an environmental toxin to the pathologic hallmark of α-synuclein aggregation. On the other hand, several studies have highlighted some critical issue such as the high variability of the nigrostriatal lesion magnitude, the mortality associated with the unspecific accumulation of the toxin and, most of all, the fact that cronically injected rotenone induced a more widespread neurotoxicity, challenging the concept that DA neurons display preferential sensitivity to complex I (Höglinger et al., 2003).

4.2.3. Paraquat

Paraquat is an herbicide that has been associated with an increased risk for PD (Liou et al., 1997).
Being a charged molecule, it doesn't cross the BBB (Shimizu et al., 2001) and it's be-

lieved to enter the brain via a neutral aminoacid transporter; the toxin is then carried inside the neurons by a sodium dependent transport, independently of DAT.
Given the low affinity of paraquat to mitochondrial complex I, its main toxic action consists in superoxide radicals formation (Day et al., 1999). When injected systemically in mice, it leads to DA SNc neuron degeneration accompanied by α-synuclein containing inclusions; although DA cell loss is moderate (20 % to 30 %) paraquat is able to reduce motor activity and induce a dose-dependent loss of striatal dopaminergic nerve fibers without a substantial decrease of striatal DA.

4.2.4. The MPTP/MPP$^+$ model

In 1982 young drug addicts developed an idiopathic parkinsonian syndrome after intravenous injection of an analogue of the narcotic meperidine containing MPTP. After investigating the causes of their condition, it was found that the toxin was the neurotoxic contaminant responsible for the parkinsonian effect.
In humans and monkeys, MPTP produces an irreversible and severe parkinsonian syndrome characterized by the major features of PD, including tremor, rigidity, slowness of movement, postural instability, and freezing. In MPTP-intoxicated humans and nonhuman primates, the beneficial response to levodopa and the development of dyskinesias after treatment are virtually identical to that seen in PD patients. Also similar to PD, the susceptibility to MPTP increases with age in both monkeys and mice (Irwin et al., 1993; Ovadia et al., 1995; Rose et al., 1993).
This model has also been used for electrophysiological studies, leading to important findings such as the use of deep brain stimulation, which is currently the best surgical method to ameliorate symptoms in PD patients.
As in PD, monkeys treated with low-dose MPTP exhibit preferential degeneration of putamenal versus caudate dopaminergic nerve terminals (Moratalla et al., 1992). In addition MPTP leads to a relatively greater cell loss in the SNc than the VTA and to a preferential loss of neurons in the ventral and lateral segments of the SNc (Sirinathsinghji et al., 1992; Varastet et al., 1994); this regional pattern is also found in MPTP-treated mice (Muthane et al., 1994; Seniuk et al., 1990). Also reminiscent of PD (Hirsch et al., 1988), dopaminergic neurons that contain neuromelanin are more susceptible to MPTP-induced degeneration (Herrero et al., 1993b).
One big limitation of the MPTP model is that it doesn't include two characteristic features of PD. First, neurons are not consistently lost from other monoaminergic nuclei, such as the locus coeruleus (Forno et al., 1993, 1986), second, although intraneuronal inclusions resembling LBs have been described (Forno et al., 1986), classical LBs have not been demonstrated convincingly in the brains of MPTP-intoxicated patients or monkeys (Forno et al., 1993). These cases were exposed to acute regimens of MPTP, so the lack of LBs-like formation in MPTP-intoxicated humans and monkeys may reflect the fact that in these cases DA neurons were rapidly injured. Chronic infusion of rotenone, another complex I inhibitor, does produce intraneuronal α-synuclein-containing proteinacious aggregates (Betarbet et al., 2000), consistent with the possibility that the speed of intoxication may influence the subsequent neuropathologic features.

4.2.5. Mechanisms of action of MPTP/MPP$^+$

MPTP is highly lipophilic pro-toxin and after systemic administration crosses the BBB within minutes (Markey et al., 1984). Once in the brain MPTP is oxidized to 1-methyl-4-phenyl-2,3-dihydropyridinium (MPDP$^+$) by MAO-B in glia and serotonergic neurons, the only cells that contain this enzyme. It is then converted to 1-methyl-4-phenylpyridinium (MPP$^+$) (probably by spontaneous oxidation), its active toxic metabolite, and released by into the extracellular space via the organic cation transporter 3 (OCT-3).
Since MPP$^+$ is a polar molecule, it depends on the plasma membrane carriers to enter cells. MPP$^+$ is a high-affinity substrate for the DAT, as well as for norepinephrine and serotonin transporters (Javitch et al., 1985; Mayer et al., 1986).
Surprisingly, the highest levels of MPP$^+$ are found in the adrenal medulla without causing the loss of chromaffin cells (Reinhard et al., 1987).
Pharmacological blockade or genetic deletion of DAT prevents MPTP-induced dopaminergic death (Bezard et al., 1999; Javitch et al., 1985), demonstrating the importance of the transporter in MPTP neurotoxicity. However, uptake by DAT does not entirely explain the selectivity of the nigrostriatal dopaminergic lesion caused by MPTP. While there are quantitative differences in DAT expression between more susceptible SNc neurons and less susceptible VTA neurons in monkeys (Haber et al., 1995), differences in DA uptake activity of comparable magnitudes between rats and mice and among mouse strains do not correlate with differences in MPTP sensitivity (Giovanni et al., 1991, 1994).

Once inside the neuron, MPP$^+$ can follow at least three routes:

1. it can bind to VMAT2, which translocates MPP$^+$ into synaptosomal vesicles (Liu et al., 1992)

2. it can be concentrated within the mitochondria by a mechanism that relies on the mitochondrial transmembrane potential (Ramsay and Singer, 1986)

3. it can remain in the cytosol to interact with cytosolic enzymes, especially those carrying negative charges (Klaidman et al., 1993).

Vesicular sequestration of MPP$^+$ appears to protect cells from MPTP-induced neurodegeneration by sequestering the toxin and preventing it from accessing mitochondria, its likely site of action. The importance of vesicular sequestration has been established by a number of experiments, including those showing that cells transfected to express greater density of VMAT2 are converted from MPP$^+$-sensitive to MPP$^+$-resistant cells (Liu et al., 1992) and that heterozygous VMAT2 null mice display enhanced sensitivity to MPTP-induced neurodegeneration (Takahashi et al., 1997). It appears that the ratio of DAT to VMAT2 expression predicts the likelihood of neuronal degeneration both in PD and the MPTP model. For instance, the putamenal dopaminergic terminals, which are most severely affected by both MPTP and PD, have a higher DAT/VMAT2 ratio than those in the caudate, which are less affected (Miller et al., 1999).
However consequences of MPP$^+$ vesicle storage is not only protective, in fact MPP$^+$ is thought to expel DA into the outer intercellular space where it can be metabolized into

a number of toxic metabolites.
Once inside the mitochondria, MPP^+ impairs oxidative phosphorylation by inhibiting the complex I (Nicklas et al., 1985), rapidly leading to a decrease in tissue ATP levels, particularly in the striatum and ventral midbrain (Chan et al., 1991; Fabre et al., 1999).
Another early effect deriving from hampering the flow of electrons through complex I may be ROS production. The importance of ROS in MPTP-induced neurodegeneration is confirmed by the finding that mice transgenic for superoxide dismutase-1 (SOD1), a key ROS scavenging enzyme, are resistant to MPTP-induced toxicity (Przedborski et al., 1992). More recent studies conducted in mice have confirmed a key role for ROS, as critical effectors in MPTP toxicity (Przedborski and Vila, 2003).
Alterations in energy metabolism and generation of ROS peak within hours of MPTP administration, days before overt neuronal death is observed (Jackson-Lewis et al., 1995). Therefore, these initial events are not likely to directly kill most cells but rather set into play downstream cellular events that ultimately kill most dopaminergic neurons (Mandir et al., 1999; Saporito et al., 2000; Vila et al., 2001).
Prolonged administration of low to moderate doses of MPTP to mice leads to morphologically defined apoptosis of SNc DA neurons (Tatton and Kish, 1997). In this study, during the MPTP application, it has been observed an upregulation of Bax, a potent agonist of programmed cell death (PCD) that triggers the release of cytochrome c and the consequent activation of caspases 9 and 3; in parallel all these effects were followed by a downregulation of Bcl-2, a PCD antagonist. Consistent with these findings, Bax null and Bcl-2 transgenic mice are both resistant to MPTP neurotoxicity Offen et al. (1998); Vila et al. (2001); Yang et al. (1998).
The mechanism by which MPTP provokes these changes in Bcl-2 family in not fully understood, however MPTP-induced oxidation of DNA could be important for both Bax translocation via JNK pathway and Bax induction via p53 activation (Mandavilli et al., 2000; Mandir et al., 1999).
Furthermore p53 null mice are resistant to MPTP-induced neurodegeneration (Trimmer et al., 1996) and pharmacological blockade of JNK results in marked attenuation of MPTP-induced SNc DA neuronal death (Saporito et al., 1999).

4.3. Unanswered issues in the mitochondrial hypothesis

Converging evidences coming from both genetic and toxin-based models point to an involvement of mitochondrial disfunction in PD development. In spite of the general consensus over the relevance of mitochondrial function in nigrostriatal degeneration underlying PD, several studies have shown that mitochondrial impairment and ROS production don't fully explain DA neuron loss and fail to account for some critical histopathological features found in both experimental and spontaneous PD. For instance, Choi and his collaborators have demonstrated that in primary mesencefalic cultures obtained from mice deficient for a protein essential for correct assembly and function of complex I ($Ndufs4^{-/-}$), basal death of DA neurons was unaffected (Choi et al., 2008). Moreover such cells still retained vulnerability to paraquat and MPP^+ toxic action. Surprisingly, these dopaminergic neurons were more sensitive to rotenone, whereas an already compromised complex I would make these cell resistant accord-

ingly to its toxic mechanism of action.
Since the doses of rotenone used did not alter mitochondrial oxygen consumption in isolated brain mitochondria (Betarbet et al., 2000), it did not appear that a bioenergetic defect could account for rotenone-induced neurodegeneration. In addition, dose-response experiments with rotenone indicated a greater effect on DA neuron toxicity than on complex I activity, moreover the hypothesis of selective nigrostriatal damage due to the interaction between mitochondrial- and DA-dependent ROS production doesn't explain why DA VTA neurons are relatively more spared than SN.
Such findings strongly suggest that complex I inhibition is not primarily responsible for MPP^+, rotenone and paraquat toxicity within DA neurons and, most of all, suggest that alternative targets could explain the selectivity of toxic action among different midbrain DA populations.

Part II.

Aim of the thesis

Chapter 5

Aim of the thesis

The aim of this PhD project was to investigate the early effects of the parkinsonian toxin MPP^+ on the neurophysiological properties of midbrain DA neurons, focusing on actions that do not dependent on mitochondrial complex I impairment. To this aim, whole-cell patch clamp and extracellular single-unit recordings were obtained from SNc and VTA DA neurons in acute midbrain slices.

Part III.

Methods

Chapter 6

Methods

6.1. Animals

Animals were purchased from Harlan Italia (Milan, Italy). Housing, handling and killing were in compliance with the European and Italian legislation (DL 116/92). All studies involving animals are reported in accordance with the ARRIVE guidelines for reporting experiments involving animals (Kilkenny et al., 2010; McGrath et al., 2010). Juvenile (2–3 weeks, $n = 119$), adult (8 weeks, $n = 5$) Wistar Han rats and C57/BL6 mice (8 weeks, $n = 8$) were used.
To better distinguish DA neurons, transgenic mice carrying the green fluorescent protein (GFP) under the TH promoter were used ($n = 5$). The generation of these mice (TH-GFP/21-31) has been described by Sawamoto et al. 2001 and Matsushita et al. 2002. The transgene construct contained the 9.0 kb 5'-flanking region of the rat TH gene, the second intron of the rabbit β-globin gene, cDNA encoding GFP, and polyadenylation signals of the rabbit β-globin and simian virus 40 early genes. Transgenic mice were identified by using PCR to detect tail DNA bearing the GFP sequence. Transgenic lines were maintained by breeding these animals to C57BL/6J inbred mice.

6.2. Midbrain slices preparation

Animals were killed by decapitation under anaesthesia with isoflurane. Brains were removed and mounted in the slicing chamber of a vibroslicer (Leica VT 1000S, Leica Microsystems, Wetzlar, Germany). Horizontal slices (250 µm in thickness) were cut from midbrain and hippocampi in chilled artificial CSF (aCSF) saturated with 95 % O_2/5 % CO_2 containing (in µM) 130 NaCl, 3.5 KCl, 1.25 NaH_2PO_4, 25 $NaHCO_3$, 10 glucose, 2 $CaCl_2$ and 2 $MgSO_4$. Slices were allowed to recover in the same solution maintained at 34 °C with constant oxygenation for 1 h prior to experiments.

6.3. The patch-clamp technique

The patch-clamp technique, invented by Erwin Neher and Bert Sakmann in 1976, consists of patching the tip of a pipette filled with a physiological solution to the

membrane of a cell, maintaining it at a specific voltage to measure currents flowing through ion channels. Alternatively the experimenter can control the current injected into the cell through the recording electrode, measuring its potential.
There are five different configurations of patch clamping: "whole-cell", "cell-attached", "inside-out", "outside-out" and "perforated". Among them the less invasive is the cell-attached configuration, where the patch electrode is sealed to the membrane (reaching an electrical resistance in the order of a GΩ), leaving the cell intact and allowing the recording of currents through single ion channels. The whole-cell configuration is obtained with the rupture of the seal, allowing the pipette to became continuous with the membrane.
If after the formation of the gigaseal the pipette is quickly withdrawn from the cell, the piece of membrane inside of it will be exposed to the extracellular media (inside-out configuration). Pulling the membrane from both sides of a whole-cell configured patch in order to let the external faces being in contact with the external solution will result in the outside-out configuration.
During whole-cell recordings an irreversible washout of diffusible intracellular constituents (e.g. ATP, phosphorylating molecules ect.) into the relatively larger volume of the pipette through dialysis can occur. As a consequence, properties and functions of ion channels can be impaired, leading to a decrease of ionic currents over time.
The permeabilized-patch whole-cell configuration overcame this problem by accessing the intracellular space not by seal rupture but by forming pores thanks to a pipette solution containing antibiotics. In this way the dialysis is much more slower and the intracellular environment is preserved for long recordings.

6.4. Electrophysiology

Patch pipettes were made from thin-walled borosilicate capillaries (Harvard Apparatus, London, UK) with a vertical puller (Narishige PP830, Narishige International Ltd, London, UK) and back-filled with an intracellular solution containing (in mM) K^+ gluconate (120), KCl (15), HEPES (10), EGTA (5), $MgCl_2$, (2), Na_2PhosphoCreatine (5), Na_2GTP (0.3), MgATP (2), resulting in a resistance of 3 MΩ to 4 MΩ in the bath. This solution was used for both cell-attached and whole-cell recordings. During whole-cell voltage clamp recordings access resistance was monitored throughout experiments with short, −10 mV steps. Recordings undergoing a variation in access resistance ∼10 % were discarded. No whole-cell compensation was used. Signals were sampled at 10 kHz, low-pass filtered at 3 kHz, acquired with an Axon Multiclamp 700B and digitized with a Digidata 1440A and Clampex 10 (Axon, Sunnyvale, CA, USA).
The recording chamber was mounted on an upright microscope (Nikon Eclipse E600 FN, Nikon Corporation, Tokyo, Japan) equipped with infrared-differential interference contrast optics and an infrared camera (Hamamatsu, Arese, Italy) for visually guided experiments. Once positioned in the recording chamber, slices were bathed with oxygenated aCSF maintained at 33–34 °C with a TC344B temperature controller (Warner, Handen, CT, USA). Flow rate was 1 ml/min and driven by gravity. Solution exchange was achieved with a remote-controlled Hamilton MVP line switch (Hamilton Bonaduz AG, Bonaduz, Switzerland). Patch pipettes were made from thin-walled borosilicate capillaries (Harvard Apparatus, London, UK) with a vertical puller

(Narishige PP830, Narishige International Ltd, London, UK) and back-filled with an intracellular solution containing (in mM) K^+ gluconate (120), KCl (15), HEPES (10), EGTA (5), MgCl2, (2), Na2PhosphoCreatine (5), Na2GTP (0.3), MgATP (4), resulting in a resistance of 3–4 MΩ in the bath. This solution was used for both cell-attached and whole-cell recordings. During whole-cell voltage clamp recordings access resistance was monitored throughout experiments with short, −10 mV steps. Recordings undergoing a variation in access resistance ∼10 % were discarded. No whole-cell compensation was used. Signals were sampled at 10 kHz, low-pass filtered at 3 kHz, acquired with an Axon Multiclamp 700B and digitized with a Digidata 1440 A and Clampex 10 (Axon, Sunnyvale, CA, USA). For the analysis of the effect on firing rate and potential, average values were calculated from 30 s frames immediately before and after 5 or 10 min of application of, respectively, MPP^+ and ZD7288. For recordings of eEPSPs in SNc, a tungsten bipolar stimulation electrode (FHC, Bowdoin, ME, USA) was placed in proximity of the STN and used to deliver trains of depolarizing stimuli (pulse frequency = 20 Hz, duration = 20 ms, amplitude = 5–15 mV generated with a computer-controlled isolated stimulator (Digitimer, Welwyn Garden City, UK). In the hippocampus, stimulation electrode was inserted in the stratum radiatum and used to elicit eEPSPs in CA1 pyramidal neurons as described for the SNc. EPSPs recordings in VTA were performed on midbrain slices from TH-GFP/21-31 mice and only GFP-positive were patched; the stimulation electrode was inserted locally. Membrane potential was maintained at −55 to −60 mV (SNc and VTA) or −65 to −70 mV (CA1) by injecting negative current, to prevent the firing of action potentials during eEPSPs trains. eEPSPs were generated under pharmacological block of NMDA and $GABA_A$ receptors with, respectively, D-AP5 50 µM and gabazine 10 µM or bicuculline 10 µM. During summation experiments, I_h was elicited with negative voltage steps (−20 mV) from −55 mV (SNc) and −65 mV (CA1).

Paired pulse recordings were performed stimulating with a bipolar electrode the STN every 15 s, generating pairs of EPSCs at 20 Hz in SNc neurons in presence and absence of 20 µM ZD7288. Inhibitory postsynaptic currents (IPSCs) were abolished by 5 min of 10 µM bicuculline pre-application. Paired pulse ratio (PPR) was calculated dividing the amplitude of the second EPSC over the first.

To produce an increased and maintained frequency of spontaneous EPSCs in SNc DA neurons, midbrain slices were challenged with 100 µM 4-AP and 10 µM bicuculline.

6.5. Drugs and chemicals

All drugs were bath-applied unless otherwise indicated. MPP^+ iodide (Sigma, Milan, Italy) was dissolved in water to 100 mM and used at 1–100 µM. Other drugs used were: ZD7288 (Tocris, 100 µM in water, used at 20-30 µM; Bristol, UK); rotenone (Sigma, 10 µM in dimethylsulfoxide (DMSO), used at 1 µM); glybenclamide (Sigma, 100 µM in DMSO, used at 10 µM); GBR12783 (Tocris, 5 mM in water, used at 5 µM); sulpiride (Sigma, 10 mM in ethanol, used at 10 µM); D-AP5 (Abcam, 100 mM in water, used at 50 µM; Abcam Biochemicals, Bristol, UK); gabazine (Abcam, 10 mM in water, used at 10 µM); bicuculline (Tocris, 20 mM in DMSO, used at 10 µM; Bristol, UK); 4-AP (Sigma, 100 mM in water, used at 100 µM); cAMP (Sigma, 100 mM in water, used at 100 µM in pipette solution); IBMX (Sigma, 50 mM in DMSO, used at 1 mM in pipette solution

with cAMP). cAMP was allowed to diffuse for 5 min before MPP^+ application.

6.6. Data analysis and statistic

Pooled data are presented as mean ± SEM of n independent experiments. Unless otherwise specified, statistical difference between means is assessed with a Student t-test for paired samples (Origin 8.1 and Graphpad Prism, Microcal, Northampton MA, USA/ La Jolla, CA, USA).
Significance at the $p < 0.05$, 0.01, 0.001 and 0.0001 level is indicated with *, **, ***, ****, respectively in figures. When single recordings are shown, they are intended to represent typical observations. Capacitance transients occurring during voltage steps, never compensated for during recordings, were graphically removed from all traces displayed in figures. Holding current was measured at −55 mV, while input resistance was determined with short (200 ms), −10 mV steps from holding. For activation curves, tail currents at −135 mV were normalized, plotted against pre-pulse potential (−45 to −135 mV) and fitted with a Boltzmann equation: $y = A_2 + (A_1 - A_2)/(1 + e^{(x-x_0)\cdot x})$. For the concentration–inhibition curve, the effect of MPP^+ on I_h elicited at −75 mV was plotted against concentration (1–100 µM). The fitting curve was obtained with a Logistic equation: $y = A_2 + (A_1 - A_2)/1 + (x - x_0)^p$. To quantify the effect of MPP^+ on the kinetic properties of I_h , currents elicited at −95, −115 and −135 mV were fitted with a double exponential: $y = y_0 + A1 \cdot e^{-x/t_1} + A2 \cdot e^{-x/t_2}$. The same equation was used to fit depolarization after the sag elicited with −200 pA current steps. The ratio eEPSP5/eEPSP1 was considered to compare temporal summation in control, MPP^+, MPP^+ + ZD7288, bicuculline and ZD7288. To avoid biases, recordings were only included in the analysis when the amplitude of eEPSP1 was stable. Traces in Figure 7.8 were baseline-adjusted to appreciate changes in summation.
Paired pulse ratio (PPR) was calculated dividing the amplitude of the second EPSC over the first.
Spontaneous EPSCs were analyzed using Clampfit 10 (Axon, Sunnyvale, CA, USA). Graphs, histograms and fittings were generated in Origin 8.1.

Part IV.

Results

Chapter 7

Results

7.1. MPP^+ causes rapid, ATP-independent, hyperpolarization and reduction of spontaneous activity in SNc DA neurons

SNc DA neurons were identified on the basis of their morphology (Figure 7.1A) and electrophysiological profile. Typical DA neurons display slow (2 Hz to 3 Hz) and regular autonomous firing activity (Figure 7.1B), and a rebound potential (sag) in response to hyperpolarizing current pulses (Figure 7.1C). In voltage clamp, slow-activating inward currents developed in response to hyperpolarizing potentials that were fully abolished by 20 µM ZD7288, a selective blocker of I_h (Figure 7.1D).
Midbrain neurons with such properties were challenged with MPP^+ 50 µM in bath application and recorded in whole-cell and cell-attached configurations. This concentration was comparable with midbrain MPP^+ levels detected by HPLC after a standard MPTP injection schedule of experiments *in vivo* (Jackson-Lewis and Przedborski, 2007).

In presence of MPP^+ 50 µM the spike rate of spontaneously firing cells dropped from 2.13 ± 0.12 Hz to 0.90 ± 0.14 Hz, (-58.0 ± 0.9 %, n = 13, $P = 7.8 \cdot 10^{-7}$, Figure 7.2A,B . In addition to a reduction of the firing rate, a substantial hyperpolarization of the membrane potential (measured from current clamp signatures as shown in Figure 7.2A, bottom) was observed (-55.28 ± 3.46 mV vs. -61.99 ± 3.50 mV, $n = 8$, $P = 0.002$, Figure 2A, B). These effects were rapid and fully developed in 5 min. A series of other parameters were measured, in control conditions and in presence of MPP^+, from current clamp protocols as the one shown in Figure 7.2A (bottom): firing threshold, rate of rise, action potential amplitude, sag amplitude and after-sag depolarization kinetics. These values are summarized in Table 1.
To test the effect of longer MPP^+ incubation, we used cell-attached recordings, in which the integrity of cell membrane and intracellular fluid are preserved (Figure 7.2 C). In line with whole-cell recordings, the effect of MPP^+ reached a first plateau within the first 5 min of application. Afterwards, after 15 min to 20 min of continuous application, silencing of spontaneous activity was generally observed, as shown for the example (Figure 7.2 C, top).
The inhibition of spontaneous firing of SNc DA upon acute administration of MPP^+

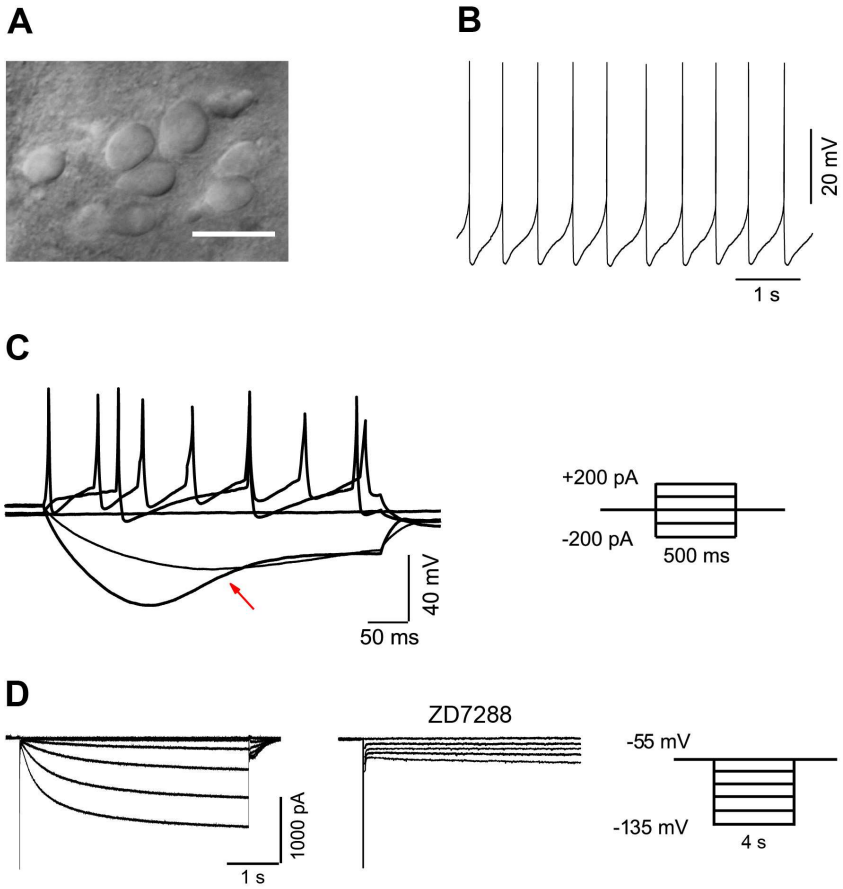

Figure 7.1.: Identification of putative SNc DA neurons within SNc in rat midbrain slices. (A) Infrared image of a microscopic field showing DA neurons (scale bar = 20 µm). (B, C) Whole-cell voltage recordings showing typical electrophysiological features of SNc DA neurons: slow and regular pace making (B) and a pronounced rebound depolarization, termed "sag", following injection of negative current (red arrow) (C). (D) Currents elicited with 4 s hyperpolarizing voltage steps from −55 mV (V_{HOLD}) to −135 mV in 20 mV increments. These currents are fully abolished by 30 µM ZD7288.

was already described before and explained as a consequence of complex I impairment and ensuing fall of cellular ATP levels (Liss et al., 2005). Reduced ATP levels lead to activation of K_{ATP} channels, membrane hyperpolarization and, eventually, cessation of firing activity.

On these premises, we tested the involvement of K_{ATP} channels on the early effects of MPP$^+$ application. Preincubation with the K_{ATP} blocker glybenclamide (10 µM) did not prevent, or dampen, the rapid drop in firing rate (2.34 ± 0.48 Hz vs. 1.18 ± 0.71 Hz, $n = 5$, $p = 0.006$, Figure 7.2 C, bottom left). In addition, the reduced ATP levels were counterbalanced by 2 mM MgATP of the intracellular solution. On the other hand, application of 30 µM ZD7288 induced a decay of firing activity, similar in extent to that induced by MPP$^+$ (2.18 ± 0.31 Hz vs. 1.50 ± 0.25 Hz, −31.20 %, $n = 4$, $p = 0.017$ vs. control, $p = 0.28$ vs. MPP$^+$, Figure 7.2 C, bottom right).

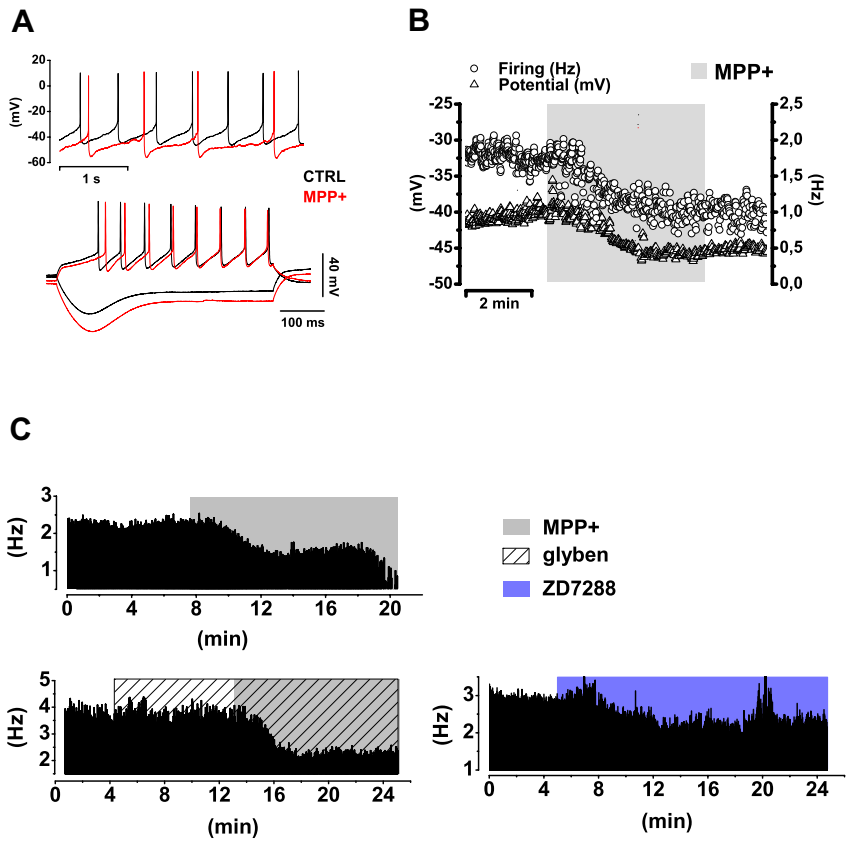

Figure 7.2.: MPP+ produces a rapid, K_{ATP} channel-independent hyperpolarization and reduction of the firing rate in SNc DA neurons. (A) Top, illustrative whole-cell current clamp recording from an SNc DA neuron before (black) and after (red) 5 min of bath application of MPP+ 50 µM. The cell membrane is hyperpolarized (-55.28 ± 3.46 mV vs. -61.99 ± 3.50 mV, $n = 8, p = 0.002$) and firing rate reduced (2.13 ± 0.12 Hz to 0.90 ± 0.14 Hz, $n = 13, p = 7.8 \cdot 10^{-7}$). Bottom, voltage response to negative (−200 pA) and positive (200 pA) currents. Note the hyperpolarization, the increase in sag amplitude and the longer time to first peak. (B) Time course of the action of MPP+ on firing frequency and membrane potential. Note the fast kinetics of the effect. (C) Cell-attached recording showing the rapid drop in SNc DA neuron firing rate followed by delayed silencing of spontaneous activity produced by MPP+ (50 µM , top). The cessation of electrical activity is often gradual. The rapid effect is not prevented by preincubation with glybenclamide (10 µM), a selective blocker of K_{ATP} channels (2.34 ± 0.48 Hz vs. 1.18 ± 0.71 Hz, $n = 5, p = 0.006$, middle). Finally, selective inhibition of I_h with the organic blocker ZD7288 (30 µM) mimics the effect of MPP+, although with slower kinetics (2.18 ± 0.31 Hz vs. 1.50 ± 0.25 Hz, $n = 4, p = 0.017$, bottom right).

7.2. MPP+ inhibits I_h by slowing its gating properties and reducing current amplitude

Previous reports have shown that pharmacological block of I_h reduces the firing rate of SNc DA neurons (Seutin et al., 2001; Zolles et al., 2006; Inyushin et al., 2010). On this basis, we tested whether the rapid action of MPP+ on firing frequency of SNc DA neurons could be caused by I_h inhibition. To this purpose, we performed whole-cell voltage clamp recordings. Consistently with the closing of an inward, cationic current, partially available at the imposed holding potential (−55 mV), application of 50 µM

MPP$^+$, caused a modest upward shift of the holding current (-59.54 ± 33.25 pA to -30.18 ± 39.36 pA, $n = 11$, $p = 0.005$) and a rise of the input resistance (222.15 ± 21.14 MΩ to -343.65 ± 41.75 MΩ, $n = 11$, $p = 0.003$). We then studied how MPP$^+$ affects I_h activation curve. We used a double-phase voltage clamp protocol in which a family of conditioning potentials (-45 mV to -135 mV, 4 s in duration, holding $= -55$ mV), are imposed, followed by a fully-activating pulse to -135 mV. With this protocol, traces as those in Figure 7.3 A are obtained, before (left) and after (right) 5 min of incubation with 50 µM MPP$^+$.

Normalized tail currents at -135 mV (magnifications) were analysed and plotted to obtain activation curves as in Figure 7.3 B, C and D. In juvenile rats ($2 - 3$ weeks old), $V_{1/2}$ was shifted from -76.29 ± 1.50 mV to -88.26 ± 1.59 mV ($n = 8$, $p = 0.001$) by 5 min of MPP$^+$. For control, the same experiment was repeated in SNc DA neurons from 8-week-old Wistar rats or 8-week-old C57/BL6 male mice, the latter being the animal model of choice in MPTP studies. In adult rats, MPP$^+$ shifted $V_{1/2}$ from -82.44 ± 1.43 mV to -90.73 ± 2.50 mV ($n = 7$, $p = 0.011$), in mice, from -76.10 ± 2.13 mV to -87.88 ± 2.31 mV ($n = 7$, $p = 0.002$). MPP$^+$-dependent $V_{1/2}$ shift was quantitatively similar in the three groups (juvenile rats vs. adult rats, $p = 0.62$; juvenile rats vs. mice, $p > 0.99$ and adult rats vs. mice $p = 0.85$, one-way ANOVA followed by Bonferroni post hoc analysis) ruling out the possibility of species- or age-related variability of the observed effect. Next, we analyzed in depth the voltage-dependence of the effect of MPP$^+$ on steady state current with a double-pulse ($-75/-135$ mV) stimulation protocol (Figure 7.4 A). As shown, steady state current reduction (black arrow in insets) is marked at -75 mV (-44.38 ± 7.39 %, $n = 8$, $p = 5.4 \cdot 10^{-4}$), while nearly absent at -135 mV (-5.0 ± 5.4 %, $n = 8$, $p = 0.4$). A concentration/inhibition curve was obtained by plotting the percentage of inhibition at -75 mV, obtained with the two-step voltage clamp protocol described earlier, versus MPP$^+$ concentration ($I_{max} = 47$ %; $IC_{50} = 7.74$ µM, Figure 7.4 B).

7.3. MPP$^+$-mediated I_h inhibition is voltage-depentent and changes I_h kinetic properties

Data reported in Figures 7.3 and 7.4 indicate that MPP$^+$-dependent inhibition of I_h shows a peculiar voltage dependence. Indeed, as the imposed potential becomes more hyperpolarized, the effect of MPP$^+$ on current amplitude at steady-state decreases, eventually approaching zero at -135 mV. Nevertheless, a sizeable alteration of the activation kinetics of I_h is present at all potentials, becoming most evident at the most physiological ones. This action was quantified by fitting inward currents elicited at -95, -115 and -135 mV with a double exponential decay function (2.1 (Franz et al., 2000), in control conditions and in presence of MPP$^+$ 50 µM (Figure 7.5 A). This equation fitted all traces under analysis with an $R^2 \geq 0.99$. MPP$^+$ increases t_{FAST} and t_{SLOW} by approximately twofold at -95 mV ($p = 0.026$ and $p = 0.047$ vs. pre-MPP$^+$, $n = 8$),by 50 % at -115 mV ($p = 0.003$ and $p = 0.01$, $n = 8$) and -135 mV ($p = 0.0015$ and $p = 0.004$, $n = 8$).

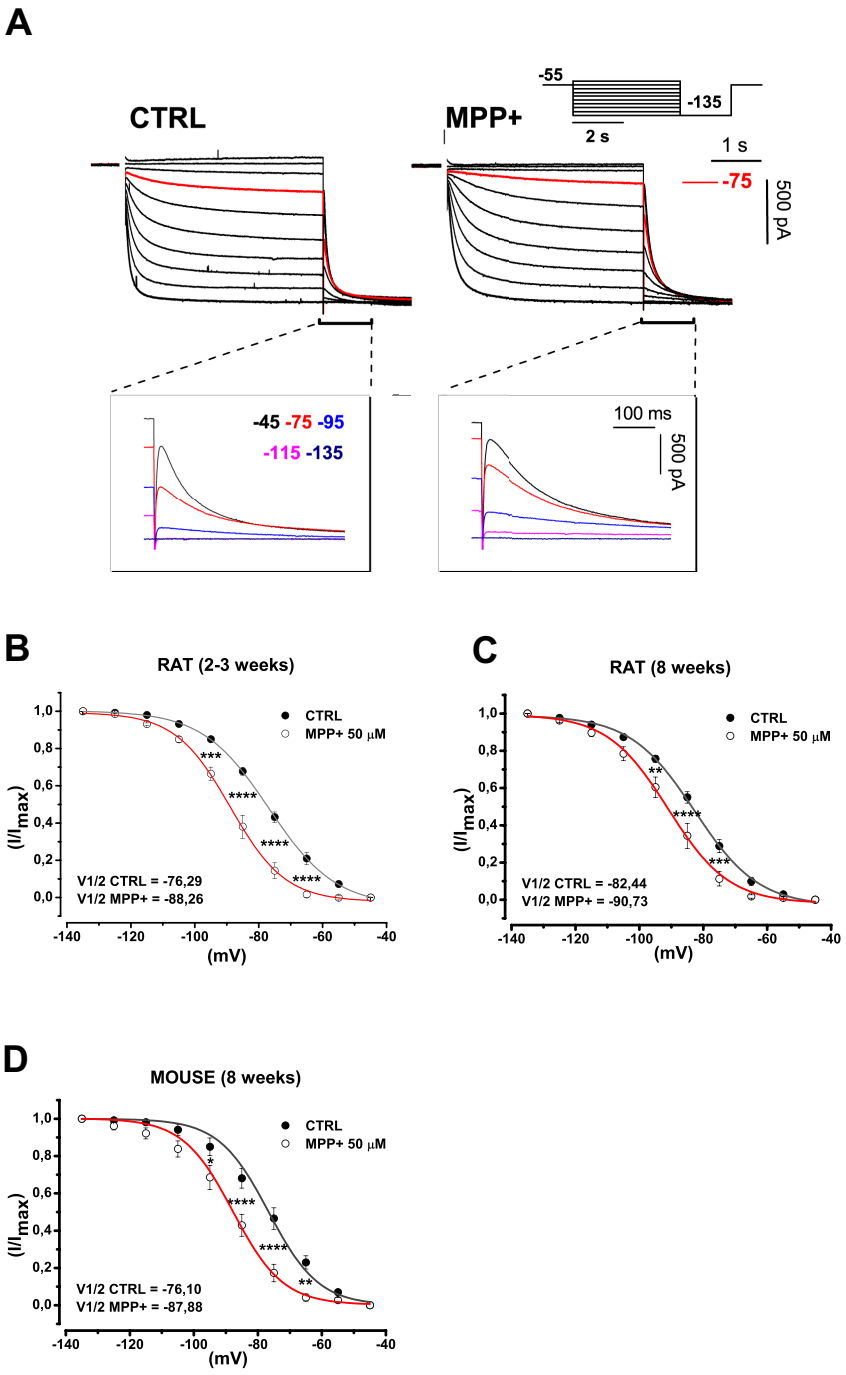

Figure 7.3.: MPP+ changes the voltage dependence of I_h . (A) Whole-cell currents elicited with a set of hyperpolarizing potentials (scheme). Currents evoked at −75 mV are highlighted in red. Enlargements show tail currents obtained at the indicated potentials. (B, C, D) I_h activation curve obtained by plotting normalized tail currents versus potential in control conditions (closed circles) and MPP+ 50 mM (open circles) in SNc DA neurons from juvenile rats (B), adult rats (C) and C57/BL6 male mice (D). *p*-values were obtained with one-way ANOVA with Bonferroni post hoc analysis. Curves were fitted with a Boltzmann equation (see methods).

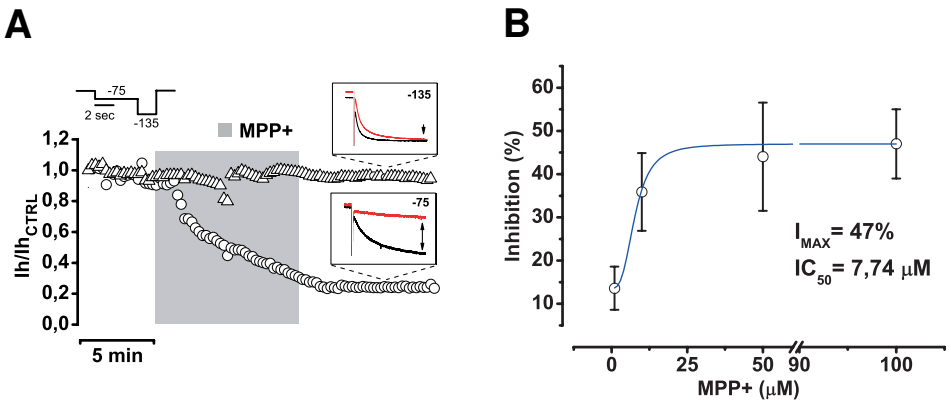

Figure 7.4.: MPP+ inhibits I_h in a voltage- and concentration-dependent manner. (A) A time course of the effect of MPP+ 50 µM on I_h at −75 (circles) and −135 mV (triangles) was obtained with the double-pulse protocol shown above. Insets show typical currents evoked before (black) and after (red) MPP+ (−75 mV = −44.38 ± 7.39 %, $n = 8$, $p = 5.4 \times 10^{-4}$; −135 mV = −5.0 ± 5.4 %, $n = 8$, $p = 0.4$. (B) Concentration-inhibition curve obtained by fitting values of inhibition (in percent- age of control) at −75 mV, in presence of 1 ($n = 5$), 10 ($n = 5$), 50 ($n = 5$) and 100 µM MPP+ ($n = 6$). Values of I_{MAX} (47 %) and IC_{50} (7.74 µM) were obtained by fitting the curve with a logistic equation (see methods).

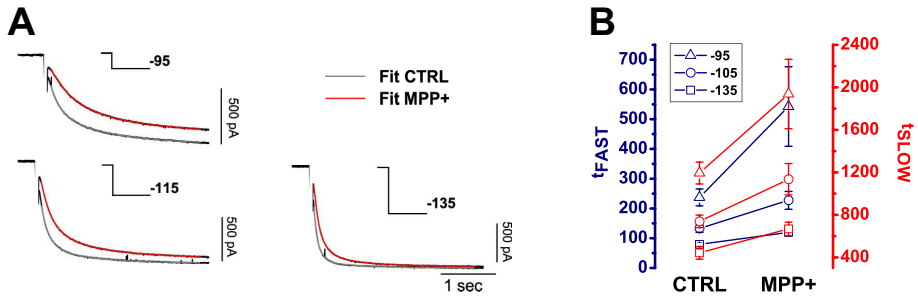

Figure 7.5.: MPP+ alters the activation kinetics of I_h in a voltage-dependent manner. (A) I_h currents elicited at −95, −115 and −135 mV evoked in control and after MPP+ 50 µM are shown. Fits are shown grey (control) and red (MPP+). Stimulation protocol is indicated in each panel. (B) Effect of MPP+ on t_{FAST} (blue) and t_{SLOW} (red) obtained at −95 (triangle), −115 (circle) and −135 mV (square) in control conditions and in MPP+ ($n = 8$).

7.4. Effect of MPP+ on I_h does not depend on complex I poisoning, D_2R signalling or cAMP metabolism

To further investigate the inhibitory action of MPP+ on I_h , we tested the involvement of pathways that, according to several reports, may provide mechanistic insight for this phenomenon (Figure 7.6 A,B). We first tested whether the effect of MPP+ on I_h was downstream of complex I blockade. We have already shown that activation of K_{ATP} channels is not responsible for the effects on spontaneous activity, as these occur in presence of ATP and are not prevented by K_{ATP} blocker glybenclamide.
As for I_h inhibition, it has been published that rotenone, a pesticide and complex I blocker, is able to open K_{ATP} channels, with an ATP-independent, ROS-dependent mechanism (Freestone et al., 2009). In turn, the opening of potassium channels active at near-rest potentials has been associated to reduced space-clamp and apparent re-

duction of I_h (Cathala and Paupardin-Tritsch, 1999). To rule out this possibility, we applied rotenone 1 µM to SNc DA neurons while eliciting I_h with 4 s pulses to −75 mV (V_{HOLD} = −55 mV), every 15 s. No significant effect on I_h amplitude was observed (95.96 ± 2.00 %, $n = 5$, $p > 0.99$; MPP$^+$ = 43.70 ± 7.43 %, $n = 8$, $p = 0.0128$; rotenone vs. MPP$^+$, $p = 0.004$, Figure 7.6 II). In addition, block of K_{ATP} channels with a preincubation with 10 µM glybenclamide failed to prevent MPP$^+$-induced inhibition of I_h ,(44.0 ± 7.8 %, $n = 4$, $p > 0.99$ vs. MPP$^+$ alone, Figure 7.6 III), providing further evidence that I_h reduction is not secondary to changes in whole-cell parameters, such as reduced clamp, due to opening of K_{ATP}. We then assessed the role of DAT, responsible for selective MPP$^+$ up accumulation in SNc DA neurons (Fuller and Hemrick-Luecke, 1985). Application of MPP$^+$ 50 µM following a 10 min pre-incubation with the specific blocker GBR12783 (5 µM) reduced I_h to an extent similar to MPP$^+$ alone (39.44 ± 5.79 %, $n = 4$, $p > 0.99$ vs. MPP$^+$, Figure 7.6 IV). Next, the hypothesis that MPP$^+$ could inhibit I_h by mimicking the action of DA on DA receptors was tested. Several laboratories have observed that activation of DA receptors on midbrain DA neurons induces effects reminiscent of those described here, namely hyperpolarization of the membrane potential, slowing of firing rate (Lacey et al., 1987) and down-modulation of I_h (Cathala and Paupardin-Tritsch, 1999; Jiang et al., 1993; Vargas and Lucero, 1999). These effects have been attributed to activation of D_2R, which inhibit adenylate cyclase and reduce cAMP levels thereby modulating a number of ion channels, such as G-protein- gated inward rectifying K^+ channels and I_h . Given the well established pharmacological similarities between MPP$^+$ and DA we reasoned that MPP$^+$ may inhibit I_h through D_2R- mediated reduction of cAMP levels. However, pre-incubation with the D_2R-selective antagonist sulpiride (10 µM, 5 min) failed to prevent the effect of 50 µM MPP$^+$ (31.63 ± 10.30 %, $n = 5$, $p > 0.99$ vs. MPP$^+$, Figure 7.6 V). In addition, we found that inclusion of 100 µM cAMP and phosphodiesterase inhibitor IBMX (1 mM) in patch pipette solution was also ineffective in preventing MPP$^+$-dependent I_h inhibition (47.45 ± 7.00 %, $n = 4$, $p > 0.99$ vs. MPP$^+$, Figure 7.6 VI). p-values for pharmacology experiments were calculated with one-way ANOVA followed by Bonferroni post hoc analysis.

7.5. MPP$^+$ increases temporal summation of EPSPs at STN-SNc glutamatergic synapse

Dendritic I_h prevents or dampens somatic temporal summation at CA3-CA1 synapse by normalizing the amplitude of eEPSPs at the soma (Magee, 1999). Pharmacological blockade of this conductance leads to temporal summation of eEPSPs and, thus, to increased spike probability and overall network excitability. Increased excitatory input has been linked to death from excitotoxicity in several pathological conditions. The SNc receives glutamatergic afferents from the STN and this axonal pathway is preserved in horizontal midbrain slices. We measured synaptic summation of eEPSPs in SNc DA neurons by delivering short trains of low frequency (train duration = 240 ms, frequency = 20 Hz) pulses in the STN. No alteration of synaptic efficacy was ever observed under these conditions. Bath application of 50 µM MPP$^+$ led to a significant increase of somatic temporal summation, measured as eEPSP5/eEPSP1 ratio, from

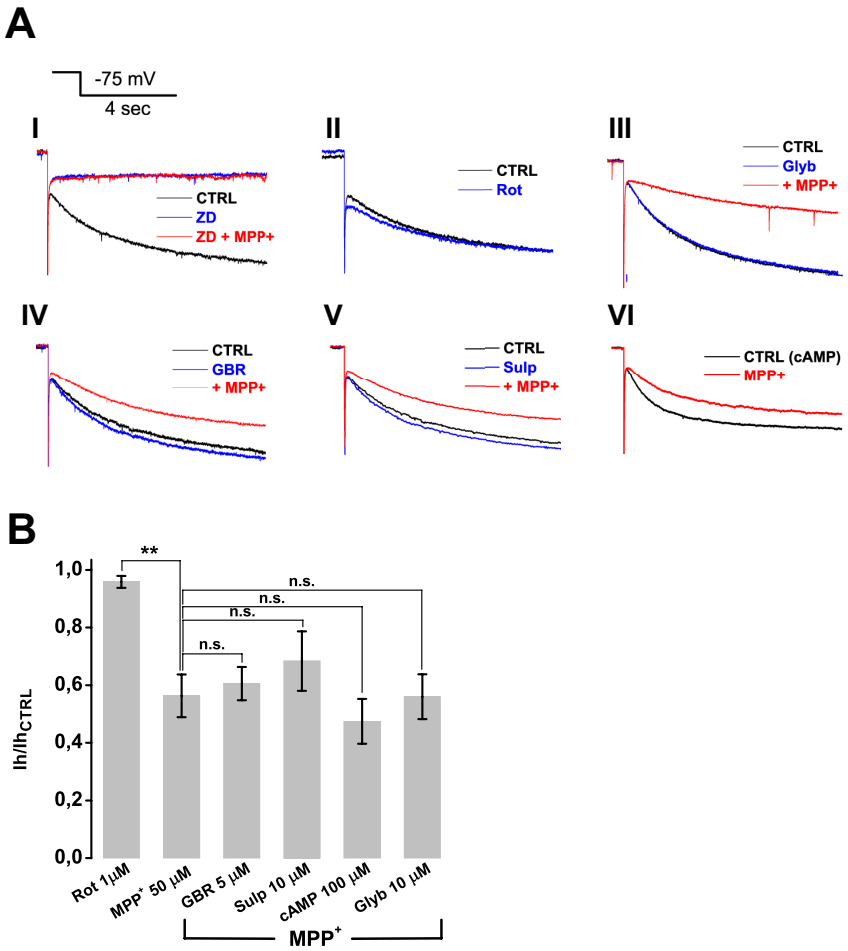

Figure 7.6.: MPP$^+$-inhibition of I_h in SNc DA neurons does not involve mitochondrial or cAMP metabolism. (A) Representative traces for each pharmacological experiment in which drugs were tested for their ability to mimic/prevent the action of MPP$^+$ 50 µM on steady-state I_h elicited with single, 4 s pulses to −75 mV (Figure 7.6 I–VI). ZD7288 30 µM completely occluded the action of MPP$^+$ (I). Rotenone 1 µM did not affect I_h , ($n = 5$, $p > 0.99$, II). Consistently, 10 µM glybenclamide did not protect I_h from MPP$^+$ inhibition ($n = 5$, $p > 0.99$, III). DAT blocker GBR12738 (5 µM, $n = 8$, $p > 0.99$, IV), D_2R antagonist sulpiride (10 µM, $n = 5$, $p > 0.99$, V) and cAMP 100 µM added to pipette solution (+ IBMX 1 mM, $n = 4$, $p > 0.99$, F), failed to prevent the inhibition caused by MPP$^+$ 50 µM. Grouped data and statistical analysis from pharmacology experiments. Statistical difference between each group and MPP$^+$ was calculated with one-way ANOVA with Bonferroni post hoc analysis.

1.69 ± 0.14 to 2.04 ± 0.13 ($n = 9$, $p = 0.0001$) in 9/14 neurons tested. In these neurons, subsequent application of the specific I_h blocker ZD7288 (30 µM) resulted in an additional increase of eEPSP5/eEPSP1 ratio from 2.04 ± 0.13 to 2.33 ± 0.13 ($n = 9$, $p = 0.037$, Figure 7A, B). In the remaining five neurons, in which MPP^+ did not affect synaptic summation, ZD7288 was also ineffective ($p = 0.47$, $n = 5$), thus suggesting that I_h , although detected with somatic current recordings, did not exert a role in synaptic summation. For this reason, ZD7288-irresponsive neurons were excluded by statistical analysis. We applied the same experimental procedure to the CA3-CA1 synapse in hippocampal slices obtained from the same brains (Figure 7.7 A, right), where ZD7288-induced enhancement of temporal summation has been well described (Magee, 1999). Here, no alteration of synaptic summation was observed in response to bath application of MPP^+ (1.18 ± 0.08 vs. 1.19 ± 0.1, $n = 7$, $p = 0.99$), whereas ZD7288 increased summation significantly (1.19 ± 0.1 vs. 1.85 ± 0.1, $n = 7$, $p = 0.048$) in all neurons tested. During eEPSP recordings in both areas, I_h amplitude was measured with single pulses to -75 mV (4 s, holding $= -55$ mV in SNc, -65 mV in hippocampus) in order to monitor the effectiveness of MPP^+ block. Interestingly, while the increase in temporal summation caused by MPP^+ was always associated to I_h inhibition in the SNc, in the hippocampus, I_h inhibition and increase in somatic summation only occurred with ZD7288, suggesting the existence of differential sensitivity towards MPP^+ among SNc- and CA1-specific HCN isoforms. p-values in eEPSP summation experiments were obtained with one-way ANOVA for repeated measures followed by Bonferroni post hoc analysis.

7.6. I_h inhibition increases temporal summation of EPSPs in VTA DA neurons

Unlike in SNc, DA neurons of the VTA can't be distinguished from non-DA on the basis of electrophysiological characterization such as I_h magnitude (Margolis 2006).
To investigate whether I_h inhibition could lead to an increase of temporal summation in VTA DA neurons too, we used midbrain slices obtained from TH-GFP mice (see methods) where DA neurons were easily identified thanks to their fluorescence.
Pure EPSPs were recorded from GFP-positive VTA neurons (see Figure 7.9B) by local stimulation of synaptic activity in presence of GABA blockers (10 µM bicuculline). As shown in Figure 7.9, bicuculline application didn't alter significantly the EPSP5/EPSP1 ratio (1.64 ± 0.39 vs. 1.54 ± 0.32, $n = 5$, $p = 0.88$), whereas a significant increase was observed after 20 µM ZD7288 bath application (from 1.54 ± 0.32 to 2.66 ± 0.50, $n = 5$, $p = 0.0028$). Only one neuron out of 5 was ZD7288-irresponsive, revealing that I_h has a pivotal role in temporal summation even in VTA.
p-values were obtained with one-way ANOVA for repeated measures followed by Bonferroni post hoc analysis.

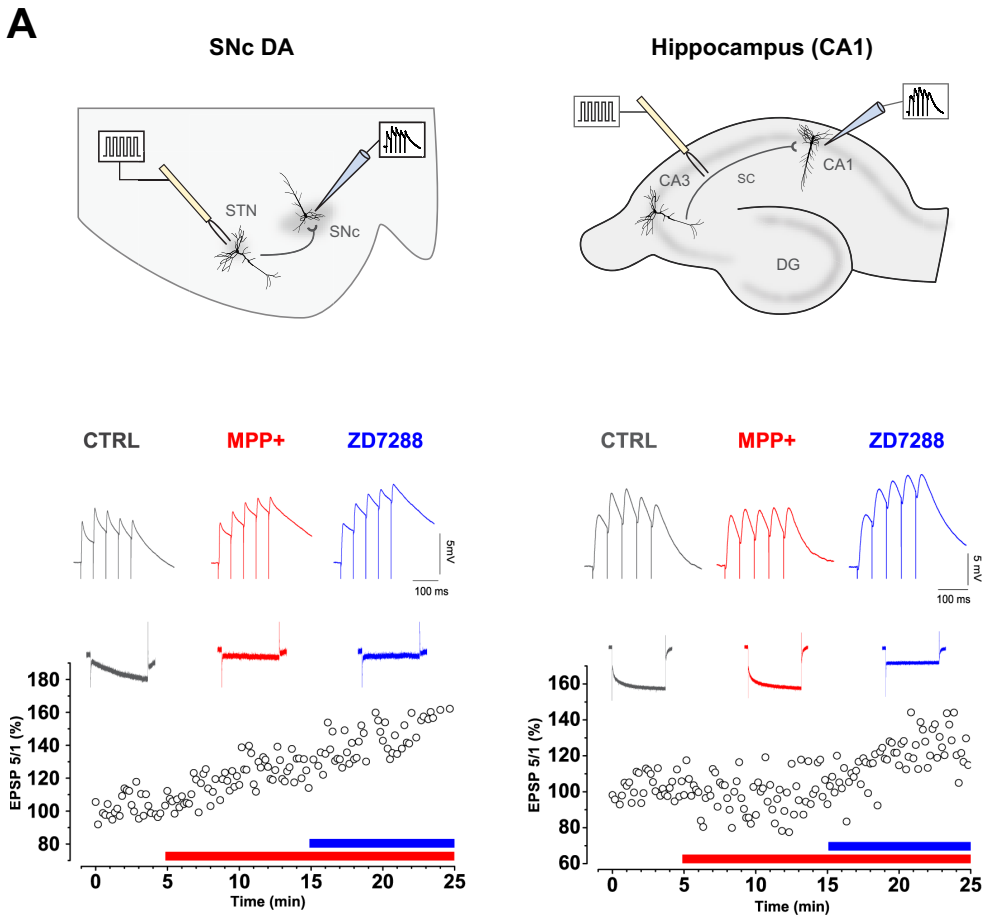

Figure 7.7.: MPP$^+$ enhances temporal summation of eEPSPs in SNc DA, but not in CA1 neurons. (A) Top: Stimulation schemes showing the position of stimulating (orange) and recording (blue) electrode in SNc (left) and hippocampus (right).
Traces showing eEPSPs trains in control (grey), MPP$^+$ 50 µM (red) and MPP$^+$ 50 µM + ZD7288 30 µM (blue) are shown for representative SNc DA and CA1 hippocampal neurons (middle). Traces were baseline adjusted to allow comparison. The time course of the ratio EPSP5/EPSP1 is shown on the bottom. Above each plot, I_h current recordings (step = −75 mV, holding = −55 mV for SNc and −65 mV for CA1) are shown for each condition in the same colour code as for eEPSPs examples.

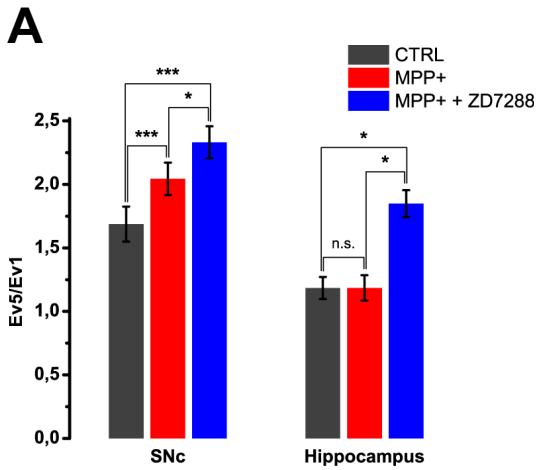

Figure 7.8.: EPSP5/EPSP1 ratio is increased by MPP$^+$ in the SNc (from 1.69 ± 0.14 to 2.04 ± 0.13, $n = 9$, $p = 0.0001$) but not in the hippocampus (from 1.18 ± 0.08 to 1.19 ± 0.10, $n = 7$, $p = 0.99$). ZD7288, as expected, increased summation in CA1 (to 1.85 ± 0.1, $n = 7$, $p = 0.048$) and produced an additional rise in SNc (to 2.33 ± 0.13, $n = 9$, $p = 0.037$). p-values were obtained with one-way ANOVA for repeated measures, followed by Bonferroni post hoc analysis.

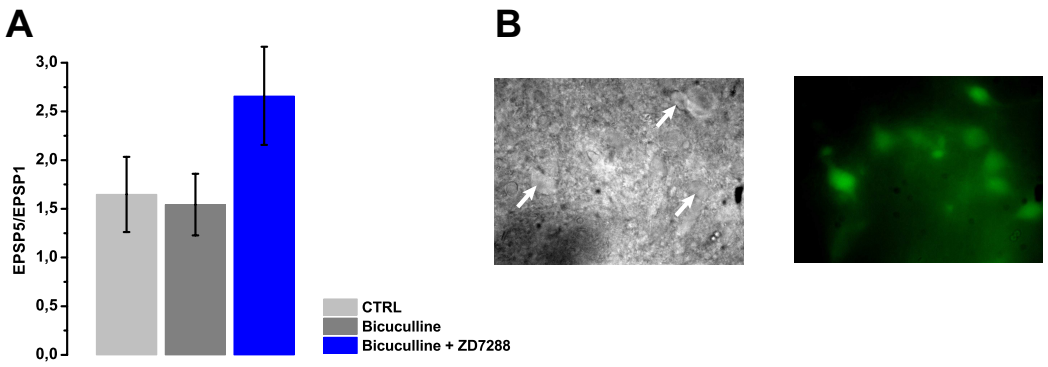

Figure 7.9.: (A) ZD7288-mediated I_h inhibition leds to an increase of EPSP5/EPSP1 ratio in DA VTA neurons from 1.64 ± 0.39 vs. 2.66 ± 0.50, $n = 5$, $p = 0.002$. In presence of bicuculline 10 µM only a small trend toward decreased temporal summation was observed (1.64 ± 0.39 vs. 1.54 ± 0.32, $n = 5$, $p = 0.88$). (B) GFP-positive VTA DA neurons (right) and the equivalent infrared field (left); neurons are indicated by white arrows.
p-values were obtained with one-way ANOVA for repeated measures followed by Bonferroni post hoc analysis.

7.7. Presynaptic I_h does not influence integration of incoming synaptic signals in SNc DA neurons

The augmented temporal summation showed in the previous experiments can be ascribed to both pre- and postsynaptic I_h inhibition. Changes in spontaneous release and paired pulse ratio (PPR) tests are normally associated with a modification of synaptic plasticity dependent on presynaptic components of the circuit. Therefore we tested whether presynaptic block of I_h leads to significant variations of these two parameters.

7.7.1. Presynaptic I_h inhibition doesn't affect evoked release

Recently it has been shown that ZD7288-mediated loss of presynaptic I_h enhances synaptic transmission onto mature Entorhinal Cortex layer III pyramidal neurons (Huang et al., 2009). An increase in miniature excitatory postsynaptic currents (mEPSC) frequency of these neurons was also observed in HCN_1 $^{-/-}$ mice, demonstrating the involvement of presynaptic HCN_1 channels in the regulation of excitatory spontaneous release from these synapses (Huang et al., 2011).
To investigate whether, in our model, I_h influences evoked release, we evoked pairs of EPSCs in absence and presence of 20 µM ZD7288. ZD7288 (20 µM) was also included in the intracellular solution to block post-synaptic HCN channels.
10 min of bath application of ZD7288 didn't affect PPR (1.00 ± 0.09 vs. 1.02 ± 0.10, $n = 8$, $p = 0.47$), suggesting that, in SNc, synaptic release is not influenced by presynaptic HCN channels block.

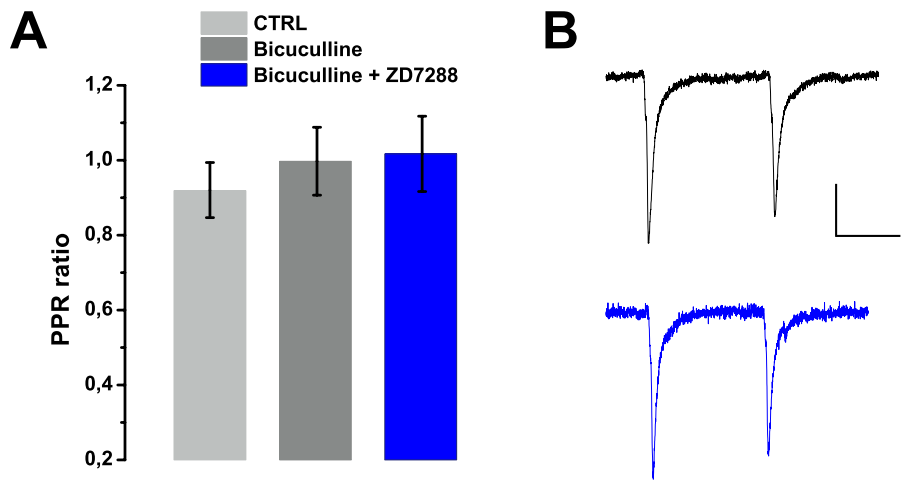

Figure 7.10.: Presynaptic I_h inhibition doesn't affect PPR in SNc DA neurons. (A) Bar graph summarizing the PPR measured at the beginning of each experiment, after 3 min bicuculline (10 µM) and after 10 min ZD7288 (20 µM). Neurons treated with bicuculline showed a small but not significant increase in PPR (from 0.92 ± 0.07 to 1.00 ± 0.09, $n = 8$, $p = 0.47$) while ZD7288-mediated I_h inhibition left PPR ratio unchanged (from 1.00 ± 0.09 to 1.02 ± 0.10, $n = 8$, $p = 0.93$. p-values were obtained with one-way ANOVA for repeated measures followed by Bonferroni post hoc analysis.)
(B) Example traces of PPR recordings before (black) and after ZD7288 application (blue). Scalebar = 50 mA · 25 ms

7.7.2. Spontaneous activity of SNc DA neurons is not affected by presynaptic I_h inhibition

To further confirm the postsynaptic nature of I_h control over EPSP integration, we tested the effect of ZD7288 on pharmacologically isolated spontaneous EPSCs.
DA neurons of the SNc rarely show spontaneous EPSCs (Caputi, 2003), therefore, to boost network activity we applied 4-AP to our slices. Neurons increased the spontaneous firing frequency from 3.40 ± 1.56 Hz to 15.70 ± 5.46 Hz. EPSCs were recorded with a ZD7288-containing solution to block postsynaptic I_h .
As shown in Figure 7.11, after 15 min of 20 µM ZD7288 application, none of responding neurons were affected in terms of spontaneous EPSCs peak amplitude (133.22 ± 20.97 pA vs. 138.93 ± 20.60 pA, $n = 7$, $p = 0.47$), frequency (15.70 ± 5.46 Hz vs. 14.12 ± 4.79 Hz, $n = 7$, $p = 0.10$) and area (594.61 ± 168.58 pA ms vs. 664.14 ± 178.42 pA ms $n = 7$, $p = 0.45$) confirming the absence of a role for presynaptic HCN channels on spontaneous activity.

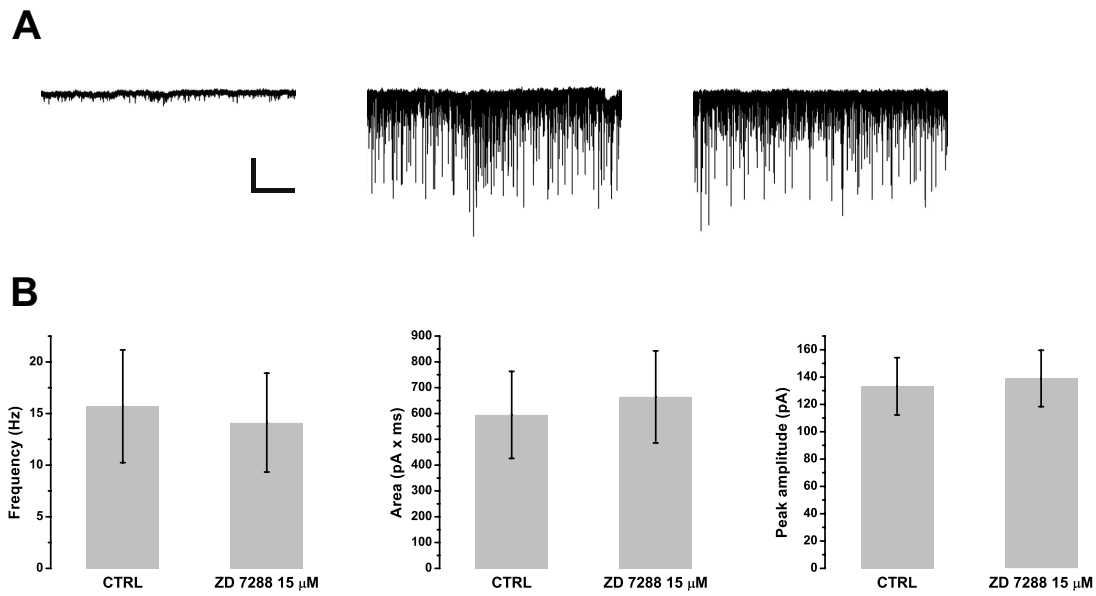

Figure 7.11.: Presynaptic I_h block does not alter peak amplitude, frequency and area of EPSCs in the SNc. (A) Example traces of spontaneous EPSCs in control conditions (left), after 5 min 4-AP 100 µM and bicuculline application (middle) and after 15 min ZD7288 20 µM (right). Scalebar = 100 pA· 10 s.
(B) Frequency (left), area (middle) and amplitude (right) histograms of spontaneous EPSCs under control conditions and in presence of ZD7288 20 µM. Bars show mean ± SEM, $n = 7$ in each case. Control and ZD7288 data are not significantly different (Student's paired t test $p = 0.10$ for frequency data, $p = 0.47$ for amplitude data; paired sample sign test $p = 0.45$ for area data.)

Part V.

Discussion

Chapter 8

Discussion

8.1. MPP^+ affects membrane potential and spontaneous activity through inhibition of I_h

Mitochondrial dysfunction and oxidative damage, probably induced by both genetic predisposition and environmental factors, are thought to play a role in the pathogenesis of PD (Vives-Bauza and Przedborski, 2011). Over the past few years this hypothesis has been reinforced by the observation that various toxins resembling principal characteristics of PD reduce complex I activity in SNc neurons, causing ATP depletion and ROS production. The importance of mitochondrial impairment has been further confirmed by the discovery that many of the genes responsible for early onset of familial forms of this disease have a role associated with mitochondrial function, including Pink1, parkin and DJ-1.

Despite evidence suggesting a role for mitochondrial dysfunction in the loss of SN neurons, there remains considerable uncertainty about the mechanisms involved. Moreover, energy failure can't account for the more pronounced degeneration of SNc neurons than VTA, a fundamental hallmark of PD.

We therefore investigated non mitochondrial effects carried by the parkinsonian toxin MPP^+ by analyzing neurophysiological properties of SNc DA neurons with patch-clamp technique in acute midbrain slices.

I_h is a non-inactivating,inward rectifying, cationic current that is very abundant in SNc and VTA DA neurons, albeit its physiological role in these regions is still unclear. In mammals, the molecular correlates of I_h is represented by four genes termed HCN_{1-4}; in both mice and rats SNc DA neurons express $HCN_{2,4}$ subunits, characterized by slower activation kinetics and strong sensitivity to cAMP levels. On the other hand, CA1 neurons express preferentially HCN_1 subunit, resulting in faster activation kinetics and very low sensibility to cAMP.

Bath application of 50 µM MPP^+ induced a rapid hyperpolarization along with a reduction of spontaneous firing activity of SNc DA neurons recorded in whole-cell configuration. These effects were already seen with perforated patch in the same region (Liss et al 2005) and linked to the opening of K_{ATP} channels due to a decrease of cellular ATP levels after mitochondrial failure. Such effects were solely dependent on I_h -inhibition since all recordings were performed in presence of 2 mM ATP and prein-

cubation with glybenclamide, even in cell-attached recordings, failed to prevent them. Notably, a rapid reduction of firing rate is also observed in the work by Liss et al. (2005) in SNc DA neurons from mice with non-functional K_{ATP} channels, upon application of MPP+ and, conversely, previous works reported a reduction of the firing activity and hyperpolarization after selective block of I_h (Inyushin et al., 2010; Seutin et al., 2001). No major alterations were found in electrophysiological properties at depolarized potentials, accordingly with the close state of HCN channels at potentials above −40 mV. In contrast with the observed I_h inhibition, MPP+ treated neurons displayed an increase in sag amplitude, interpreted as a result of the increased input resistance. When I_h is inhibited by MPP+, the membrane, in addition to being more negative at rest, hyperpolarizes more in response to negative current steps, thereby recruiting a larger fraction of HCN channels and overcoming the inhibitory effect of MPP+. In agreement with the increment of I_h time constants, sag activation kinetics were slower after MPP+ treatment.

8.2. MPP+ likely inhibits I_h in a direct way

MPP+-dependent inhibition of I_h was found to be voltage and concentration dependent. A significant shift of the curve towards negative potentials is observed after application of 50 µM MPP+. This effect was not species- or age-dependent since no differences were found between juvenile and adult rats or between rats and mice.
In contrast with the shift of voltage dependence evenly distributed after cAMP application (Biel, 2009; Postea and Biel, 2011), MPP+ showed a not symmetrical shift, more evident at physiological potentials. The greatest MPP+ mediated I_h inhibition was observed at physiological potentials whereas it was almost totally relieved during strong and long hyperpolarizing steps (−135 mV, 4 s).
Interestingly, block by ZD7288 is also relieved by prolonged hyperpolarization (Gasparini and DiFrancesco, 1997), although this process unfolds in minutes, compared with few hundred milliseconds for MPP+. A slowdown of current activation was observed at every potentials, being more pronounced near RMP.
These findings concur to suggest a direct interaction of the toxin with the channel. Additional support to this hypothesis has come from the investigation of metabolic and signalling pathways. First we investigated if MPP+-induced effects could depend on mitochondrial impairment and consequent ATP depletion and ROS production. As our pipette contained 2 mM ATP, depletion of ATP was deemed not influent. In addition, MPP+-dependent reduction of firing activity was also observed in cell-attached configuration. The involvement of oxidative stress was tested with rotenone, a complex I blocker previously found to bring about ROS elevation, K_{ATP} channels opening and consequent cessation of firing activity in SNc DA neurons (Freestone et al., 2009; Liss et al., 2005). In our experiments, rotenone left I_h unaffected. Besides, the effect of MPP+ on firing activity and I_h occurred also in presence of the specific K_{ATP} blocker glybenclamide and, in whole-cell recordings, 2 mM ATP.
We then looked for extra-mitochondrial mechanism explaining MPP+ effects. The observation that I_h inhibition carried by MPP+ also occurred in slices preincubated with DAT blocker GBR 12783, indicates that the toxin does not need to enter the cell to exert its action. Of the many signalling pathways reported to modulate I_h , we focused

on those already described in SNc DA neurons. PIP_2 is a positive modulator of I_h in SNc DA neurons (Zolles et al., 2006). However, block of PIP_2-synthesizing enzyme PI 3- kinase with the specific inhibitor wortmannin leads to the inhibition of I_h in 30 min. As MPP+ is nearly five times faster we discarded the hypothesis of an interaction with this signalling pathway.
Given the MPP+ affinity for DA specific enzymes and trasporters, we tested whether MPP+ could mimic DA action on DA receptors, in particular on D_2R, which are coupled to $G_{i/o}$ proteins. Preincubation with D_2R antagonist sulpiride was unable to protect I_h from MPP+ inhibitory action and the effect was also not prevented by increased intracellular levels of cAMP, further confirming that DA-mimicking action of MPP+ is not relevant here.

8.3. MPP+ increases temporal summation of eEPSPs in SNc DA neurons via inhibition of I_h

Normalization of EPSPs is afforded by the remarkable distribution of I_h conductance along dendritic arborization found in many neurons (Magee, 1999; Sheets et al., 2011). Thanks to this action, synaptic inputs are conveyed to the soma with temporal precision. This helps avoiding long and potentially noxious depolarizing episodes resulting from temporal summation. When I_h is not functional, due to pharmacological or molecular ablation (Kim et al., 2012), the ability of dendrites to compute and integrate synaptic inputs is lost and robust temporal summation of EPSPs may occur at the soma, leading to greater depolarization and higher firing probability. In the hippocampus and cortex, this promotes the generation of an epileptic focus (Jung et al., 2010; Strauss et al., 2004). Our results suggest that something similar may occur in the SNc in presence of MPP+.
Significant elevation of temporal summation of EPSPs originating in STN glutamatergic terminals has been observed during MPP+- and ZD7288-induced block of I_h . Interestingly, MPP+ did not inhibit I_h in CA1 neurons and did not facilitate temporal summation at CA3-CA1 synapse. This supports the conclusion that MPP+ enhances temporal summation in SNc DA neurons through inhibition of I_h and that differential effect may be due to different HCN subunit composition in the two areas.
The same role of I_h current is confirmed in VTA region by the increased temporal summation observed in the soma after ZD7288 application.

8.4. I_h contribution to DA synaptic activity is mainly due to postsynaptic HCN channels

The functional involvement of I_h in synaptic transmission can be pre- or postsynaptic depending on the synapse considered. It appears to be exclusively postsynaptic at CA3-CA1 synapse (Magee, 1999) while a contribution to release probability was described at the EC-CA1 synapse (Huang et al., 2011). The increased temporal summation observed after I_h block observed at glutamatergic synapses of midbrain DA neurons suggests a postsynaptic action of I_h . To obtain further confirmation we per-

formed electrophysiological protocols classically employed to discriminate between the two cases, that is measurement of sEPSCs frequency and paired pulse ratio (PPR) following ZD7288 application. Preliminary data obtained in rat SNc DA neurons indicate that neither the frequency of 4-AP-stimulated sEPSCs nor PPR are significantly altered by block of HCN channels. Considering the strong similarities in ZD7288 action on temporal summation in SNc and VTA, we presume that results of sEPSCs frequency and PPR can be extended to VTA DA neurons.
However these experiments will be repeated in midbrain slices of TH-GFP mice where DA neurons within the VTA where they are readily recognizable.

8.5. Relevance of I_h inhibition in PD pathogenesis

Acute inhibition of I_h by MPP^+ leads to hyperpolarization, reduction of spontaneous firing activity and increased temporal summation of excitatory inputs in SNc DA neurons. Firing activity of these neurons is very regular *in vitro*, whereas it shows a bursting pattern *in vivo* or in organotypic cultures (Rohrbacher et al., 2000). Given this marked difference, one cannot assume that I_h inhibition by MPP^+ reduces discharge frequency of SNc DA neurons *in vivo*. Moreover, a reduction in excitability can hardly be considered noxious in general. Nonetheless, it was reported that the firing activity of SNc DA neurons from adult mice, driven by dendritic voltage-gated calcium channels (Cav 1.3), can be reverted to a juvenile specific, I_h -driven firing by pharmacological block of such oscillating calcium conductance (Chan et al., 2007). This phenomenon, named "rejuvenation" by the authors, was found to be protective *in vitro* and *in vivo*. In this respect, it could be hypothesized that the observed MPP^+-dependent suppression of I_h could lead to the inverse process, that is the shift from a "safe" I_h -driven to a "noxious" Cav 1.3-driven firing pattern, although this would seem rather speculative. On the other hand, the finding that MPP^+ enhances synaptic summation of excitatory inputs in SNc DA neurons may have high-potential pathogenic relevance.
Temporal summation leads to greater and more sustained depolarization epochs at the soma and, likely, in dendrites. This may, in turn, result in increased calcium entry through voltage-gated calcium channels. In keeping with this, Surmeier and co-workers have shown that isradipine, a Cav 1.3 blocker, is able to stop dendritic calcium oscillations and accumulation and to protect from MPTP- induced degeneration *in vitro* and *in vivo* (Chan et al., 2007; Meredith et al., 2008b). Interestingly, it has been reported that I_h is more abundant in calbindin-negative SNc DA neurons and that this subpopulation is more vulnerable in weaver and MPTP-lesioned mice (German et al., 1996; Neuhoff et al., 2002). The observation that I_h block leads to an increased temporal summation in the VTA region too, apparently argues against the hypothesis that I_h loss of function is responsible of SNc neurodegeneration in experimental and spontaneous PD; however one need to consider that the two DA populations belong to different neuronal pathways.
The SNc, as opposed to the VTA, receives extensive glutamatergic innervations from the STN, a nucleus undergoing marked disinhibition during PD pathogenesis. This could lead to a toxic excitatory drive toward the SNc, thus explaining the differential vulnerability. In this respect, Wallace and collaborators have demonstrated that lesion

of the STN protects midbrain DA neurons in a monkey MPTP model (Wallace et al., 2007), thus suggesting a contribution of the STN excitatory drive to excitatory process. In this view I_h loss of function is not to be considered an aetiological factor, rather a mechanism promoting SNc specific vulnerability, as seen in MitoPark mice, where I_h loss of function accompanies, and perhaps leads to, the early stages of nigrostriatal degeneration triggered by genetic mitochondrial dysfunction (Good et al., 2011). The actual pathogenic significance of I_h loss of function in MitoPark mice is still to be investigated. Furthermore our hypothesis requires confirmation from *in vivo* experiments aimed at evaluating whether, first, selective I_h inhibition is intrinsically able to result in nigrostriatal degeneration and, second, functional rescue of I_h in presymptomatic MitoPark mice is able to stop or slow down cell loss.

Chapter 9

List of abbreviations

4-AP 4-Aminopyridine

ATP Adenosine-5'-triphosphate

BBB Blood-brain barrier

cAMP Cyclic adenosine monophosphate

CNBD Cyclic nucleotide binding domain

CNS Central nervous system

CSD cAMP-sensing domain

D_1R Dopamine 1-type receptor

D_2R Dopamine 2-type receptor

DA Dopamine

DAT Dopamine transporter

DMSO Dimethylsulfoxide

EC Entorhinal cortex

EPSC Excitatory postsynaptic current

EPSCs Excitatory postsynaptic currents

EPSP Excitatory postsynaptic potential

EPSPs Excitatory postsynaptic potentials

GABA γ-aminobutyric acid

GFP Green fluorescent protein

GP Globus pallidus

GPe Globus pallidus externus

GPi Globus pallidus internus

GSH Glutathione

HCN Hyperpolarization-activated cyclic nucleotide-gated channels

IPSCs Inhibitory postsynaptic currents

JNK c-Jun N-terminal kinase

KIR Inwardly rectifying potassium channels

LBs Lewi's bodies

MAO-A Monoamine oxidase A

MAO-B Monoamine oxidase B

MAPK Mitogen associated protein kinase

$MPDP^+$ 1-methyl-4-phenyl-2,3-dihydropyridinium

MPP^+ 1-methyl-4-phenylpyridinium

MPTP n-methyl-4-phenyl-1,2,3,6-tetrahydropyridine

MSNs Medium spiny neurons

NAC non-$\alpha\beta$ component

OCT-3 Organic cation transporter 3

PCD Programmed cell death

PD Parkinson's disease

PIP_2 Phosphatidylinositol 4,5-bisphosphate

PPR Paired pulse ratio

RMP Resting membrane potential

ROS Reactive oxygen species

SN Substantia nigra

SNc Substantia nigra pars compacta

SNr Substantia nigra pars reticulata

SOD1 Superoxide dismutase-1

STN Subthalamic nucleus

TEA Tetraethylammonium

TH Tyrosine hydroxyalse

VMAT Vesicular monoamine transporter

VMAT1 Vesicular monoamine transporter 1

VMAT2 Vesicular monoamine transporter 2

VTA Ventral tegmental area

Bibliography

Albin, R. L.; Young, A. B.; and Penney, J. B., *The functional anatomy of basal ganglia disorders. Trends Neurosci*, 12 (10): (1989) 366–75.

Alexander, G. E. and Crutcher, M. D., *Functional architecture of basal ganglia circuits: neural substrates of parallel processing. Trends Neurosci*, 13 (7): (1990) 266–71.

Auluck, P. K.; Chan, H. Y. E.; Trojanowski, J. Q.; Lee, V. M. Y.; and Bonini, N. M., *Chaperone suppression of alpha-synuclein toxicity in a drosophila model for parkinson's disease. Science*, 295 (5556): (2002) 865–8. doi:10.1126/science.1067389.

Baruscotti, M.; Bucchi, A.; and Difrancesco, D., *Physiology and pharmacology of the cardiac pacemaker ("funny") current. Pharmacol Ther*, 107 (1): (2005) 59–79. doi:10.1016/j.pharmthera.2005.01.005.

Beaumont, V.; Zhong, N.; Froemke, R. C.; Ball, R. W.; and Zucker, R. S., *Temporal synaptic tagging by i(h) activation and actin: involvement in long-term facilitation and camp-induced synaptic enhancement. Neuron*, 33 (4): (2002) 601–13.

Beckman, K. B. and Ames, B. N., *The free radical theory of aging matures. Physiol Rev*, 78 (2): (1998) 547–81.

Bender, R. A. and Baram, T. Z., *Hyperpolarization activated cyclic-nucleotide gated (hcn) channels in developing neuronal networks. Prog Neurobiol*, 86 (3): (2008) 129–40. doi:10.1016/j.pneurobio.2008.09.007.

Bender, R. A.; Kirschstein, T.; Kretz, O.; Brewster, A. L.; Richichi, C.; Rüschenschmidt, C.; Shigemoto, R.; Beck, H.; Frotscher, M.; and Baram, T. Z., *Localization of hcn1 channels to presynaptic compartments: novel plasticity that may contribute to hippocampal maturation. J Neurosci*, 27 (17): (2007) 4697–706. doi:10.1523/JNEUROSCI.4699-06.2007.

Berman, S. B. and Hastings, T. G., *Dopamine oxidation alters mitochondrial respiration and induces permeability transition in brain mitochondria: implications for parkinson's disease. J Neurochem*, 73 (3): (1999) 1127–37.

Bernheimer, H.; Birkmayer, W.; Hornykiewicz, O.; Jellinger, K.; and Seitelberger, F., *Brain dopamine and the syndromes of parkinson and huntington. clinical, morphological and neurochemical correlations. J Neurol Sci*, 20 (4): (1973) 415–55.

Betarbet, R.; Sherer, T. B.; MacKenzie, G.; Garcia-Osuna, M.; Panov, A. V.; and Greenamyre, J. T., *Chronic systemic pesticide exposure reproduces features of parkinson's disease. Nat Neurosci*, 3 (12): (2000) 1301–6. doi:10.1038/81834.

Bezard, E.; Gross, C. E.; Fournier, M. C.; Dovero, S.; Bloch, B.; and Jaber, M., *Absence of mptp-induced neuronal death in mice lacking the dopamine transporter. Exp Neurol*, 155 (2): (1999) 268–73. doi:10.1006/exnr.1998.6995.

Bezard, E. and Przedborski, S., *A tale on animal models of parkinson's disease. Mov Disord*, 26 (6): (2011) 993–1002. doi:10.1002/mds.23696.

Biel, M., *Cyclic nucleotide-regulated cation channels. J Biol Chem*, 284 (14): (2009) 9017–21. doi:10.1074/jbc.R800075200.

Biel, M.; Wahl-Schott, C.; Michalakis, S.; and Zong, X., *Hyperpolarization-activated cation channels: from genes to function. Physiol Rev*, 89 (3): (2009) 847–85. doi:10.1152/physrev.00029.2008.

Blanchard, V.; Raisman-Vozari, R.; Vyas, S.; Michel, P. P.; Javoy-Agid, F.; Uhl, G.; and Agid, Y., *Differential expression of tyrosine hydroxylase and membrane dopamine transporter genes in subpopulations of dopaminergic neurons of the rat mesencephalon. Brain Res Mol Brain Res*, 22 (1-4): (1994) 29–38.

Blandini, F.; Levandis, G.; Bazzini, E.; Nappi, G.; and Armentero, M.-T., *Time-course of nigrostriatal damage, basal ganglia metabolic changes and behavioural alterations following intrastriatal injection of 6-hydroxydopamine in the rat: new clues from an old model. Eur J Neurosci*, 25 (2): (2007) 397–405. doi:10.1111/j.1460-9568.2006.05285.x.

Blandini, F.; Nappi, G.; Tassorelli, C.; and Martignoni, E., *Functional changes of the basal ganglia circuitry in parkinson's disease. Prog Neurobiol*, 62 (1): (2000) 63–88.

Briggs, I.; BoSmith, R. E.; and Heapy, C. G., *Effects of zeneca zd7288 in comparison with alinidine and ul-fs 49 on guinea pig sinoatrial node and ventricular action potentials. J Cardiovasc Pharmacol*, 24 (3): (1994) 380–7.

Bucchi, A.; Baruscotti, M.; Nardini, M.; Barbuti, A.; Micheloni, S.; Bolognesi, M.; and DiFrancesco, D., *Identification of the molecular site of ivabradine binding to hcn4 channels. PLoS One*, 8 (1): (2013) e53.132. doi:10.1371/journal.pone.0053132.

Bussell, R., Jr and Eliezer, D., *Residual structure and dynamics in parkinson's disease-associated mutants of alpha-synuclein. J Biol Chem*, 276 (49): (2001) 45.996–6003. doi:10.1074/jbc.M106777200.

Cannon, J. R.; Tapias, V.; Na, H. M.; Honick, A. S.; Drolet, R. E.; and Greenamyre, J. T., *A highly reproducible rotenone model of parkinson's disease. Neurobiol Dis*, 34 (2): (2009) 279–90.

Cathala, L. and Paupardin-Tritsch, D., *Effect of catecholamines on the hyperpolarization-activated cationic ih and the inwardly rectifying potassium i(kir) currents in the rat substantia nigra pars compacta. Eur J Neurosci*, 11 (2): (1999) 398–406.

Chan, C. S.; Glajch, K. E.; Gertler, T. S.; Guzman, J. N.; Mercer, J. N.; Lewis, A. S.; Goldberg, A. B.; Tkatch, T.; Shigemoto, R.; Fleming, S. M.; Chetkovich, D. M.; Osten, P.; Kita, H.; and Surmeier, D. J., *Hcn channelopathy in external globus pallidus neurons in models of parkinson's disease. Nat Neurosci*, 14 (1): (2011) 85–92. doi:10.1038/nn.2692.

Chan, C. S.; Guzman, J. N.; Ilijic, E.; Mercer, J. N.; Rick, C.; Tkatch, T.; Meredith, G. E.; and Surmeier, D. J., *'rejuvenation' protects neurons in mouse models of parkinson's disease. Nature*, 447 (7148): (2007) 1081–6. doi:10.1038/nature05865.

Chan, P.; DeLanney, L. E.; Irwin, I.; Langston, J. W.; and Di Monte, D., *Rapid atp loss caused by 1-methyl-4-phenyl-1,2,3,6-tetrahydropyridine in mouse brain. J Neurochem*, 57 (1): (1991) 348–51.

Chaplan, S. R.; Guo, H.-Q.; Lee, D. H.; Luo, L.; Liu, C.; Kuei, C.; Velumian, A. A.; Butler, M. P.; Brown, S. M.; and Dubin, A. E., *Neuronal hyperpolarization-activated pacemaker channels drive neuropathic pain. J Neurosci*, 23 (4): (2003) 1169–78.

Chen, J.; Mitcheson, J. S.; Lin, M.; and Sanguinetti, M. C., *Functional roles of charged residues in the putative voltage sensor of the hcn2 pacemaker channel. J Biol Chem*, 275 (46): (2000) 36.465–71. doi:10.1074/jbc.M007034200.

Chen, S.; Wang, J.; and Siegelbaum, S. A., *Properties of hyperpolarization-activated pacemaker current defined by coassembly of hcn1 and hcn2 subunits and basal modulation by cyclic nucleotide. J Gen Physiol*, 117 (5): (2001) 491–504.

Chipuk, J. E. and Green, D. R., *Cytoplasmic p53: bax and forward. Cell Cycle*, 3 (4): (2004) 429–31.

Choi, W.-S.; Kruse, S. E.; Palmiter, R. D.; and Xia, Z., *Mitochondrial complex i inhibition is not required for dopaminergic neuron death induced by rotenone, mpp+, or paraquat. Proc Natl Acad Sci U S A*, 105 (39): (2008) 15.136–41. doi:10.1073/pnas.0807581105.

Cohen, G., *Oxidative stress, mitochondrial respiration, and parkinson's disease. Ann N Y Acad Sci*, 899: (2000) 112–20.

Colbert, C. M. and Johnston, D., *Axonal action-potential initiation and na+ channel densities in the soma and axon initial segment of subicular pyramidal neurons. J Neurosci*, 16 (21): (1996) 6676–86.

Conway, K. A.; Rochet, J. C.; Bieganski, R. M.; and Lansbury, P. T., Jr, *Kinetic stabilization of the alpha-synuclein protofibril by a dopamine-alpha-synuclein adduct. Science*, 294 (5545): (2001) 1346–9. doi:10.1126/science.1063522.

Cummings, C. J.; Reinstein, E.; Sun, Y.; Antalffy, B.; Jiang, Y.; Ciechanover, A.; Orr, H. T.; Beaudet, A. L.; and Zoghbi, H. Y., *Mutation of the e6-ap ubiquitin ligase reduces nuclear inclusion frequency while accelerating polyglutamine-induced pathology in sca1 mice. Neuron*, 24 (4): (1999) 879–92.

Cummings, C. J.; Sun, Y.; Opal, P.; Antalffy, B.; Mestril, R.; Orr, H. T.; Dillmann, W. H.; and Zoghbi, H. Y., *Over-expression of inducible hsp70 chaperone suppresses neuropathology and improves motor function in sca1 mice. Hum Mol Genet*, 10 (14): (2001) 1511–8.

Dauer, W. and Przedborski, S., *Parkinson's disease: mechanisms and models. Neuron*, 39 (6): (2003) 889–909.

Dawson, T. M.; Ko, H. S.; and Dawson, V. L., *Genetic animal models of parkinson's disease. Neuron*, 66 (5): (2010) 646–61. doi:10.1016/j.neuron.2010.04.034.

Day, B. J.; Patel, M.; Calavetta, L.; Chang, L. Y.; and Stamler, J. S., *A mechanism of paraquat toxicity involving nitric oxide synthase. Proc Natl Acad Sci U S A*, 96 (22): (1999) 12.760–5.

Day, M.; Carr, D. B.; Ulrich, S.; Ilijic, E.; Tkatch, T.; and Surmeier, D. J., *Dendritic excitability of mouse frontal cortex pyramidal neurons is shaped by the interaction among hcn, kir2, and kleak channels. J Neurosci*, 25 (38): (2005) 8776–87. doi: 10.1523/JNEUROSCI.2650-05.2005.

DeLong, M. R., *Primate models of movement disorders of basal ganglia origin. Trends Neurosci*, 13 (7): (1990) 281–5.

Deuschl, G.; Raethjen, J.; Baron, R.; Lindemann, M.; Wilms, H.; and Krack, P., *The pathophysiology of parkinsonian tremor: a review. J Neurol*, 247 Suppl 5: (2000) V33–48.

DiFrancesco, D., *Characterization of single pacemaker channels in cardiac sino-atrial node cells. Nature*, 324 (6096): (1986) 470–3. doi:10.1038/324470a0.

Ekstrand, M. I. and Galter, D., *The mitopark mouse - an animal model of parkinson's disease with impaired respiratory chain function in dopamine neurons. Parkinsonism Relat Disord*, 15 Suppl 3: (2009) S185–8. doi:10.1016/S1353-8020(09)70811-9.

El-Agnaf, O. M.; Bodles, A. M.; Guthrie, D. J.; Harriott, P.; and Irvine, G. B., *The n-terminal region of non-a beta component of alzheimer's disease amyloid is responsible for its tendency to assume beta-sheet and aggregate to form fibrils. Eur J Biochem*, 258 (1): (1998a) 157–63.

El-Agnaf, O. M.; Jakes, R.; Curran, M. D.; Middleton, D.; Ingenito, R.; Bianchi, E.; Pessi, A.; Neill, D.; and Wallace, A., *Aggregates from mutant and wild-type alpha-synuclein proteins and nac peptide induce apoptotic cell death in human neuroblastoma cells by formation of beta-sheet and amyloid-like filaments. FEBS Lett*, 440 (1-2): (1998b) 71–5.

Erickson, J. D.; Schafer, M. K.; Bonner, T. I.; Eiden, L. E.; and Weihe, E., *Distinct pharmacological properties and distribution in neurons and endocrine cells of two isoforms of the human vesicular monoamine transporter. Proc Natl Acad Sci U S A*, 93 (10): (1996) 5166–71.

Fabre, E.; Monserrat, J.; Herrero, A.; Barja, G.; and Leret, M. L., *Effect of mptp on brain mitochondrial h2o2 and atp production and on dopamine and dopac in the striatum. J Physiol Biochem*, 55 (4): (1999) 325–31.

Fearnley, J. M. and Lees, A. J., *Ageing and parkinson's disease: substantia nigra regional selectivity. Brain*, 114 (Pt 5): (1991) 2283–301.

Forloni, G.; Bertani, I.; Calella, A. M.; Thaler, F.; and Invernizzi, R., *Alpha-synuclein and parkinson's disease: selective neurodegenerative effect of alpha-synuclein fragment on dopaminergic neurons in vitro and in vivo. Ann Neurol*, 47 (5): (2000) 632–40.

Forno, L. S.; DeLanney, L. E.; Irwin, I.; and Langston, J. W., *Similarities and differences between mptp-induced parkinsonsim and parkinson's disease. neuropathologic considerations. Adv Neurol*, 60: (1993) 600–8.

Forno, L. S.; Langston, J. W.; DeLanney, L. E.; Irwin, I.; and Ricaurte, G. A., *Locus ceruleus lesions and eosinophilic inclusions in mptp-treated monkeys. Ann Neurol*, 20 (4): (1986) 449–55. doi:10.1002/ana.410200403.

Franz, O.; Liss, B.; Neu, A.; and Roeper, J., *Single-cell mrna expression of hcn1 correlates with a fast gating phenotype of hyperpolarization-activated cyclic nucleotide-gated ion channels (ih) in central neurons. Eur J Neurosci*, 12 (8): (2000) 2685–93.

Freestone, P. S.; Chung, K. K. H.; Guatteo, E.; Mercuri, N. B.; Nicholson, L. F. B.; and Lipski, J., *Acute action of rotenone on nigral dopaminergic neurons–involvement of reactive oxygen species and disruption of ca2+ homeostasis. Eur J Neurosci*, 30 (10): (2009) 1849–59. doi:10.1111/j.1460-9568.2009.06990.x.

Fuller, R. W. and Hemrick-Luecke, S. K., *Mechanisms of mptp (1-methyl-4-phenyl-1,2,3,6-tetrahydropyridine) neurotoxicity to striatal dopamine neurons in mice. Prog Neuropsychopharmacol Biol Psychiatry*, 9 (5-6): (1985) 687–90.

Gasparini, S. and DiFrancesco, D., *Action of the hyperpolarization-activated current (ih) blocker zd 7288 in hippocampal ca1 neurons. Pflugers Arch*, 435 (1): (1997) 99–106.

German, D. C. and Manaye, K. F., *Midbrain dopaminergic neurons (nuclei a8, a9, and a10): three-dimensional reconstruction in the rat. J Comp Neurol*, 331 (3): (1993) 297–309. doi:10.1002/cne.903310302.

German, D. C.; Nelson, E. L.; Liang, C. L.; Speciale, S. G.; Sinton, C. M.; and Sonsalla, P. K., *The neurotoxin mptp causes degeneration of specific nucleus a8, a9 and a10 dopaminergic neurons in the mouse. Neurodegeneration*, 5 (4): (1996) 299–312.

Giasson, B. I.; Uryu, K.; Trojanowski, J. Q.; and Lee, V. M., *Mutant and wild type human alpha-synucleins assemble into elongated filaments with distinct morphologies in vitro. J Biol Chem*, 274 (12): (1999) 7619–22.

Gibb, W. R.; Scott, T.; and Lees, A. J., *Neuronal inclusions of parkinson's disease. Mov Disord*, 6 (1): (1991) 2–11. doi:10.1002/mds.870060103.

Giovanni, A.; Sieber, B. A.; Heikkila, R. E.; and Sonsalla, P. K., *Correlation between the neostriatal content of the 1-methyl-4-phenylpyridinium species and dopaminergic neurotoxicity following 1-methyl-4-phenyl-1,2,3,6-tetrahydropyridine administration to several strains of mice. J Pharmacol Exp Ther*, 257 (2): (1991) 691–7.

Giovanni, A.; Sieber, B. A.; Heikkila, R. E.; and Sonsalla, P. K., *Studies on species sensitivity to the dopaminergic neurotoxin 1-methyl-4-phenyl-1,2,3,6-tetrahydropyridine. part 1: Systemic administration. J Pharmacol Exp Ther*, 270 (3): (1994) 1000–7.

Good, C. H.; Hoffman, A. F.; Hoffer, B. J.; Chefer, V. I.; Shippenberg, T. S.; Bäckman, C. M.; Larsson, N.-G.; Olson, L.; Gellhaar, S.; Galter, D.; and Lupica, C. R., *Impaired nigrostriatal function precedes behavioral deficits in a genetic mitochondrial model of parkinson's disease. FASEB J*, 25 (4): (2011) 1333–44. doi:10.1096/fj.10-173625.

Grace, A. A. and Bunney, B. S., *Intracellular and extracellular electrophysiology of nigral dopaminergic neurons–1. identification and characterization. Neuroscience*, 10 (2): (1983) 301–15.

Grace, A. A. and Bunney, B. S., *The control of firing pattern in nigral dopamine neurons: burst firing. J Neurosci*, 4 (11): (1984a) 2877–90.

Grace, A. A. and Bunney, B. S., *The control of firing pattern in nigral dopamine neurons: single spike firing. J Neurosci*, 4 (11): (1984b) 2866–76.

Graham, D. G.; Tiffany, S. M.; Bell, W. R., Jr; and Gutknecht, W. F., *Autoxidation versus covalent binding of quinones as the mechanism of toxicity of dopamine, 6-hydroxydopamine, and related compounds toward c1300 neuroblastoma cells in vitro. Mol Pharmacol*, 14 (4): (1978) 644–53.

Haber, S. N.; Ryoo, H.; Cox, C.; and Lu, W., *Subsets of midbrain dopaminergic neurons in monkeys are distinguished by different levels of mrna for the dopamine transporter: comparison with the mrna for the d2 receptor, tyrosine hydroxylase and calbindin immunoreactivity. J Comp Neurol*, 362 (3): (1995) 400–10. doi:10.1002/cne.903620308.

Harris, N. C. and Constanti, A., *Mechanism of block by zd 7288 of the hyperpolarization-activated inward rectifying current in guinea pig substantia nigra neurons in vitro. J Neurophysiol*, 74 (6): (1995) 2366–78.

Häusser, M. and Clark, B. A., *Tonic synaptic inhibition modulates neuronal output pattern and spatiotemporal synaptic integration. Neuron*, 19 (3): (1997) 665–78.

Herrero, M. T.; Hirsch, E. C.; Javoy-Agid, F.; Obeso, J. A.; and Agid, Y., *Differential vulnerability to 1-methyl-4-phenyl-1,2,3,6-tetrahydropyridine of dopaminergic and cholinergic neurons in the monkey mesopontine tegmentum. Brain Res*, 624 (1-2): (1993a) 281–5.

Herrero, M. T.; Hirsch, E. C.; Kastner, A.; Ruberg, M.; Luquin, M. R.; Laguna, J.; Javoy-Agid, F.; Obeso, J. A.; and Agid, Y., *Does neuromelanin contribute to the vulnerability of catecholaminergic neurons in monkeys intoxicated with mptp? Neuroscience*, 56 (2): (1993b) 499–511.

Höglinger, G. U.; Féger, J.; Prigent, A.; Michel, P. P.; Parain, K.; Champy, P.; Ruberg, M.; Oertel, W. H.; and Hirsch, E. C., *Chronic systemic complex i inhibition induces a hypokinetic multisystem degeneration in rats. J Neurochem*, 84 (3): (2003) 491–502.

Hornykiewicz, O. and Kish, S. J., *Biochemical pathophysiology of parkinson's disease. Adv Neurol*, 45: (1987) 19–34.

Huang, Z.; Lujan, R.; Kadurin, I.; Uebele, V. N.; Renger, J. J.; Dolphin, A. C.; and Shah, M. M., *Presynaptic hcn1 channels regulate cav3.2 activity and neurotransmission at select cortical synapses. Nat Neurosci*, 14 (4): (2011) 478–86. doi:10.1038/nn.2757.

Huang, Z.; Walker, M. C.; and Shah, M. M., *Loss of dendritic hcn1 subunits enhances cortical excitability and epileptogenesis. J Neurosci*, 29 (35): (2009) 10.979–88. doi:10.1523/JNEUROSCI.1531-09.2009.

Inyushin, M. U.; Arencibia-Albite, F.; Vázquez-Torres, R.; Vélez-Hernández, M. E.; and Jiménez-Rivera, C. A., *Alpha-2 noradrenergic receptor activation inhibits the hyperpolarization-activated cation current (ih) in neurons of the ventral tegmental area. Neuroscience*, 167 (2): (2010) 287–97. doi:10.1016/j.neuroscience.2010.01.052.

Irwin, I.; DeLanney, L. E.; and Langston, J. W., *Mptp and aging. studies in the c57bl/6 mouse. Adv Neurol*, 60: (1993) 197–206.

Ishikawa, A. and Takahashi, H., *Clinical and neuropathological aspects of autosomal recessive juvenile parkinsonism. J Neurol*, 245 (11 Suppl 3): (1998) P4–9.

Jackson-Lewis, V.; Jakowec, M.; Burke, R. E.; and Przedborski, S., *Time course and morphology of dopaminergic neuronal death caused by the neurotoxin 1-methyl-4-phenyl-1,2,3,6-tetrahydropyridine. Neurodegeneration*, 4 (3): (1995) 257–69.

Jackson-Lewis, V. and Przedborski, S., *Protocol for the mptp mouse model of parkinson's disease. Nat Protoc*, 2 (1): (2007) 141–51. doi:10.1038/nprot.2006.342.

Jaffe, D. B. and Carnevale, N. T., *Passive normalization of synaptic integration influenced by dendritic architecture. J Neurophysiol*, 82 (6): (1999) 3268–85.

Javitch, J. A.; D'Amato, R. J.; Strittmatter, S. M.; and Snyder, S. H., *Parkinsonism-inducing neurotoxin, n-methyl-4-phenyl-1,2,3,6 -tetrahydropyridine: uptake of the metabolite n-methyl-4-phenylpyridine by dopamine neurons explains selective toxicity. Proc Natl Acad Sci U S A*, 82 (7): (1985) 2173–7.

Javoy, F.; Sotelo, C.; Herbet, A.; and Agid, Y., *Specificity of dopaminergic neuronal degeneration induced by intracerebral injection of 6-hydroxydopamine in the nigrostriatal dopamine system. Brain Res*, 102 (2): (1976) 201–15.

Jenner, P., *Oxidative stress in parkinson's disease. Ann Neurol*, 53 Suppl 3: (2003) S26–36; discussion S36–8. doi:10.1002/ana.10483.

Jiang, Z. G.; Pessia, M.; and North, R. A., *Dopamine and baclofen inhibit the hyperpolarization-activated cation current in rat ventral tegmental neurones. J Physiol*, 462: (1993) 753–64.

Jonsson, G., *Chemical neurotoxins as denervation tools in neurobiology. Annu Rev Neurosci*, 3: (1980) 169–87. doi:10.1146/annurev.ne.03.030180.001125.

Jung, S.; Bullis, J. B.; Lau, I. H.; Jones, T. D.; Warner, L. N.; and Poolos, N. P., *Downregulation of dendritic hcn channel gating in epilepsy is mediated by altered phosphorylation signaling. J Neurosci*, 30 (19): (2010) 6678–88. doi:10.1523/JNEUROSCI.1290-10.2010.

Juraska, J. M.; Wilson, C. J.; and Groves, P. M., *The substantia nigra of the rat: a golgi study. J Comp Neurol*, 172 (4): (1977) 585–600. doi:10.1002/cne.901720403.

Keeney, P. M.; Xie, J.; Capaldi, R. A.; and Bennett, J. P., Jr, *Parkinson's disease brain mitochondrial complex i has oxidatively damaged subunits and is functionally impaired and misassembled. J Neurosci*, 26 (19): (2006) 5256–64. doi:10.1523/JNEUROSCI.0984-06.2006.

Kim, C. S.; Chang, P. Y.; and Johnston, D., *Enhancement of dorsal hippocampal activity by knockdown of hcn1 channels leads to anxiolytic- and antidepressant-like behaviors. Neuron*, 75 (3): (2012) 503–16. doi:10.1016/j.neuron.2012.05.027.

Kish, S. J.; Shannak, K.; Rajput, A.; Deck, J. H.; and Hornykiewicz, O., *Aging produces a specific pattern of striatal dopamine loss: implications for the etiology of idiopathic parkinson's disease. J Neurochem*, 58 (2): (1992) 642–8.

Klaidman, L. K.; Adams, J. D., Jr; Leung, A. C.; Kim, S. S.; and Cadenas, E., *Redox cycling of mpp+: evidence for a new mechanism involving hydride transfer with xanthine oxidase, aldehyde dehydrogenase, and lipoamide dehydrogenase. Free Radic Biol Med*, 15 (2): (1993) 169–79.

Kopito, R. R., *Aggresomes, inclusion bodies and protein aggregation. Trends Cell Biol*, 10 (12): (2000) 524–30.

Kuhn, D. M.; Arthur, R. E., Jr; Thomas, D. M.; and Elferink, L. A., *Tyrosine hydroxylase is inactivated by catechol-quinones and converted to a redox-cycling quinoprotein: possible relevance to parkinson's disease. J Neurochem*, 73 (3): (1999) 1309–17.

Lacey, M. G.; Mercuri, N. B.; and North, R. A., *Dopamine acts on d2 receptors to increase potassium conductance in neurones of the rat substantia nigra zona compacta. J Physiol*, 392: (1987) 397–416.

Lang, A. E. and Lozano, A. M., *Parkinson's disease. first of two parts. N Engl J Med*, 339 (15): (1998a) 1044–53. doi:10.1056/NEJM199810083391506.

Lang, A. E. and Lozano, A. M., *Parkinson's disease. second of two parts. N Engl J Med*, 339 (16): (1998b) 1130–43. doi:10.1056/NEJM199810153391607.

Langston, J. W.; Ballard, P.; Tetrud, J. W.; and Irwin, I., *Chronic parkinsonism in humans due to a product of meperidine-analog synthesis. Science*, 219 (4587): (1983) 979–80.

Langston, J. W.; Forno, L. S.; Tetrud, J.; Reeves, A. G.; Kaplan, J. A.; and Karluk, D., *Evidence of active nerve cell degeneration in the substantia nigra of humans years after 1-methyl-4-phenyl-1,2,3,6-tetrahydropyridine exposure. Ann Neurol*, 46 (4): (1999) 598–605.

Lee, C. S.; Han, J. H.; Jang, Y. Y.; Song, J. H.; and Han, E. S., *Differential effect of catecholamines and mpp(+) on membrane permeability in brain mitochondria and cell viability in pc12 cells. Neurochem Int*, 40 (4): (2002) 361–9.

Liou, H. H.; Tsai, M. C.; Chen, C. J.; Jeng, J. S.; Chang, Y. C.; Chen, S. Y.; and Chen, R. C., *Environmental risk factors and parkinson's disease: a case-control study in taiwan. Neurology*, 48 (6): (1997) 1583–8.

Liss, B.; Haeckel, O.; Wildmann, J.; Miki, T.; Seino, S.; and Roeper, J., *K-atp channels promote the differential degeneration of dopaminergic midbrain neurons. Nat Neurosci*, 8 (12): (2005) 1742–51. doi:10.1038/nn1570.

Liu, Y.; Peter, D.; Roghani, A.; Schuldiner, S.; Privé, G. G.; Eisenberg, D.; Brecha, N.; and Edwards, R. H., *A cdna that suppresses mpp+ toxicity encodes a vesicular amine transporter. Cell*, 70 (4): (1992) 539–51.

Lörincz, A.; Notomi, T.; Tamás, G.; Shigemoto, R.; and Nusser, Z., *Polarized and compartment-dependent distribution of hcn1 in pyramidal cell dendrites. Nat Neurosci*, 5 (11): (2002) 1185–93. doi:10.1038/nn962.

Lotharius, J. and Brundin, P., *Impaired dopamine storage resulting from alpha-synuclein mutations may contribute to the pathogenesis of parkinson's disease. Hum Mol Genet*, 11 (20): (2002) 2395–407.

Ludwig, A.; Zong, X.; Jeglitsch, M.; Hofmann, F.; and Biel, M., *A family of hyperpolarization-activated mammalian cation channels. Nature*, 393 (6685): (1998) 587–91. doi:10.1038/31255.

Maccaferri, G. and McBain, C. J., *The hyperpolarization-activated current (ih) and its contribution to pacemaker activity in rat ca1 hippocampal stratum oriens-alveus interneurones. J Physiol*, 497 (Pt 1): (1996) 119–30.

Macri, V. and Accili, E. A., *Structural elements of instantaneous and slow gating in hyperpolarization-activated cyclic nucleotide-gated channels. J Biol Chem*, 279 (16): (2004) 16.832–46. doi:10.1074/jbc.M400518200.

Macri, V.; Proenza, C.; Agranovich, E.; Angoli, D.; and Accili, E. A., *Separable gating mechanisms in a mammalian pacemaker channel. J Biol Chem*, 277 (39): (2002) 35.939–46. doi:10.1074/jbc.M203485200.

Magee, *Dendritic ih normalizes temporal summation in hippocampal ca1 neurons. Nat Neurosci*, 2 (9): (1999) 848. doi:10.1038/12229.

Magee, J. C., *Dendritic hyperpolarization-activated currents modify the integrative properties of hippocampal ca1 pyramidal neurons. J Neurosci*, 18 (19): (1998) 7613–24.

Magee, J. C., *Dendritic integration of excitatory synaptic input. Nat Rev Neurosci*, 1 (3): (2000) 181–90. doi:10.1038/35044552.

Mainen, Z. F. and Sejnowski, T. J., *Influence of dendritic structure on firing pattern in model neocortical neurons. Nature*, 382 (6589): (1996) 363–6. doi:10.1038/382363a0.

Mandavilli, B. S.; Ali, S. F.; and Van Houten, B., *Dna damage in brain mitochondria caused by aging and mptp treatment. Brain Res*, 885 (1): (2000) 45–52.

Mandir, A. S.; Przedborski, S.; Jackson-Lewis, V.; Wang, Z. Q.; Simbulan-Rosenthal, C. M.; Smulson, M. E.; Hoffman, B. E.; Guastella, D. B.; Dawson, V. L.; and Dawson, T. M., *Poly(adp-ribose) polymerase activation mediates 1-methyl-4-phenyl-1, 2,3,6-tetrahydropyridine (mptp)-induced parkinsonism. Proc Natl Acad Sci U S A*, 96 (10): (1999) 5774–9.

Margolis, E. B.; Lock, H.; Hjelmstad, G. O.; and Fields, H. L., *The ventral tegmental area revisited: is there an electrophysiological marker for dopaminergic neurons? J Physiol*, 577 (Pt 3): (2006) 907–24. doi:10.1113/jphysiol.2006.117069.

Markey, S. P.; Johannessen, J. N.; Chiueh, C. C.; Burns, R. S.; and Herkenham, M. A., *Intraneuronal generation of a pyridinium metabolite may cause drug-induced parkinsonism. Nature*, 311 (5985): (1984) 464–7.

Marsden, C. D., *Neuromelanin and parkinson's disease. J Neural Transm Suppl*, 19: (1983) 121–41.

Martinez-Vicente, M.; Talloczy, Z.; Kaushik, S.; Massey, A. C.; Mazzulli, J.; Mosharov, E. V.; Hodara, R.; Fredenburg, R.; Wu, D.-C.; Follenzi, A.; Dauer, W.; Przedborski, S.; Ischiropoulos, H.; Lansbury, P. T.; Sulzer, D.; and Cuervo, A. M., *Dopamine-modified alpha-synuclein blocks chaperone-mediated autophagy. J Clin Invest*, 118 (2): (2008) 777–88. doi:10.1172/JCI32806.

Mayer, R. A.; Kindt, M. V.; and Heikkila, R. E., *Prevention of the nigrostriatal toxicity of 1-methyl-4-phenyl-1,2,3,6-tetrahydropyridine by inhibitors of 3,4-dihydroxyphenylethylamine transport. J Neurochem*, 47 (4): (1986) 1073–9.

McCormack, A. L.; Thiruchelvam, M.; Manning-Bog, A. B.; Thiffault, C.; Langston, J. W.; Cory-Slechta, D. A.; and Di Monte, D. A., *Environmental risk factors and parkinson's disease: selective degeneration of nigral dopaminergic neurons caused by the herbicide paraquat. Neurobiol Dis*, 10 (2): (2002) 119–27.

McGeer, P. L.; Itagaki, S.; Akiyama, H.; and McGeer, E. G., *Rate of cell death in parkinsonism indicates active neuropathological process. Ann Neurol*, 24 (4): (1988) 574–6. doi:10.1002/ana.410240415.

Meredith, G. E.; Sonsalla, P. K.; and Chesselet, M.-F., *Animal models of parkinson's disease progression. Acta Neuropathol*, 115 (4): (2008a) 385–98. doi:10.1007/s00401-008-0350-x.

Meredith, G. E.; Totterdell, S.; Potashkin, J. A.; and Surmeier, D. J., *Modeling pd pathogenesis in mice: advantages of a chronic mptp protocol. Parkinsonism Relat Disord*, 14 Suppl 2: (2008b) S112–5. doi:10.1016/j.parkreldis.2008.04.012.

Michels, G.; Brandt, M. C.; Zagidullin, N.; Khan, I. F.; Larbig, R.; van Aaken, S.; Wippermann, J.; and Hoppe, U. C., *Direct evidence for calcium conductance of hyperpolarization-activated cyclic nucleotide-gated channels and human native if at physiological calcium concentrations. Cardiovasc Res*, 78 (3): (2008) 466–75. doi:10.1093/cvr/cvn032.

Miller, G. W.; Erickson, J. D.; Perez, J. T.; Penland, S. N.; Mash, D. C.; Rye, D. B.; and Levey, A. I., *Immunochemical analysis of vesicular monoamine transporter (vmat2) protein in parkinson's disease. Exp Neurol*, 156 (1): (1999) 138–48. doi:10.1006/exnr.1998.7008.

Mizuno, Y.; Sone, N.; Suzuki, K.; and Saitoh, T., *Studies on the toxicity of 1-methyl-4-phenylpyridinium ion (mpp+) against mitochondria of mouse brain. J Neurol Sci*, 86 (1): (1988) 97–110.

Moosmang, S.; Biel, M.; Hofmann, F.; and Ludwig, A., *Differential distribution of four hyperpolarization-activated cation channels in mouse brain. Biol Chem*, 380 (7-8): (1999) 975–80. doi:10.1515/BC.1999.121.

Moosmang, S.; Stieber, J.; Zong, X.; Biel, M.; Hofmann, F.; and Ludwig, A., *Cellular expression and functional characterization of four hyperpolarization-activated pacemaker channels in cardiac and neuronal tissues. Eur J Biochem*, 268 (6): (2001) 1646–52.

Moratalla, R.; Quinn, B.; DeLanney, L. E.; Irwin, I.; Langston, J. W.; and Graybiel, A. M., *Differential vulnerability of primate caudate-putamen and striosome-matrix dopamine systems to the neurotoxic effects of 1-methyl-4-phenyl-1,2,3,6-tetrahydropyridine. Proc Natl Acad Sci U S A*, 89 (9): (1992) 3859–63.

Much, B.; Wahl-Schott, C.; Zong, X.; Schneider, A.; Baumann, L.; Moosmang, S.; Ludwig, A.; and Biel, M., *Role of subunit heteromerization and n-linked glycosylation in the formation of functional hyperpolarization-activated cyclic nucleotide-gated channels. J Biol Chem*, 278 (44): (2003) 43.781–6. doi:10.1074/jbc.M306958200.

Muchowski, P. J., *Protein misfolding, amyloid formation, and neurodegeneration: a critical role for molecular chaperones? Neuron*, 35 (1): (2002) 9–12.

Muthane, U.; Ramsay, K. A.; Jiang, H.; Jackson-Lewis, V.; Donaldson, D.; Fernando, S.; Ferreira, M.; and Przedborski, S., *Differences in nigral neuron number and sensitivity to 1-methyl-4-phenyl-1,2,3,6-tetrahydropyridine in c57/bl and cd-1 mice. Exp Neurol*, 126 (2): (1994) 195–204. doi:10.1006/exnr.1994.1058.

Neuhoff, H.; Neu, A.; Liss, B.; and Roeper, J., *I(h) channels contribute to the different functional properties of identified dopaminergic subpopulations in the midbrain. J Neurosci*, 22 (4): (2002) 1290–302.

Nicklas, W. J.; Vyas, I.; and Heikkila, R. E., *Inhibition of nadh-linked oxidation in brain mitochondria by 1-methyl-4-phenyl-pyridine, a metabolite of the neurotoxin, 1-methyl-4-phenyl-1,2,5,6-tetrahydropyridine. Life Sci*, 36 (26): (1985) 2503–8.

Nolan, M. F.; Malleret, G.; Lee, K. H.; Gibbs, E.; Dudman, J. T.; Santoro, B.; Yin, D.; Thompson, R. F.; Siegelbaum, S. A.; Kandel, E. R.; and Morozov, A., *The hyperpolarization-activated hcn1 channel is important for motor learning and neuronal integration by cerebellar purkinje cells. Cell*, 115 (5): (2003) 551–64.

Noma, A. and Irisawa, H., *A time- and voltage-dependent potassium current in the rabbit sinoatrial node cell. Pflugers Arch*, 366 (2-3): (1976) 251–8.

Notomi, T. and Shigemoto, R., *Immunohistochemical localization of ih channel subunits, hcn1-4, in the rat brain. J Comp Neurol*, 471 (3): (2004) 241–76. doi:10.1002/cne.11039.

Obeso, J. A.; Rodriguez-Oroz, M.; Marin, C.; Alonso, F.; Zamarbide, I.; Lanciego, J. L.; and Rodriguez-Diaz, M., *The origin of motor fluctuations in parkinson's disease: importance of dopaminergic innervation and basal ganglia circuits. Neurology*, 62 (1 Suppl 1): (2004) S17–30.

O'Callaghan, J. P. and Miller, D. B., *Quantification of reactive gliosis as an approach to neurotoxicity assessment. NIDA Res Monogr*, 136: (1993) 188–212.

Offen, D.; Beart, P. M.; Cheung, N. S.; Pascoe, C. J.; Hochman, A.; Gorodin, S.; Melamed, E.; Bernard, R.; and Bernard, O., *Transgenic mice expressing human bcl-2 in their neurons are resistant to 6-hydroxydopamine and 1-methyl-4-phenyl-1,2,3,6- tetrahydropyridine neurotoxicity. Proc Natl Acad Sci U S A*, 95 (10): (1998) 5789–94.

Olijslagers, J. E.; Werkman, T. R.; McCreary, A. C.; Kruse, C. G.; and Wadman, W. J., *Modulation of midbrain dopamine neurotransmission by serotonin, a versatile interaction between neurotransmitters and significance for antipsychotic drug action. Curr Neuropharmacol*, 4 (1): (2006) 59–68.

Ovadia, A.; Zhang, Z.; and Gash, D. M., *Increased susceptibility to mptp toxicity in middle-aged rhesus monkeys. Neurobiol Aging*, 16 (6): (1995) 931–7.

Pape, H. C., *Queer current and pacemaker: the hyperpolarization-activated cation current in neurons. Annu Rev Physiol*, 58: (1996) 299–327. doi:10.1146/annurev.ph.58.030196.001503.

Pappolla, M. A., *Lewy bodies of parkinson's disease. immune electron microscopic demonstration of neurofilament antigens in constituent filaments. Arch Pathol Lab Med*, 110 (12): (1986) 1160–3.

Parker, W. D., Jr; Parks, J. K.; and Swerdlow, R. H., *Complex i deficiency in parkinson's disease frontal cortex. Brain Res*, 1189: (2008) 215–8. doi:10.1016/j.brainres.2007.10.061.

Parsons, S. M., *Transport mechanisms in acetylcholine and monoamine storage. FASEB J*, 14 (15): (2000) 2423–34. doi:10.1096/fj.00-0203rev.

Perkins, K. L. and Wong, R. K., *Intracellular qx-314 blocks the hyperpolarization-activated inward current iq in hippocampal ca1 pyramidal cells. J Neurophysiol*, 73 (2): (1995) 911–5.

Pettit, D. L. and Augustine, G. J., *Distribution of functional glutamate and gaba receptors on hippocampal pyramidal cells and interneurons. J Neurophysiol*, 84 (1): (2000) 28–38.

Pian, P.; Bucchi, A.; Robinson, R. B.; and Siegelbaum, S. A., *Regulation of gating and rundown of hcn hyperpolarization-activated channels by exogenous and endogenous pip2. J Gen Physiol*, 128 (5): (2006) 593–604. doi:10.1085/jgp.200609648.

Poller, W. C.; Bernard, R.; Derst, C.; Weiss, T.; Madai, V. I.; and Veh, R. W., *Lateral habenular neurons projecting to reward-processing monoaminergic nuclei express hyperpolarization-activated cyclic nucleotid-gated cation channels. Neuroscience*, 193: (2011) 205–16. doi:10.1016/j.neuroscience.2011.07.013.

Poolos, N. P.; Bullis, J. B.; and Roth, M. K., *Modulation of h-channels in hippocampal pyramidal neurons by p38 mitogen-activated protein kinase. J Neurosci*, 26 (30): (2006) 7995–8003. doi:10.1523/JNEUROSCI.2069-06.2006.

Postea, O. and Biel, M., *Exploring hcn channels as novel drug targets. Nat Rev Drug Discov*, 10 (12): (2011) 903–14. doi:10.1038/nrd3576.

Price, K. S.; Farley, I. J.; and Hornykiewicz, O., *Neurochemistry of parkinson's disease: relation between striatal and limbic dopamine. Adv Biochem Psychopharmacol*, 19: (1978) 293–300.

Proenza, C.; Angoli, D.; Agranovich, E.; Macri, V.; and Accili, E. A., *Pacemaker channels produce an instantaneous current. J Biol Chem*, 277 (7): (2002) 5101–9. doi:10.1074/jbc.M106974200.

Przedborski, S.; Kostic, V.; Jackson-Lewis, V.; Naini, A. B.; Simonetti, S.; Fahn, S.; Carlson, E.; Epstein, C. J.; and Cadet, J. L., *Transgenic mice with increased cu/zn-superoxide dismutase activity are resistant to n-methyl-4-phenyl-1,2,3,6-tetrahydropyridine-induced neurotoxicity. J Neurosci*, 12 (5): (1992) 1658–67.

Przedborski, S. and Vila, M., *The 1-methyl-4-phenyl-1,2,3,6-tetrahydropyridine mouse model: a tool to explore the pathogenesis of parkinson's disease. Ann N Y Acad Sci*, 991: (2003) 189–98.

Puopolo, M.; Raviola, E.; and Bean, B. P., *Roles of subthreshold calcium current and sodium current in spontaneous firing of mouse midbrain dopamine neurons. J Neurosci*, 27 (3): (2007) 645–56. doi:10.1523/JNEUROSCI.4341-06.2007.

Raman, I. M. and Bean, B. P., *Ionic currents underlying spontaneous action potentials in isolated cerebellar purkinje neurons. J Neurosci*, 19 (5): (1999) 1663–74.

Ramsay, R. R. and Singer, T. P., *Energy-dependent uptake of n-methyl-4-phenylpyridinium, the neurotoxic metabolite of 1-methyl-4-phenyl-1,2,3,6-tetrahydropyridine, by mitochondria. J Biol Chem*, 261 (17): (1986) 7585–7.

Reinhard, J. F., Jr; Diliberto, E. J., Jr; Viveros, O. H.; and Daniels, A. J., *Subcellular compartmentalization of 1-methyl-4-phenylpyridinium with catecholamines in adrenal medullary chromaffin vesicles may explain the lack of toxicity to adrenal chromaffin cells. Proc Natl Acad Sci U S A*, 84 (22): (1987) 8160–4.

Rinzel, J. and Rall, W., *Transient response in a dendritic neuron model for current injected at one branch. Biophys J*, 14 (10): (1974) 759–90. doi:10.1016/S0006-3495(74)85948-5.

Rodríguez, M.; Barroso-Chinea, P.; Abdala, P.; Obeso, J.; and González-Hernández, T., *Dopamine cell degeneration induced by intraventricular administration of 6-hydroxydopamine in the rat: similarities with cell loss in parkinson's disease. Exp Neurol*, 169 (1): (2001) 163–81. doi:10.1006/exnr.2000.7624.

Rohrbacher, J.; Ichinohe, N.; and Kitai, S. T., *Electrophysiological characteristics of substantia nigra neurons in organotypic cultures: spontaneous and evoked activities. Neuroscience*, 97 (4): (2000) 703–14.

Rose, S.; Nomoto, M.; Jackson, E. A.; Gibb, W. R.; Jaehnig, P.; Jenner, P.; and Marsden, C. D., *Age-related effects of 1-methyl-4-phenyl-1,2,3,6-tetrahydropyridine treatment of common marmosets. Eur J Pharmacol*, 230 (2): (1993) 177–85.

Samii, A.; Nutt, J. G.; and Ransom, B. R., *Parkinson's disease. Lancet*, 363 (9423): (2004) 1783–93. doi:10.1016/S0140-6736(04)16305-8.

Saner, A. and Thoenen, H., *Model experiments on the molecular mechanism of action of 6-hydroxydopamine. Mol Pharmacol*, 7 (2): (1971) 147–54.

Santens, P.; Boon, P.; Van Roost, D.; and Caemaert, J., *The pathophysiology of motor symptoms in parkinson's disease. Acta Neurol Belg*, 103 (3): (2003) 129–34.

Santoro, B.; Chen, S.; Luthi, A.; Pavlidis, P.; Shumyatsky, G. P.; Tibbs, G. R.; and Siegelbaum, S. A., *Molecular and functional heterogeneity of hyperpolarization-activated pacemaker channels in the mouse cns. J Neurosci*, 20 (14): (2000) 5264–75.

Santoro, B.; Liu, D. T.; Yao, H.; Bartsch, D.; Kandel, E. R.; Siegelbaum, S. A.; and Tibbs, G. R., *Identification of a gene encoding a hyperpolarization-activated pacemaker channel of brain. Cell*, 93 (5): (1998) 717–29.

Saporito, M. S.; Brown, E. M.; Miller, M. S.; and Carswell, S., *Cep-1347/kt-7515, an inhibitor of c-jun n-terminal kinase activation, attenuates the 1-methyl-4-phenyl tetrahydropyridine-mediated loss of nigrostriatal dopaminergic neurons in vivo. J Pharmacol Exp Ther*, 288 (2): (1999) 421–7.

Saporito, M. S.; Thomas, B. A.; and Scott, R. W., *Mptp activates c-jun nh(2)-terminal kinase (jnk) and its upstream regulatory kinase mkk4 in nigrostriatal neurons in vivo. J Neurochem*, 75 (3): (2000) 1200–8.

Satoh, T. O. and Yamada, M., *A bradycardiac agent zd7288 blocks the hyperpolarization-activated current (i(h)) in retinal rod photoreceptors. Neuropharmacology*, 39 (7): (2000) 1284–91.

Saudou, F.; Finkbeiner, S.; Devys, D.; and Greenberg, M. E., *Huntingtin acts in the nucleus to induce apoptosis but death does not correlate with the formation of intranuclear inclusions. Cell*, 95 (1): (1998) 55–66.

Sayer, R. J.; Friedlander, M. J.; and Redman, S. J., *The time course and amplitude of epsps evoked at synapses between pairs of ca3/ca1 neurons in the hippocampal slice. J Neurosci*, 10 (3): (1990) 826–36.

Schapira, A. H.; Cooper, J. M.; Dexter, D.; Clark, J. B.; Jenner, P.; and Marsden, C. D., *Mitochondrial complex i deficiency in parkinson's disease. J Neurochem*, 54 (3): (1990) 823–7.

Scherman, D.; Desnos, C.; Darchen, F.; Pollak, P.; Javoy-Agid, F.; and Agid, Y., *Striatal dopamine deficiency in parkinson's disease: role of aging. Ann Neurol*, 26 (4): (1989) 551–7. doi:10.1002/ana.410260409.

Seniuk, N. A.; Tatton, W. G.; and Greenwood, C. E., *Dose-dependent destruction of the coeruleus-cortical and nigral-striatal projections by mptp. Brain Res*, 527 (1): (1990) 7–20.

Seutin, V.; Massotte, L.; Renette, M. F.; and Dresse, A., *Evidence for a modulatory role of ih on the firing of a subgroup of midbrain dopamine neurons. Neuroreport*, 12 (2): (2001) 255–8.

Sheets, P. L.; Suter, B. A.; Kiritani, T.; Chan, C. S.; Surmeier, D. J.; and Shepherd, G. M. G., *Corticospinal-specific hcn expression in mouse motor cortex: I(h)-dependent synaptic integration as a candidate microcircuit mechanism involved in motor control. J Neurophysiol*, 106 (5): (2011) 2216–31. doi:10.1152/jn.00232.2011.

Shimizu, K.; Ohtaki, K.; Matsubara, K.; Aoyama, K.; Uezono, T.; Saito, O.; Suno, M.; Ogawa, K.; Hayase, N.; Kimura, K.; and Shiono, H., *Carrier-mediated processes in blood–brain barrier penetration and neural uptake of paraquat. Brain Res*, 906 (1-2): (2001) 135–42.

Shin, M. and Chetkovich, D. M., *Activity-dependent regulation of h channel distribution in hippocampal ca1 pyramidal neurons. J Biol Chem*, 282 (45): (2007) 33.168–80. doi: 10.1074/jbc.M703736200.

Sirinathsinghji, D. J.; Kupsch, A.; Mayer, E.; Zivin, M.; Pufal, D.; and Oertel, W. H., *Cellular localization of tyrosine hydroxylase mrna and cholecystokinin mrna-containing cells in the ventral mesencephalon of the common marmoset: effects of 1-methyl-4-phenyl-1,2,3,6-tetrahydropyridine. Brain Res Mol Brain Res*, 12 (1-3): (1992) 267–74.

Spencer, J. P.; Jenner, P.; Daniel, S. E.; Lees, A. J.; Marsden, D. C.; and Halliwell, B., *Conjugates of catecholamines with cysteine and gsh in parkinson's disease: possible mechanisms of formation involving reactive oxygen species. J Neurochem*, 71 (5): (1998) 2112–22.

Stieber, J.; Herrmann, S.; Feil, S.; Löster, J.; Feil, R.; Biel, M.; Hofmann, F.; and Ludwig, A., *The hyperpolarization-activated channel hcn4 is required for the generation of pacemaker action potentials in the embryonic heart. Proc Natl Acad Sci U S A*, 100 (25): (2003) 15.235–40. doi:10.1073/pnas.2434235100.

Strauss, U.; Kole, M. H. P.; Bräuer, A. U.; Pahnke, J.; Bajorat, R.; Rolfs, A.; Nitsch, R.; and Deisz, R. A., *An impaired neocortical ih is associated with enhanced excitability and absence epilepsy. Eur J Neurosci*, 19 (11): (2004) 3048–58. doi:10.1111/j.0953-816X.2004.03392.x.

Takahashi, N.; Miner, L. L.; Sora, I.; Ujike, H.; Revay, R. S.; Kostic, V.; Jackson-Lewis, V.; Przedborski, S.; and Uhl, G. R., *Vmat2 knockout mice: heterozygotes display reduced amphetamine-conditioned reward, enhanced amphetamine locomotion, and enhanced mptp toxicity. Proc Natl Acad Sci U S A*, 94 (18): (1997) 9938–43.

Tatton, N. A. and Kish, S. J., *In situ detection of apoptotic nuclei in the substantia nigra compacta of 1-methyl-4-phenyl-1,2,3,6-tetrahydropyridine-treated mice using terminal deoxynucleotidyl transferase labelling and acridine orange staining. Neuroscience*, 77 (4): (1997) 1037–48.

Tepper, J. M. and Lee, C. R., *Gabaergic control of substantia nigra dopaminergic neurons. Prog Brain Res*, 160: (2007) 189–208. doi:10.1016/S0079-6123(06)60011-3.

Trimmer, P. A.; Smith, T. S.; Jung, A. B.; and Bennett, J. P., Jr, *Dopamine neurons from transgenic mice with a knockout of the p53 gene resist mptp neurotoxicity. Neurodegeneration*, 5 (3): (1996) 233–9.

Uéda, K.; Fukushima, H.; Masliah, E.; Xia, Y.; Iwai, A.; Yoshimoto, M.; Otero, D. A.; Kondo, J.; Ihara, Y.; and Saitoh, T., *Molecular cloning of cdna encoding an unrecognized component of amyloid in alzheimer disease. Proc Natl Acad Sci U S A*, 90 (23): (1993) 11.282–6.

Uhl, G. R.; Hedreen, J. C.; and Price, D. L., *Parkinson's disease: loss of neurons from the ventral tegmental area contralateral to therapeutic surgical lesions. Neurology*, 35 (8): (1985) 1215–8.

Ungerstedt, U., *Striatal dopamine release after amphetamine or nerve degeneration revealed by rotational behaviour. Acta Physiol Scand Suppl*, 367: (1971) 49–68.

van Ginneken, A. C. and Giles, W., *Voltage clamp measurements of the hyperpolarization-activated inward current i(f) in single cells from rabbit sino-atrial node. J Physiol*, 434: (1991) 57–83.

Van Laar, V. S.; Mishizen, A. J.; Cascio, M.; and Hastings, T. G., *Proteomic identification of dopamine-conjugated proteins from isolated rat brain mitochondria and sh-sy5y cells. Neurobiol Dis*, 34 (3): (2009) 487–500. doi:10.1016/j.nbd.2009.03.004.

Varastet, M.; Riche, D.; Maziere, M.; and Hantraye, P., *Chronic mptp treatment reproduces in baboons the differential vulnerability of mesencephalic dopaminergic neurons observed in parkinson's disease. Neuroscience*, 63 (1): (1994) 47–56.

Vargas, G. and Lucero, M. T., *Dopamine modulates inwardly rectifying hyperpolarization-activated current (ih) in cultured rat olfactory receptor neurons. J Neurophysiol*, 81 (1): (1999) 149–58.

Vila, M.; Jackson-Lewis, V.; Vukosavic, S.; Djaldetti, R.; Liberatore, G.; Offen, D.; Korsmeyer, S. J.; and Przedborski, S., *Bax ablation prevents dopaminergic neurodegeneration in the 1-methyl- 4-phenyl-1,2,3,6-tetrahydropyridine mouse model of parkinson's disease. Proc Natl Acad Sci U S A*, 98 (5): (2001) 2837–42. doi:10.1073/pnas.051633998.

Vives-Bauza, C. and Przedborski, S., *Mitophagy: the latest problem for parkinson's disease. Trends Mol Med*, 17 (3): (2011) 158–65. doi:10.1016/j.molmed.2010.11.002.

Wallace, B. A.; Ashkan, K.; Heise, C. E.; Foote, K. D.; Torres, N.; Mitrofanis, J.; and Benabid, A.-L., *Survival of midbrain dopaminergic cells after lesion or deep brain stimulation of the subthalamic nucleus in mptp-treated monkeys. Brain*, 130 (Pt 8): (2007) 2129–45. doi:10.1093/brain/awm137.

Watts, A. E.; Williams, J. T.; and Henderson, G., *Baclofen inhibition of the hyperpolarization-activated cation current, ih, in rat substantia nigra zona compacta neurons may be secondary to potassium current activation. J Neurophysiol*, 76 (4): (1996) 2262–70.

Weihe, E. and Eiden, L. E., *Chemical neuroanatomy of the vesicular amine transporters. FASEB J*, 14 (15): (2000) 2435–49. doi:10.1096/fj.00-0202rev.

Wells, J. E.; Rowland, K. C.; and Proctor, E. K., *Hyperpolarization-activated channels in trigeminal ganglia innervating healthy and pulp-exposed teeth. Int Endod J*, 40 (9): (2007) 715–21. doi:10.1111/j.1365-2591.2007.01297.x.

Wichmann, T. and DeLong, M. R., *Basal ganglia discharge abnormalities in parkinson's disease. J Neural Transm Suppl*, (70): (2006) 21–5.

Williams, S. R. and Stuart, G. J., *Site independence of epsp time course is mediated by dendritic i(h) in neocortical pyramidal neurons. J Neurophysiol*, 83 (5): (2000) 3177–82.

Winner, B.; Jappelli, R.; Maji, S. K.; Desplats, P. A.; Boyer, L.; Aigner, S.; Hetzer, C.; Loher, T.; Vilar, M.; Campioni, S.; Tzitzilonis, C.; Soragni, A.; Jessberger, S.; Mira, H.; Consiglio, A.; Pham, E.; Masliah, E.; Gage, F. H.; and Riek, R., *In vivo demonstration that alpha-synuclein oligomers are toxic. Proc Natl Acad Sci U S A*, 108 (10): (2011) 4194–9. doi:10.1073/pnas.1100976108.

Wollmuth, L. P. and Hille, B., *Ionic selectivity of ih channels of rod photoreceptors in tiger salamanders. J Gen Physiol*, 100 (5): (1992) 749–65.

Womble, M. D. and Moises, H. C., *Hyperpolarization-activated currents in neurons of the rat basolateral amygdala. J Neurophysiol*, 70 (5): (1993) 2056–65.

Yamada, T.; McGeer, E.; and Schelper, R., *Histological and biochemical pathology in a family with autosomal dominant histochemical and biochemical pathology in a family with autosomal dominant parkinsonism and dementia. Neurol Psychiat Brain Res*, 2: (1993) 26–35.

Yang, L.; Matthews, R. T.; Schulz, J. B.; Klockgether, T.; Liao, A. W.; Martinou, J. C.; Penney, J. B., Jr; Hyman, B. T.; and Beal, M. F., *1-methyl-4-phenyl-1,2,3,6-tetrahydropyride neurotoxicity is attenuated in mice overexpressing bcl-2. J Neurosci*, 18 (20): (1998) 8145–52.

Yu, F. H. and Catterall, W. A., *The vgl-chanome: a protein superfamily specialized for electrical signaling and ionic homeostasis. Sci STKE*, 2004 (253): (2004) re15. doi:10.1126/stke.2532004re15.

Yue, B. W. and Huguenard, J. R., *The role of h-current in regulating strength and frequency of thalamic network oscillations. Thalamus Relat Syst*, 1 (2): (2001) 95–103. doi:10.1016/S1472-9288(01)00009-7.

Zecca, L.; Tampellini, D.; Gerlach, M.; Riederer, P.; Fariello, R. G.; and Sulzer, D., *Substantia nigra neuromelanin: structure, synthesis, and molecular behaviour. Mol Pathol*, 54 (6): (2001) 414–8.

Zecca, L.; Wilms, H.; Geick, S.; Claasen, J.-H.; Brandenburg, L.-O.; Holzknecht, C.; Panizza, M. L.; Zucca, F. A.; Deuschl, G.; Sievers, J.; and Lucius, R., *Human neuromelanin induces neuroinflammation and neurodegeneration in the rat substantia nigra: implications for parkinson's disease. Acta Neuropathol*, 116 (1): (2008) 47–55. doi:10.1007/s00401-008-0361-7.

Zolles, G.; Klöcker, N.; Wenzel, D.; Weisser-Thomas, J.; Fleischmann, B. K.; Roeper, J.; and Fakler, B., *Pacemaking by hcn channels requires interaction with phosphoinositides. Neuron*, 52 (6): (2006) 1027–36. doi:10.1016/j.neuron.2006.12.005.